

*"This is the peer reviewed version of the following article: Paddock K, Zeigler L, Harvey B, Prufrock KA, Liptak JM, Ficorilli CM, Hogg RT, Bonar CJ, Evans S, Williams L, Vinyard CJ. 2020. Comparative dental anatomy in newborn primates: Cusp mineralization. The Anatomical Record 303: 2415–2475, which has been published in final form at <https://doi.org/10.1002/ar.24326>. This article may be used for non-commercial purposes in accordance with Wiley Terms and Conditions for Use of Self-Archived Versions."*

## **Comparative dental anatomy in newborn primates: Cusp mineralization**

Kelsey Paddock<sup>1</sup>, Larissa Zeigler<sup>1</sup>, Brianna Harvey<sup>1</sup>, Kristen A. Prufrock<sup>2</sup>, Jordan M. Liptak<sup>1</sup>, Courtney M. Ficorilli<sup>1</sup>, Russell T. Hogg<sup>3</sup>, Christopher J. Bonar<sup>4</sup>, Sian Evans<sup>5</sup>, Lawrence Williams<sup>6</sup>, Christopher J. Vinyard<sup>7</sup>, Valerie B. DeLeon<sup>8</sup>, Timothy D. Smith<sup>1</sup>

1, School of Physical Therapy, Slippery Rock University, Slippery Rock, PA 16057; 2, Center for Functional Anatomy and Evolution, Johns Hopkins University School of Medicine, Baltimore, MD, 21205; 3, Department of Rehabilitation Sciences; Florida Gulf Coast University; 4, Dallas Zoo, Dallas, Texas 75203; 5, DuMond Conservancy, Miami, Florida 33170; 6, Department of Veterinary Sciences, UT MD Anderson Cancer Center, Michale E. Keeling Center for Comparative Medicine and Research, Bastrop, Texas 78602; 7, Department of Anatomy and Neurobiology, Northeast Ohio Medical University, Rootstown, OH 44272; 8, Department of Anthropology, University of Florida, Gainesville, FL 32611.

**Funding: NSF; grant numbers BCS-1830894, BCS-1830919, BCS-1231717, BCS-1231350, BCS-1728263; BCS-0959438; NIH; Grant numbers: P40 OD010938, P51 OD011106; Duke Lemur Center's Director's Fund.**

Correspondence to:

Address: TD Smith, Ph.D.

School of Physical Therapy

Slippery Rock University

Slippery Rock, PA 16057

E-mail: [timothy.smith@sru.edu](mailto:timothy.smith@sru.edu)

Fax: 724-738-2113

## ABSTRACT

Previous descriptive work on deciduous dentition of primates has focused disproportionately on great apes and humans. To address this bias in the literature, we studied 131 subadult non-hominoid specimens (including 110 newborns) describing deciduous tooth morphology and assessing maximum hydroxyapatite density (MHD). All specimens were CT scanned at 70 kVp and reconstructed at 20.5 to 39  $\mu\text{m}$  voxels. Grayscale intensity from scans was converted to hydroxyapatite (HA) density ( $\text{mg HA/cm}^3$ ) using a linear conversion of grayscale values to calibration standards of known HA density ( $R^2=0.99$ ). Using Amira software, mineralized dental tissues were captured by segmenting the tooth cusps first, and then capturing the remainder of the teeth at descending thresholds of gray levels. We assessed the relationship of MHD of selected teeth to cranial length using Pearson correlation coefficients. In monkeys, anterior teeth are more mineralized than postcanine teeth. In tarsiers and most lemurs and lorises, postcanine teeth are the most highly mineralized. This suggests that monkeys have a more prolonged process of dental mineralization that begins with incisors and canines, while mineralization of postcanine teeth is delayed. This may in part be a result of relatively late weaning in most anthropoid primates. Results also reveal that in lemurs and lorises, MHD of the mandibular first permanent molar ( $M_1$ ) negatively correlates with cranial length. In contrast, the MHD of  $M_1$  positively correlates with cranial length in monkeys. This supports the hypothesis that natural selection acts independently on dental growth as opposed to mineralization, and indicates clear phylogenetic differences among primates.

KEY WORDS: deciduous, catarrhine, platyrhine, dentition

## INTRODUCTION

Our understanding of mammalian dentition has been gleaned through painstaking methodologies. Three-dimensional reconstructions of developing jaws have informed us of early tooth morphogenesis. These models were at first produced by stacking aligned physical cross-sections (e.g., composed of wax plates or paper) based on histological sections (Ahrens, 1913; Blechschmidt, 1954; Ooë, 1979; Luckett and Maier, 1982). Computer generated models, also based on histology, have produced further insights in more recent years (e.g., Radlanski 1995). In vitro or immunohistochemical data can be embedded within these models to identify genetic control or signaling mechanisms (e.g., Jernvall et al., 1994). Similarly labor-intensive procedures, such as clearing and staining whole tooth germs, have helped us to understand patterns of cusp mineralization (e.g., Tarrant and Swindler, 1973; Winkler et al., 1991). The germs are painstakingly dissected out of the jaws and stained by soaking in alizarin red S solution. Then the outer collagenous capsule, the follicle, is cut open to reveal the mineralized portion of the crown, which may include only cusp tips. Radiological methods have historically failed to identify some teeth in such early stages of mineralization (see Garn et al., 1959; Winkler et al., 1991). More recently, micro-computed tomography ( $\mu$ -CT) has significantly increased knowledge on dental development, particularly regarding the dentition of small-bodied primates, including both living and extinct taxa, and increased scan resolution has allowed detailed study of deciduous teeth in smaller primates (e.g., Franzen et al., 2009; Smith et al., 2011). In the present study, we employ  $\mu$ -CT to further our understanding of the extent of cusp mineralization in primates at birth, a timeframe for which we currently lack a broad comparative perspective.

Compared to our understanding of the sequence in which teeth pierce the gingiva (gingival emergence) and transition from within alveolar crypts into occlusion (dental eruption), we have a far poorer comparative understanding of how the crown forms. Prior to the widespread availability of  $\mu$ -CT, our most extensive and detailed observations centered on larger and medium sized primates, which could be studied grossly or as whole-mount stained specimens (e.g., Kraus and Jordan, 1965; Tarrant and Swindler, 1973). The most comprehensive descriptions have focused on human deciduous teeth (e.g., Kraus and Jordan, 1965), but our extant and extinct closest relatives have also attracted much attention (e.g., Mann, 1988, Macchiarelli et al., 2006). The rare studies of smaller primates have relied on histologically

sectioned material (e.g., Luckett and Maier, 1982). The advantages of histological methods are the fine resolution through microscopy and the ability to identify tissue types using a variety of staining procedures. However, the resolution of  $\mu$ -CT has improved, now reaching interslice distances that can match that achieved during routine paraffin histology. In the present study we use  $\mu$ -CT in a comparative study of maxillary and mandibular tooth crowns in perinatal primates.

### ***Dentition of the newborn***

In the newborn primate, there is most likely a mix of deciduous and permanent teeth that have at least initiated mineralization (Smith et al., 2015). For simplicity, our terminology here divides teeth into three groups, deciduous teeth (i1, i2, dc, dp2-dp4), “replacement” teeth (I1, I2, C, P2, P3, P4, i.e., the secondary teeth), and “permanent” teeth (the molars M1, M2, M3). Maxillary teeth are denoted by superscript numbers (e.g., M<sup>1</sup>) and mandibular teeth are denoted by subscript numbers (e.g., M<sub>1</sub>). The nomenclature used for postcanine deciduous teeth, “deciduous premolars,” is meant to facilitate a discussion of tooth location in the developing jaw. These teeth are often discussed as “deciduous molars” in the literature (morphologically, this is a more appropriate term for the primary teeth replaced by the adult premolars - e.g., Schwartz, 2007).

Nearly all newborn primates possess at least one partially mineralized permanent tooth at birth: M1 (Smith et al., 2015). This is one trait that universally distinguishes primates from altricial mammals such as scandentians. However, primates vary enormously in the rate at which replacement teeth mineralize and erupt. In some, deciduous teeth have already been shed at birth, and replacement teeth have initiated crown formation; in others, deciduous teeth are maintained postnatally to weaning age and beyond (Luckett and Maier, 1982; Godfrey et al., 2001, 2004; Smith et al., 2015). The extent of variation may relate to the relatively protracted parenting period for primates compared to most mammals. The newborn primate is at first fully dependent on, and later supplemented by maternal milk for a variable amount of time. This might be thought to give natural selection an unusually light hand on the dentition of the newborn. However, certain specializations can be observed at birth, such as precocious mineralization of

cusps in folivorous primates (Smith et al., 2015). Hence, we expect certain adaptive characteristics of primate tooth cusps may be already apparent at birth.

### ***Crown mineralization in newborn anthropoid primates***

The literature on crown mineralization in primates is centered mostly on hominoid primates (apes and humans). Using whole mount preparations that stained enamel and dentin, Kraus and Jordan (1965) studied developing tooth crowns of fetal and neonatal humans. The teeth of newborn great apes were studied by Siebert and Swindler (1991) and Winkler et al. (1991) using similar methods and radiography. In hominoids, mineralization of deciduous tooth crowns is well underway at birth, but the roots have yet to develop; the deciduous incisor crowns are the most complete, while deciduous canine and premolar crowns are still forming, particularly in the cervical region. Maxillary or mandibular dp<sub>4</sub> may lag behind dp<sub>3</sub> in mineralization (e.g., only two to three cusps of dp<sup>4</sup> are mineralized in some newborns). Siebert and Swindler (1991) note that all cusps of mandibular dp<sub>4</sub> of *Pan troglodytes* are mineralized, but the central basin is incomplete. Among three extant hominoids studied, *Pongo* (Winkler et al., 1991) may be more advanced than *Pan* and *Homo*, although great apes have not been studied using large samples. M<sup>1</sup>/M<sub>1</sub> cusp mineralization is initiated (at least more mesial cusps), but has not yet extended to the tooth basin at birth. Replacement teeth have not commenced mineralization.

Other anthropoids studied regarding crown formation include *Alouatta caraya* (Tarrant and Swindler, 1973), *Macaca mulatta* (Swindler and McCoy, 1964) and *Papio anubis* (Swindler et al., 1968). In *A. caraya* the fetal stages were studied, but the state of mineralization of teeth in the largest specimens allows us to infer that most deciduous tooth crowns are nearly complete or complete in mineralization at birth. In the largest fetus, isolated cusps of all upper and lower permanent molars had formed. In the catarrhines, most detailed descriptions have centered on the deciduous premolars, and the crowns are described as fully formed in newborns, in terms of occlusal features at least.

The sequence of cusp mineralization has also been addressed in anthropoids. Siebert and Swindler (1991) describe the sequence of cusp mineralization in *Pan* as follows. For the

maxillary dps and  $M^1$ : paracone, protocone, metacone, then hypocone. For the mandibular dps and  $M_1$ : protoconid, metaconid, hypoconid, entoconid, and hypoconulid (if present). This sequence of mineralization corresponds to that in humans (Kraus and Jordan, 1965). Moreover, the above pattern of cusp formation for  $M_1$  applies to all extant hominoids (Oka and Kraus, 1969), *Macaca mulatta* (Swindler and McCoy, 1964), *Papio anubis* (Swindler et al., 1968) and *Theropithecus gelada* (Swindler and Beynon, 1993), suggesting the sequence may be identical across Catarrhini. Whether the sequence of cusp mineralization is similar among all anthropoids, or all primates, is unknown. In *A. caraya* it is uncertain whether the metacone or protocone of  $dp^4$  calcify first (Tarrant and Swindler, 1973). Tarrant and Swindler also observed that in *A. caraya*, the mesial cusp pair coalesces (i.e., the protocristid mineralizes) before the distal cusp pair initiates calcification. This is in contrast to other known anthropoids in which the primary cusps form prior to crests (e.g., Swindler and McCoy, 1964; Kraus and Jordan, 1965). Since we have scarce information on platyrhines, and no information on cusp morphology in strepsirrhines, common patterns and subtle variations among primates remain unclear.

In part, the present study is intended to resolve the paucity of morphological observations on the deciduous teeth of non-human primates, as noted by Daris Swindler in his book, Primate Dentition (2002). As of that date, detailed observations accompanied by pictorial accounts were only available on hominoids, some catarrhines, a single platyrhine (Swindler, 2002) and descriptions of Malagasy strepsirrhines (Tattersall and Schwartz, 1974). Unfortunately, this particular aim is only partially achieved, because the majority of our sample is of an age in which the extent of crown mineralization varies greatly. This relates to our second and more important aim: to further assess the state of crown maturation in newborn primates. In our previous work (Smith et al., 2015), we sought to definitively establish the presence of mineralized teeth using histology. Here, we expand the diversity of primates studied by using a larger sample of specimens examined with  $\mu$ -CT, thereby creating a better context for understanding the far more detailed existing knowledge base on hominoid crown formation, and a point of comparison for information on deciduous teeth of extinct primates. We directly compare the capacity of histology and  $\mu$ -CT to locate developing teeth, and establish patterns of crown maturation using the latter method. Finally, we assess the sequence of cusp mineralization using selected species and compare the trajectory of cusp mineralization at similar ages. In sum, we make a preliminary

attempt to discern differences in the pace and pattern of mineralization achieved during gestation and early postnatal age.

## Materials and Methods

### *Sample*

Specimens included a large sample of non-human primates that were previously examined to establish dental maturity (Smith et al., 2015), and more recently acquired samples. All specimens died of natural causes and were obtained as cadavers. In sum, 110 primates considered to be neonates (or newborns; for criteria, see Smith et al., 2015) and 21 fetal or older subadult specimens were studied. Throughout the text, subadult age is indicated in postnatal days (e.g., day 1 = a one-day-old), in months, or as “fetal,” based on collection records at the point of origin.

The head of each specimen was  $\mu$ -CT scanned using a viva-CT 75  $\mu$ -CT scanner at Northeast Ohio Medical University (NEOMED) using the Scanco vivaCT scanner (scan parameters: 70kVp; 114 $\mu$ A). The volumes were reconstructed using 20.5 $\mu$ m to 25  $\mu$ m cubic voxels with 8-bit grayscale values ranging from 0 to 255 (see DeLeon and Smith, 2014; Smith et al., 2014). Three-dimensional digital reconstructions from the  $\mu$ -CT volume for selected specimens were rendered using Amira® 6.1 software (Thermo Fisher). Three-dimensional surfaces for the dentition shown in this paper are freely available for download at MorphoSource ([https://www.morphosource.org/Detail/ProjectDetail>Show/project\\_id/879](https://www.morphosource.org/Detail/ProjectDetail>Show/project_id/879)).

A histological sample of selected heads from this sample was consulted to establish the identity of dental tissues (see below). The material was previously sectioned at 10  $\mu$ m and stained with Gomori trichrome and other stains (see Smith et al., 2015 for further details).

Terminology for cusp morphology used throughout the text is primarily derived from Swindler (2002; see Supplemental Document 1). In our tabulations of data, primate systematics are based on Fleagle (2013) except for Platyrrhini, which is arranged according to Rosenberger (2011).

## ***Identification of mineralized tissues using $\mu$ -CT***

The grayscale intensity of teeth in microCT scans was converted to hydroxyapatite (HA) density with a linear conversion of grayscale values. Each grayscale value was converted to an HA density using the calibration standard of HA density ( $R^2=0.99$ ). Using this regression equation ( $y = 6.9269 x - 222.8126$ ), HA density reaches 0 at approximately a gray level of 32. Based on this, we assume most of the  $\mu$ -CT voxels below this gray level in the presumptive tooth are either predentin or noise.

To assess the ability of  $\mu$ -CT to faithfully identify dentin and enamel, we compared  $\mu$ -CT slices to histology of the same specimens. Because enamel becomes fragmented during sectioning, due to a lack of fibrous matrix (Nanci, 2007), we selected specimens in which the enamel survived decalcification and subsequent serial sectioning. In these specimens, Amira 6.0 was used to align the volume of  $\mu$ -CT image data with micrographs of serial histological sections of the same specimen (see DeLeon and Smith, 2014, for further details). As a result, we were able to make paired comparisons of serial histological sections to matching  $\mu$ -CT slices (Figs. 1-2).

Based on the comparisons at matching cross-sectional levels, crown thickness (Fig. 1) and degree of mineralization (Fig. 2) are potentially limiting factors for crown segmentation. One match (Figs. 1a, b) is of a well mineralized tooth. In the  $\mu$ -CT slice, enamel and dentin are distinct in the protocone, especially near the tip, but this distinction fades near the base of the cusps (Fig. 1c), in the basins (Fig. 1d) and closer to the cervical parts of the crown; this is true even in locations where histology confirms the presence of both tissues (e.g., Fig. 1c).

Voxel size may be one limiting factor that prevents  $\mu$ -CT-based discrimination of enamel and dentin at these locations, and may also limit the ability to detect dentin alone where it is especially thin (Fig. 1d). However, since enamel in basins and nearer the crown base is deposited after cusp enamel (Swindler, 2002), it is also likely that the enamel and dentin of the basins and crown cervix have a greater overlap in range of HA density.

Generally, the least mineralized teeth in newborn primates are permanent molars. In newborn *Tarsius*,  $M^1$  is actually highly mineralized (Fig. 1), as are parts of  $M^2$ .  $M^3$  has nascent mineralization of its protocone (Fig. 2), and this tooth illustrates the capacity of  $\mu$ -CT slices to

identify teeth just entering the late bell stage.  $M^3$  at first resides beneath the orbit with little/no ossification of the surrounding tissue (Fig. 2a). The tooth still has plentiful stellate reticulum, and the paracone solely consists of dentin (Fig. 2b), although newly secreted predentin is extending further toward the basin (Fig. 2c). As a consequence, the paracone is an isolated small structure as detected in CT slices at matching levels (Fig. 2d). Gray levels between 30 and 50 capture the entirety of the mineralized dentin, although likely at an exaggerated thickness by comparison to histology (Fig. 2e); the cusp tip is captured at a narrower range of gray levels, between 39 and 50 (Fig. 2f),

### ***Correspondence between morphology as viewed in $\mu$ -CT and histology***

The two methods used in our matched cross-sectional comparison each have advantages and disadvantages. For many tissues, histology remains the gold-standard for microanatomical description, and for poorly mineralized or newly mineralizing tissue it remains the better method for discerning detail (Fig 2). However,  $\mu$ -CT is approaching the ability to resolve fine structure of skeletonized tissues (Reinholt et al., 2009; Bouxsein et al., 2010). Using our matched comparisons, we assessed the advantages and disadvantages of  $\mu$ -CT.

Both methods distort our view of dental tissues. Histological distortions depend on the methodology, but the commonly used procedure of paraffin embedding and sectioning produces both compositional alterations to tissue and physical artifacts. An example of the former is the change to enamel during decalcification, a required step for microtome sectioning. Dentin survives decalcification well because, like bone, it has a densely collagenous matrix, which stains intensely using connective tissue staining procedures (e.g., green in Gomori trichrome – Figs. 1-2). Enamel lacks a fibrous extracellular matrix and once decalcified it often shatters and flakes away during microtome sectioning, leaving the so-called “enamel space,” a gap between dentin and the outer enamel epithelium of teeth at the late bell stage (Nanci, 2007; although newly mineralized enamel survives decalcification far better). Shrinkage due to dehydration and folds or tearing are additional examples of physical alterations introduced by histology.

Imaging by  $\mu$ -CT creates less severe distortions than histology, but scan parameters can affect the capacity to detect microanatomical detail (e.g., Bouxsein et al., 2010). Optimal energy

levels used during radiographic methods such as  $\mu$ -CT vary according to age, with subadult morphology better discerned with lower energy output than for adults. However, there is a tradeoff between discerning the presence of mineralized tissues and surface detail. Figure 3 shows  $\mu$ -CT slices through the head of a neonatal marmoset (*Callithrix jacchus*) scanned at two energy levels. Matching slice levels at the level of deciduous anterior teeth (Figs. 3a, b) and  $dp^4$  (Figs 3c, d) illustrate a basic challenge of studying subadult dentition using radiological methods: teeth mature at different rates. In many anthropoids, the posterior deciduous teeth mineralize later than the deciduous incisors and canine cusp tips. Therefore, selecting a single parameter may provide optimal detail in one tooth but not another. This is not just an age-related phenomenon. Newborns of different species may vary to a similar degree in tissue level maturity of any given tooth (Smith et al., 2015).

Each energy parameter shown in Figure 3 has advantages and disadvantages. The lower energy level (45 kVp) accentuates enamel, especially at the tip (Fig. 3b), and also more clearly reveals thinner mineralized crown parts that are closer to the cervix (Fig. 3d). However, the higher energy level (70 kVp) provides a clearer apical margin of the crowns (Fig. 3a), with more distinct spaces between teeth compared to 45 kVp scan slices (Fig. 3d). Since our study focuses on crown mineralization patterns, we opted to use the higher energy level (70kVp). We acknowledge a tradeoff: we are optimizing surface detail of the cusps, while potentially losing the ability to resolve the presence of the least mineralized or thinnest dentin and enamel.

With any energy level there are some voxels, especially near the pulp chamber, that are ambiguous in their composition, i.e., whether they represent dentin. Thus, we assessed our ability to identify dentin using samples that were scanned and subsequently sectioned by doing a paired comparison of histology and  $\mu$ -CT-derived measurements of dentin thickness. Using *Tarsius*, we selected  $dp^4$  and  $M^1$ . Using *Saimiri*, we selected  $dp^4$  (in *Saimiri*, the dentin-enamel junction could not yet be well distinguished in  $M^1$ ). These teeth are all well-advanced in the late bell stage or erupted (*Tarsius*  $dp^4$ ). Enamel and dentin appeared to be distinguishable at the cusp tips and buccal marginal ridges, based on comparisons to matching histological levels (Fig. 4a,b). A specific gray level range is needed to isolate dentin during segmentation. A low range in gray levels capture the least mineralized dentin, but excludes the more mature dentin of the cusps (Fig. 4c). Expanding the gray level range to include all dentin may capture some enamel, and also

bleed irregularly onto the apical surface, presumably capturing peripheral “noise” (Fig. 4d). Thus, cusp dentin is best segmented using a range of gray levels that excludes both poorly mineralized dentin and enamel (Fig. 4e).

To compare the two methods (histology and  $\mu$ -CT), we measured buccal dentin thickness (along basoapical axis) for the buccal cusps and the marginal ridge in every histological section (amounting to every 5<sup>th</sup> 10  $\mu$ m thick section) in which the cusp was present. Next, we measured the same distance using matching  $\mu$ -CT slices. Measurements were made using ImageJ, after entering linear scale dimensions for each imaging method (histology scale: based on a stage micrometer photograph at the same magnification as the section;  $\mu$ -CT scale: based on known voxel dimension of 20  $\mu$ m). In  $\mu$ -CT slices, dentin was first captured as a range of gray levels using the threshold function in ImageJ. For each  $\mu$ -CT slice, we manually selected a gray level range that visually appeared to correspond to dentin. The lowest gray level was selected to produce a smooth dentin surface contour at the pulp cavity (irregular surfaces produce by wider ranges do not match the smooth histological contours). A peak gray level was selected to occur at the amelodentinal junction, as surmised by an abrupt change in gray level (Fig. 4). Paired t-tests reveal no significant ( $p > 0.05$ ) differences between measurements of buccal apical dentin thickness using  $\mu$ -CT slices versus histology (*Saimiri* dp<sup>4</sup>:  $t(19) = 1.49$ ;  $p = 0.15$ ; *Tarsius* dp<sup>4</sup>:  $t(16) = 1.09$ ;  $p = 0.29$ ; *Tarsius* M<sup>1</sup>:  $t(33) = 0.36$ ;  $p = 0.72$ ). The measurements are correlated at  $r = 0.83$  to 0.99. Based on plots of the paired measurements for one buccal cusp, the paracone, there appears to be no systematic bias that would suggest  $\mu$ -CT consistently under- or overestimates the thickness measured via histology (Fig. 5). The degree of discordance between the two measurement series is virtually none for *Saimiri*, and limited for *Tarsius*. The measurements follow identical curves, suggesting that divergence could be explained by error in alignment of sections to  $\mu$ -CT slices.

These results suggest that at least in regions where dentin is more mature (which tends to be in cusp regions of newborn), we may rely on thresholding to produce faithful reconstructions of the tooth crowns, with the caveat that the least mineralized portions of the tooth in our reconstructions may be somewhat exaggerated in the crown basins, and regions closer to the cervix. Interestingly, the close correspondence also suggests that dentin does not shrink

significantly, even though distortions to soft parts of the tooth germ may be quite severe, especially in less mature germs (Fig. 2).

Lastly, we assessed the reliability of two different observers (TDS and JML) to detect dentin in the same tooth (dp<sup>4</sup> of the newborn *Tarsius syrichta*). In the first trial, each observer selected a gray level range corresponding to dentin in all  $\mu$ -CT slices along the apical margin on the buccal side. This was accomplished using the threshold function of ImageJ, and the pixel range corresponding to dentin was measured in basoapical distance. Observers visually identified the dentin of the buccal cusps and intervening crest in every 4<sup>th</sup> CT-slice (total = 34 slices). Basoapical dentin height was measured from its pulp interface to its enamel interface. Results of the measurement series on identical  $\mu$ -CT slices were highly correlated (Pearson  $r = 0.97$ ).

### ***A step-wise (cusp-first) method for crown segmentation***

The immaturity of dentin and enamel at the tissue level is a final issue complicating reconstruction of subadult teeth. Histology at matched levels of  $\mu$ -CT slices indicates that the dentin and enamel surfaces (dentin facing the pulp cavity, at the dentin-enamel junction [DEJ], and apical enamel) are smooth (Figs. 1, 4). And yet, using teeth that are not fully mineralized, threshold ranges that encompass all gray levels, from the softest dentin to cusp enamel, capture surface noise (Fig. 6a, b). In erupted teeth, by contrast, all surfaces are far smoother within the threshold range. This difference may be explained by the process of enamel mineralization. In mature teeth, apical enamel is denser than that near the DEJ (He et al., 2011). However, during dental development, the enamel near the DEJ mineralizes first (Avery, 2002). As a result, most of the enamel at the apical surface is relatively less mineralized and this may lead to the tendency of some apical enamel to differentiate poorly from adjacent gray levels in terms of radio-opacity; because of this, reconstructions accomplished by segmentation using a large range of gray levels may recruit voxels from adjacent tissues or even scattered photons into the reconstructed volume (Fig. 4d).

Based on these observations, we devised a sequence of segmentation using Amira 6.1 software which minimizes the capture of adjacent voxels at the tooth surface, and thus presumably producing contours with better fidelity to the actual apical enamel surface. In this

step-wise method of segmentation, the cusp is captured first, using a relatively high range of grayscale values. This range varies by species, but in all cases the goal is to capture the cusp with smooth apical surfaces (Fig. 6a). Subsequently, the remainder of the crown is captured at descending threshold ranges, which capture increasingly more basal parts of the crown (Figs. 6b to d). Each descending range was chosen without allowing the selected voxels to “bleed” onto the apical surface and capture additional voxels presumed to be noise. Segmentation was complete when the last voxels in the cervical region or root (when present) were captured. Our reconstructions focus most on capturing the crown, and may exclude some of the deepest parts of the root since these were difficult to segment without capturing adjacent bone.

### ***Assessing maximum HA density on tooth crowns***

Once teeth were reconstructed we examined the crown to assess where hydroxyapatite densities are greatest or least. This was first assessed qualitatively in five percentile ranges: 0-25%, 25-50%, 50-75%, 75-85%, and 85-100% of maximum hydroxyapatite density. As explained above, 8-bit images allowed a range of possible grayscale values from 0 to 255. Based on our regression analysis against an HA standard, we exclude voxels below 30 as we presume them to represent unmineralized material. The total range of density for each tooth was from 30 to the peak for the individual tooth. For this total range, the gray level corresponding to the 25<sup>th</sup>, 50<sup>th</sup>, 75<sup>th</sup>, and 85<sup>th</sup> percentiles were calculated. Using Amira, these were then used to create five reconstructions of the upper and lower tooth rows in occlusal view: the portion of voxels of the tooth within 1) the 0-25% range, 2) the 0 to 50% range, 3) the 0 to 75% range, 4) the 0 to 85% range, and 5) the 0 to 100% range (i.e., all tooth voxels).

Next, the first four ranges were sequentially superimposed over the last range, beginning with the entire tooth row (all tooth voxels), represented as a 2D white profile of the tooth crown. The four superimposed layers were colored and partially transparent to create “maps” of hydroxyapatite density for the entire tooth row (e.g., Fig. 7; and see Supplemental document 2). For each species, this map shows which parts of which teeth represent the highest density of hydroxyapatite, revealing patterns of mineralization across the tooth row at birth.

Qualitatively, hydroxyapatite density of the crowns was examined using occlusal views of at least one specimen of each species under study. In addition, maximum hydroxyapatite density (MHD) was recorded for a total of 86 neonates from our overall sample, and then averaged for each of 40 species (20 haplorhines; 20 strepsirrhines). These were  $\log_{10}$  transformed for normalization and then plotted against  $\log_{10}$  transformed cranial length (prosthion-ion), used here as a proxy for body size. Previously, we found cranial length to be a good proxy for body size (Smith et al., 2015). This provides a means to test the hypothesis, based on that histological study, that small-bodied and folivorous primates have the most highly mineralized teeth at birth.

## RESULTS

### **Morphology of the dentition in newborn catarrhine monkeys**

#### *General considerations*

The crown morphology of all deciduous teeth as well as  $M^1/M_1$  are clear in these catarrhine monkeys even at birth, because crown mineralization is at an advanced state (Tables 1-3).  $Di^1/di_1$  is wider than  $di^2/di_2$ . In upper and lower jaws,  $di^2/di_2$  is caniniform to a varying extent (Swindler, 2002). Thus, there is a varied gradation of morphology from  $di^1/di_1$  to  $dc$ . A striking characteristic of the postcanine deciduous teeth is the bilophodont form, that is, there are pronounced transverse crests between mesial and distal cusp pairs, seen on  $dp^3/dp_3$  and  $dp^4/dp_4$ , and beginning to mineralize on  $M_1$ . Four primary cusps are present on deciduous premolars. But in the lower jaw, an additional cusplet may be present at the mesial end of the paracristid, a possible paraconid. This cusp, when present, is more buccally positioned than the paraconid in *Tarsius*. In addition, the paraconid is typically more mineralized than the paracristid, suggesting mineralization begins earlier. Thus, putative paraconids are included in the total count of primary cusps when present (Table 3), but more developmental work is needed to understand whether these form similarly to the other cusps. The only permanent tooth present in any of the cercopithecoids is  $M^1$ . Histological work has verified this, and neither  $M^2$  nor any replacement teeth have even progressed to the bud stage (Smith et al., 2015).

Maps of the MHD of the crowns reveal contrasts with other primates. Cusps, transverse crests, and even the marginal ridges are intense foci of hydroxyapatite density, whereas the primary cusps are more of an emphasis of MHD in other anthropoids. This suggests that perhaps aside from the sequence of primary cusp mineralization, there are subtle differences in crown mineralization patterns among primates. Further consideration of hydroxyapatite density follows morphological descriptions.

### ***Maxillary dentition***

#### **Subfamily Cercopithecinae**

*Allenopithecus nigroviridis*, newborn (Fig. 7)

$Di^1$  has a slightly rounded incisal border. The incisal margin of  $di^2$  reaches a central rounded tip and has a slight distal heel.  $Dc$  has a nearly conical cusp, slight distal and mesial marginal ridges, and a lingual cingulum. Each of the incisors has a lingual cingulum with a spike-like tubercle near its base. Much of the crowns of the anterior teeth, especially apically and near the cingulum, have at least 50% MHD. The incisal margins of the incisors and the tip of  $dc$  reach 85% MHD.

$Dp^3$  and  $dp^4$  are roughly quadrate in shape.  $Dp^3$  is more rounded, and slightly compressed in an ovoid contour on the mesial side. A trigon basin is present, as are mesial and distal fovea. Both maxillary dps also have the following features: the mesial and distal pairs of cusps are connected by transverse crests; well demarcated marginal ridges border anterior and posterior fovea; parastyles and metastyles are present. The anterior transverse crest of  $dp^3$  is raised prominently compared to that of the posterior transverse crest. Both transverse crests of  $dp^4$  resemble that of  $dp^3$ . All cusps of  $dp^3$  reach or exceed 85% of MHD.  $Dp^4$  is less mineralized than  $Dp^3$  because only a single cusp (the paracone) reaches MHD of 85%. The trigon basin of  $dp^3$  is also more highly mineralized than that of  $dp^4$ .  $M^1$  has four well mineralized cusps and transverse crests that are almost mineralized, but the trigon basin is as yet, not mineralized. The paracone and a very small portion of the protocone of  $M^1$  reach 50% MHD.

*Cercocebus atys*, newborn (Fig. 7)

$Di^1$  has a rounded incisal border; there is a slight lingual cingulum that is continuous with a vertical ridge that leads only partway toward the incisal margin. Its root is beginning to mineralize.  $Di^2$  is caniniform with a slight distal heel.  $Dc$  has a slightly compressed cusp, with distal and mesial marginal ridges. Compared to the other anterior teeth,  $dc$  is the least mineralized near the crown base. All anterior teeth have extensive portions of the crown reaching at least 50% MHD. The apical margins of the incisors and the cusp tip of  $dc$  have particularly high densities of hydroxyapatite and reach the 85<sup>th</sup> percentile of MHD.

$Dp^3$  and  $dp^4$  each have roughly quadrate well-mineralized crowns. The transverse crests are moderately raised on each, accentuating the basin and foveae. Both maxillary dps also have parastyles.  $M^1$  has four mineralized cusps and the anterior transverse crest is mineralized, but the trigon basin is not. Buccal cusps of  $dp^3$  reach or exceed the 85<sup>th</sup> percentile of MHD; the protocone reaches the 75<sup>th</sup> percentile while the hypocone is the least mineralized. The trigon basin of  $dp^3$  reaches 50% MHD.  $Dp^4$  is less mineralized than  $Dp^3$ . None of the cusps exceed the 50<sup>th</sup> percentile of MHD. The two buccal cusps and the tip of the protocone of  $M^1$  reach 50% MHD.

*Macaca mulatta*, newborn

$Di^1$  is spatulate with a rounded incisal border. Its root is beginning to mineralize.  $Di^2$  is caniniform. The cusp tip of  $dc$  tapers slightly in the lingual direction. All anterior teeth have extensive portions of the crown reaching at least 50 % MHD. The apical margins of the incisors and the cusp tip of  $dc$  reach the 85<sup>th</sup> percentile of MHD.

$Dp^3$  and  $dp^4$  each have a well-delineated basin and foveae. Buccal cusps are slightly more robust and parastyles are present. The former is somewhat trapezoidal, being longer on the buccal margin than lingually;  $dp^4$  is more quadrate. In both dps, the anterior transverse crest is more elevated than the posterior crest.  $Dp^3$  is much more mineralized than  $dp^4$ , with all cusps but the hypocone reaching the 85<sup>th</sup> percentile of MHD. The transverse crests and the parastyle also represent peaks of mineralization in  $dp^3$ . In  $dp^4$  the four primary cusps as well as the anterior marginal ridge represent the peaks in MHD, with the paracone highest at 75% MHD. Four

isolated crests of  $M^1$  are mineralized with the two mesial cusps having the highest MHD, reaching 50% at the cusp tips.

#### *Papio anubis*, neonate (Fig. 7)

$Di^1$  is wider with a rounded incisal border. Its root is beginning to mineralize.  $Di^2$  is caniniform, with the cusp leading to mesial and distal ridges, and has a small shelf-like lingual swelling.  $Dc$  is poorly mineralized at the crown base; the cusp is buccolingually compressed. On all anterior teeth the apical margins reach the 85<sup>th</sup> percentile of MHD.  $Di^1$  is the best mineralized overall, with most of the crown at > 50% MHD.

$Dp^3$  and  $dp^4$  each have transverse crests to delineate a trigon basin and mesial/distal foveae. Buccal cusps are slightly more robust and small parastyles are present. Both teeth are elongated mesiodistally and quadrate in shape. Four crests of  $M^1$  are mineralized, with the proximal two already connected by a transverse crest.  $Dp^3$  is much more mineralized than  $dp^4$ , with all cusps (with the exception of the hypocone) reaching at least the 75<sup>th</sup> percentile of MHD and the paracone reaching 85% MHD. The mesial transverse crest and the parastyle also have high levels of mineralization in  $dp^3$  relative to adjacent areas of the crown. In  $dp^4$  the four primary cusps represent the peaks in MHD, with them all reaching 50% MHD. Similarly, in  $M^1$  all four cusp tips reach 50% MHD.

### Subfamily Colobinae

#### *Colobus guereza*, neonate

A single newborn is described based on a skeletonized hemisected head.

$Di^1$  has a straight incisal margin adorned with three mamelons. There is a low vertical lingual pillar with furrows on either side. These meet a lingual heel near the base of the crown. The mesial and distal margins are slightly raised lingually, but they are not distinct ridges.  $Di^2$  comes to a caniniform apex, which tapers to rounded incisal margins.  $Dc$  is a partially mineralized crown, pyramidal in form, with a stout lingual pillar. The crown base appears mostly unmineralized.

$Dp^3$  and  $dp^4$  each have a large central basin, with smaller fovea mesial and distal to transverse ridges. The mesial fovea of  $dp^3$  is a triangular projection, while it has a rounded mesial margin in  $dp^4$ . The transverse crests are higher in  $dp^4$  than  $dp^3$ .  $Dp^4$  is less mineralized than  $dp^3$ , with a thin central basin, and a poorly mineralized posterior margin. Three cusps of  $M^1$  are mineralized; the hypocone remains unmineralized.

#### *Trachypithecus francoisi*, neonate (Fig. 7)

$Di^1$  has a rounded incisal margin.  $Di^2$  has a more triangular, almost caniniform shape, except for the concave lingual fossa.  $Dc$  has pronounced mesial and distal marginal ridges tapering from the cusp, and a more rounded lingual surface compared to the incisors.

$Dp^3$  and  $dp^4$  are both quadrate in shape. The anterior transverse crest of  $dp^3$  is raised compared to that of the posterior transverse crest, and compared to either transverse crest of  $dp^4$ . There are weakly pronounced parastyles on each  $dp$  (parastyles and metastyles were described as absent in colobines by Swindler, 2002). A trigon basin is present, as are mesial and distal fovea, separated from the latter by transverse crests.  $M^1$  has four well mineralized cusps; but the trigon basin is as yet, unmineralized. Transverse crests also remain barely mineralized and the marginal crests have not, as yet, started to mineralize.  $M^2$  is not mineralized (and has not progressed to even the bud stage - Smith et al., 2015).

### ***Mandibular dentition***

#### **Subfamily Cercopithecinae**

##### *Allenopithecus nigroviridis*, neonate (Fig. 8)

$Di_1$  is tall and narrow. By comparison,  $di_2$  is relatively lower, more rounded on the labial side, and the incisal margin reaches a pointed apex.  $Dc$  is broad at the base and slightly rounded on its lingual surface. Distal to the cusp there is a slight depression and then a raised heel with a small tubercle. The bulk of the crown is less erupted than adjacent teeth, save for the cusp tip. The cusp tips of all anterior teeth reach or exceed 85% MHD.

$Dp_3$  is compressed and ovoid in shape;  $dp_4$  is nearly quadrate. Each has four primary cusps and a mesial marginal ridge that at least partly outlines the trigonid basin. In  $dp_3$ , the ridge is low on the lingual side, so that the basin is open adjacent to the metaconid.  $Dp_4$  has much more prominent cusps than  $dp_3$ ; the marginal ridge is raised on both lingual and buccal sides. In both deciduous premolars, the paracristid leads to a small cusp, a putative paraconid.  $Dp_3$  has higher hydroxyapatite densities at each of the cusps as compared to  $dp_4$ . Three cusps of  $dp_3$  (protoconid, hypoconid, and, to the least extent, the metaconid) are at or beyond the 85th percentile of MHD. The protoconid is the most mineralized of the four cusps in  $dp_4$  (a small portion of the tip exceeds 85% MHD), and the hypoconid is the least mineralized. The small tubercle on the mesial marginal ridge is similar in MHD to the ridge as a whole.  $M_1$  has four prominent cusps, with a possible fifth cusp mesially. None of these cusps exceed 50% MHD, and the hypoconid is least mineralized.  $M_2$  is not observed.

No replacement teeth are mineralized.

#### *Cercocebus atys*, newborn (Fig. 8)

$Di_1$  is spatulate with a straight incisive margin. By comparison,  $di_2$  has a longer incisive margin, coming to a pointed apex leading to a slightly sloping mesial margin and a deeply sloping distal margin. The dc is rounded on its lingual side, rather than slightly concave like the deciduous incisors. Yet it still has mesial and distal marginal ridges, reminiscent of an incisal ridge. The marginal ridges or cusp tips of all anterior teeth reach or exceed 85% MHD.

$Dp_3$  is mesiodistally elongated. The mesial side is narrow compared to the wider and flatter distal end. The tooth is rotated obliquely compared to  $dp_4$ , such that the mesial side of  $dp_3$  nearly faces in a buccal direction. This is true of all of the cercopithecines but especially so in this *C. atys* specimen.  $Dp_4$  has a wider mesial end. Both deciduous premolars have a raised paracristid arcing around a mesial fovea and in  $dp_4$  this leads to a small cusplet resembling a paraconid. Transverse crests are pronounced in  $dp_4$ , but not  $dp_3$ .  $Dp_3$  is better mineralized than  $dp_4$ , with the mesial cusp pairs reaching the 85<sup>th</sup> percentile of MHD and the distal pair reaching 75% MHD. In  $dp_4$ , all cusps reach the 50th percentile of MHD; the paracristid represents a peak in MHD relative to the adjacent basin.  $M_1$  has four mineralized cusps. They are isolated although

the mesial pair has nearly come in contact along a transverse crest. All cusps of  $M_1$  except the entoconid reach the 50th percentile of MHD.

*Macaca mulatta*, newborn

Both deciduous incisors are spatulate with broad incisal margins.  $Di_1$  has a mostly flattened apex with three small mamelons. In  $di_2$  the incisal margin slopes downward from a central peak to a distal heel. The dc is incompletely mineralized but a pointed distolingual heel is beginning to form. All anterior teeth reach the 85<sup>th</sup> percentile of MHD along the incisal margins, or in dc, at the cusp tip and along ridges departing the mesial and distal sides of the cusp.

$Dp_3$  is mesiodistally elongated with four prominent primary cusps and a raised paracristid. The mesial fovea is narrow compared to the distal fovea, but not as buccolingually compressed as in *C. atys*. There is a small cusplet at the end of the paracristid, toward the lingual side of the mesial fovea. The distal fovea is small.  $Dp_4$  has all of the same characteristics as  $dp_3$  except the mesial end and the fovea within it are broader and roughly equal in breadth to the central (talonid) region. Transverse crests are equally pronounced in both deciduous molars.  $Dp_3$  is better mineralized than  $dp_4$ , with the mesial cusp pairs and the hypoconid reaching the 85<sup>th</sup> percentile of MHD and the entoconid reaching 75% MHD. The mesial and distal foveae are more mineralized than the talonid basin. In  $dp_4$ , all cusps and the paracristid reach the 50th percentile of MHD.  $M_1$  has four isolated mineralized cusps. The protoconid of  $M_1$  is the only cusp to reach the 50th percentile of MHD, whereas the entoconid reaches < 25% MHD.

*Papio anubis*, neonate (Fig. 8)

The deciduous anterior teeth are all very well-rounded buccally, and the incisors have a more exaggerated lingual convexity than the other cercopithecine specimens we examined. The incisal margin of  $di_2$  comes to a slight caniniform peak, and the cusp of dc leads to sharp mesial and distal marginal ridges. All three deciduous anterior teeth reach the 85<sup>th</sup> percentile of MHD, the dc only at the cusp tip.

Both deciduous premolars are mesiodistally elongated. Each has a large mesial fovea, mesiodistally elongate in  $dp_3$  and rounded in  $dp_4$ . The talonid basin is bounded by transverse crests, and is open buccally and lingually via grooves between mesial and distal cusp pairs; the basin is larger in  $dp_4$ . The distal fovea is small in both premolars. Each deciduous premolar has four primary cusps and a rounded swelling at the mesial end, positioned slightly to the buccal side of the raised “paraconid shelf”.  $Dp_4$  has a small cusplet distal to the metaconid, near the groove between the lingual primary cusps.  $Dp_3$  is better mineralized than  $dp_4$ , with the protoconid reaching the 85<sup>th</sup> percentile of MHD, the metaconid and the hypoconid reaching 75% MHD, and the entoconid reaching 50% MHD. The mesial fovea is more mineralized than the talonid basin or distal fovea.  $M_1$  has four isolated cusps with the mesial pair almost connected by the mineralizing transverse crest. In  $dp_4$  and  $M_1$ , all cusps reach the 50th percentile of MHD.

### **Subfamily Colobinae**

*Colobus guereza*, neonate

$Di_1$  has straight incisal margin that inclines distally downward; centrally there is a slight notch that is continuous with an incisive fossa. By comparison, the incisal margin of  $di_2$  reaches a rounded central peak and there is a more rounded lingual surface and a distal, lingual heel. The  $dc$  has a mesial marginal ridge next to a slight lingual fossa. The cusp leads to a more rounded distal margin that leads in a straight line to the base of the mineralized crown. In  $di_1$  and  $dc$ , this line of maximum hydroxyapatite density reaches 75%.  $Di_2$  reaches a MHD of 85% near the rounded apex of the incisal margin.

In occlusal view,  $dp_3$  has a squared profile distally, but mesially the anterior marginal ridge comes to a triangular apex. The trigonid basin is thus quite elongated.  $Dp_4$  is more closely quadrate, with higher cusps than  $dp_3$ ; the trigonid basin is smaller than in  $dp_3$ , and the talonid basin is deep.  $Dp_3$  has a MHD reaching 75%, at the protoconid and metaconid. In  $dp_4$  all four cusps reach a MHD of 50%. Three cusps of  $M_1$  are mineralized with the protoconid reaching a MHD of 50%. The entoconid remains unmineralized.

No replacement teeth are mineralized.

### *Trachypithecus francoisi*, neonate (Fig. 8)

In  $di_1$ , the incisal margin is straight with a central depression. On both  $di_2$  and  $dc$  the incisal margin reaches a central peak.  $Di_2$  has a lingual longitudinal ridge. Anterior teeth lack prominent anterior and posterior marginal ridges.

The trigonid basin of  $dp_3$  is more elongated than in  $dp_4$ . In the latter, the trigonid basin has a more pronounced ridge on the lingual side. From  $dp_3$  to  $M_1$ , teeth become increasingly quadrate in the occlusal view.  $M_1$  is present with four cusps and a mineralized crest between the mesial cusp pair. The tooth basin remains unmineralized.

## **Morphology of the dentition in newborn platyrhine monkeys**

### ***General considerations***

There is arguably more ontogenetic dental variation among New world monkeys than among Old World monkeys. There is also much variation in the status of crown maturation in newborn platyrhines (Tables 1-3). Callitrichines have the least mineralized postcanine teeth at birth (especially  $dp^4/dp_4$  crowns), implying altricial mineralization. *Alouatta*, *Aotus* and many other platyrhines are far more advanced in cusp mineralization at birth.

### ***Maxillary dentition***

#### **Family Atelidae**

##### *Alouatta seniculus*, neonate (Fig. 9)

$Di^1$  has a rounded incisal margin.  $Di^2$ , though buccolingually compressed like  $di^1$ , possesses a caniniform cusp.  $Dc$  is very broad and flattened buccolingually near the cusp tip. Nearer the base it is broad and possesses a pronounced lingual cingulum. The tooth lacks the

vertical lingual ridge described in *A. palliata* (Swindler, 2002). Dc is less erupted and displaced buccally relative to  $dp^2$ . The apices of  $di^1$  and dc are the most mineralized parts of the anterior teeth, reaching the 85th percentile of hydroxyapatite density (of MHD for all teeth).  $Di^2$  reaches 75% MHD.

$Dp^2$  and  $dp^3$  are each broad with pronounced paracones. Each has a pronounced lingual cingulum with two or more small cusps; on each, one is positionally consistent with a small protocone. Swindler noted two cusps on  $dp^3$  of *A. palliata*.  $Dp^4$  has a quadrate shape and four cusps. A distinct but low crista obliqua is present, which intersects the lingual side distal to the protocone, and traverses to the base of the metacone. Three styles are present on the buccal side of  $dp^4$  (para-, meso-, and metastyles), whereas only the parastyle is evident on  $dp^3$ . These cusplets may be common on the deciduous premolars of *Alouatta* (see also Swindler, 2002). The most mineralized cusp of each upper dp is the paracone, reaching or exceeding 85% MHD. The presumptive protocone of  $dp^2$  and  $dp^3$  reaches a MHD of 50%. On  $dp^4$ , the protocone and hypocone reach 75%; the hypocone is least mineralized, reaching 50% MHD. The basins of all dps are mineralized at 25 to 50% of MHD. Tarrant and Swindler (1973) noted that the styles of dps do not derive from their own calcification centers. Consistent with this observation, none of the styles observed here are notable “peaks” in hydroxyapatite density, distinguishing them from the ridge along which the styles form.  $M^1$  has three isolated mineralized cusps, reaching 50% MHD, for both the paracone and metacone.  $M^2$  is not present or mineralized (also see Smith et al., 2015).

Histological observations reveal that the permanent incisors are at the cap or bud stage, and other replacement teeth are not even that advanced at birth (Smith et al., 2015).

## Family Cebidae

*Callithrix jacchus* and *C. penicillata*, neonate

Morphologically, deciduous teeth of the two *Callithrix* spp. are similar.  $Di^1$  has a rounded apex.  $Di^2$  is caniniform with a distally curving cusp, and a distolingual heel (in specimens in which the crown base is mineralized). Dc is similar in form to  $di^2$ , but with a broader base; the base of dc may be deficient compared to the incisors.  $Di^1$  is mostly mineralized at 50% MHD or higher, and the incisal margin reaches 85% MHD. In *C. jacchus*,  $di^2$  reaches 75% MHD at the

cusp tip, and 50% along mesial and distal margins and at the lingual heel. Additionally, the MHD of dc is highly localized near the cusp, with the tip at 85% MHD or higher. In *C. penicillata*, all anterior teeth reach or exceed the 85<sup>th</sup> percentile of MHD at the cusp apex.

$Dp^2$  is nearly triangular in profile (occlusal view) with a highly projecting paracone, and distinct mesial and distal ridges.  $Dp^3$  also has a small protocone and a parastyle is visible in some but may not be mineralized in others. Hershkovitz (1977) also noted stylar cusps on older infants.  $Dp^4$  has three cusps, with the paracone the most pronounced, and a sharp ridge connecting the two buccal cusps. The trigon basin is poorly mineralized as is the distal marginal ridge. The parastyle is present (and a mesostyle in *C. penicillata*) but other stylar cusps are as yet unmineralized in *C. jacchus*. However, a mesostyle is visible in *C. penicillata*. It is distinctly more molariform than  $dp^3$  and  $dp^2$ .  $Dp^2$  reaches a MHD of 50% at the cusp.  $Dp^3$  reaches a MHD of 75% at the paracone. The paracone of  $dp^4$  reaches a MHD of 75 percent. In all deciduous premolars, much of the crown base is at < 25% MHD.  $M^1$  is not mineralized.

No replacement teeth are mineralized in newborns.

#### *Cebuella pygmaea*, neonate (Fig. 9)

*Cebuella* has the most advanced mineralization of deciduous teeth at birth compared to other callitrichines.  $Di^1$  has a rounded incisal margin and can commence root formation.  $Di^2$  is rotated lingually compared to  $di^1$  and caniniform. Dc is broad-based with a high, backwardly-tilting cusp. In two specimens examined regarding hydroxyapatite density, dc reached the 85<sup>th</sup> percentile of MHD. The cusps of  $di^1$  and  $di^2$  reach a hydroxyapatite density at the 50th to 85<sup>th</sup> percentiles of MHD; in one specimen  $di^1$  exceeds the MHD of  $di^2$ , and the reverse is true of the other specimen. The anterior teeth reach higher levels of MHD than the postcanine teeth.

$Dp^2$  resembles dc, except with pronounced cingula.  $Dp^3$  possesses two cusps and in at least one subadult, a weakly developed parastyle.  $Dp^4$  is triangular with three cusps. The trigon basin may be incompletely mineralized in  $dp^4$ , but in some newborns it appears to be nearly complete with poorly mineralized matrix. Two specimens have para- and mesostyles on  $dp^4$  (in other cases the buccal cingula is not mineralized enough to locate them). On an older infant, a weakly pronounced metastyle is also observed. Older subadults also possess pronounced lingual

cingula on  $dp^4$ , which is not yet mineralized in the newborns. Both  $dp^2$  and  $dp^3$  reach 75% MHD. In the one perinatal specimen examined for hydroxyapatite density, the paracone of  $dp^4$  also reaches the 75th percentile of MHD, but in the other the paracone only reaches the 50<sup>th</sup> percentile. The paracone of  $M^1$  is mineralized in two neonates (day 0, day 5), but is not detected in a third specimen of similar size (but unrecorded specific age). Previously, mineralization of  $M^1$  was detected in a day 0 newborn using histology (Smith et al., 2015). In a specimen possessing a mineralized paracone of  $M^1$ , the tip reaches the 25<sup>th</sup> percentile of MHD.

In the day 0 and day 5 neonates, no replacement teeth are mineralized. In an older infant (estimated at 1 month of age) the apical part of  $I^1$  and  $C$  are mineralized.

#### *Leontopithecus rosalia*, juvenile

The deciduous teeth of this species were briefly described and figured by Hershkovitz (1977, Fig. V.28). Deciduous incisors resemble those of other callitrichines (rounded  $di^1$  apex, caniniform  $di^2$ ).  $Dc$  is pictured as robust and having a vertical lingual ridge.  $Dc$  and deciduous premolars are indicated to possess parastyles and distostyles/metastyles. Hershkovitz (1977) wrote that the molarization of deciduous premolars was “more extensive” in *Leontopithecus* compared to the same teeth in other callitrichines. Smith et al. (2011) measured the dental follicle volume of maxillary postcanine teeth and found *Leontopithecus* has large deciduous premolars, significantly larger compared to *Callithrix*. In contrast,  $M^1$  is poorly mineralized in *Leontopithecus* newborns – some fail to exceed the early bell stage of development (Smith et al., 2011, 2015).

#### *Saguinus* spp.

$Di^1$  and  $di^2$  are both buccolingually compressed.  $Di^1$  has a rounded incisal ridge while  $di^2$  is caniniform with a parastyle; in one *S. geoffroyi* neonate a small distostyle is apparent.  $Dc$  is a nearly conical cusp except for a slightly flattened lingual surface, and lacks any cingula at birth. In a day 27 *S. oedipus* infant, para- and distostyles are present, as described in Hershkovitz (1977). In both *S. midas* and *S. oedipus*, the anterior teeth are of greater overall mineral density

compared to postcanine teeth (the latter having more poorly mineralized crown bases, by comparison).  $Di^1$  and  $di^2$  reach 75% of MHD at the incisal margin in newborn *S. geoffroyi*, and reach the 85<sup>th</sup> percentile in the other two species.  $Dc$  reaches or exceeds the 85<sup>th</sup> percentile of MHD in all three species.

$Dp^2$  and  $dp^3$  have broad cusps with incomplete mineralization of the base. Parastyles are typically beginning to mineralize at birth, but the lingual cingulum and the protocone of  $dp^3$  may or may not be mineralized, as yet. In one *S. geoffroyi* neonate, para- and distostyles are present on  $dp^2$  and  $dp^3$ , and the protocone of  $dp^3$  has begun to mineralize. The day 27 *S. oedipus* has a lingual heel on  $dp^2$ ;  $dp^3$  has a fully mineralized crown with a protocone, a parastyle, and a distostyle. At birth,  $dp^4$  has three mineralized cusps and a parastyle. The basin is poorly mineralized. At best, the mesial margin and a portion of the trigon basin of the same side are mineralized. The buccal cusps are connected by a low, sharp crest. The crown of  $dp^4$  is nearly completely mineralized at P27 in *S. oedipus*, except for the lingual cingulum (shown by Hershkovitz, 1977 in this species). No metastyle is apparent. All deciduous premolars have more poorly mineralized crown compared to anterior teeth.  $Dp^2$  and  $dp^3$  reach a MHD of 75 to 85% at the paracone in *S. geoffroyi* and *S. oedipus*, while  $dp^4$  reaches the 50<sup>th</sup> percentile of MHD at the two buccal cusps.  $M^1$  is typically unmineralized at birth;  $M^1$  paracone and protocone tips are mineralized in P27 *S. oedipus*. In *S. midas* all three of these teeth have a lesser MHD, perhaps reflecting their less mineralized state overall in the specimen studied.

Absence of replacement teeth at birth was histologically confirmed by Smith et al. (2015). The P27 *S. oedipus* has a mineralized  $I^1$ .

#### *Saimiri boliviensis*, neonate

$Di^1$  has a rounded incisal margin.  $Di^2$  is similar but the margin slopes distally, making the cusp taller and more rounded mesially. Both incisors have mesial crests.  $Dc$  is broad with a distally curved cusp, sharp mesial and distal ridges, and a flattened lingual surface. The crown base of the  $Dc$  is only partially mineralized.

Features of the dps resemble the illustration (Fig. V.28) provided by Hershkovitz (1977) for *S. sciureus*.  $Dp^2$  has a large paracone and a smaller protocone; projecting para- and

distostyles give it a triangular appearance in occlusal profile. With a more expanded cingulum,  $dp^3$  and  $dp^4$  all have a more quadrate appearance.  $Dp^3$  has two primary cusps (paracone, protocone), para- and distostyles, and a metaconule.  $Dp^4$  has four cusps, the paracone, protocone, metacone, and hypocone; para- and metastyles are also present. A crista obliqua is pronounced, traversing to the base of the metacone. The distolingual side of the deciduous premolars appears least mineralized, with the lingual cingulum of  $dp^3$  and  $dp^4$  incompletely mineralized in all newborns. In the newborn with the most mineralized deciduous premolars,  $dp^4$  has a hypocone as well as a small cusplet lingual to the protocone. However, overall the crown base is far better mineralized than in callitrichines. Smith et al. (2011) demonstrated that the posterior-most deciduous premolars, especially  $dp^4$ , are large in *Saimiri* relative to their facial size. This may partially explain the absence of a maxillary sinus in the genus. The paracone and protocone of  $M^1$  are mineralized.

#### *Cebus apella* (older infant, day 9)

No perinatal material of *Cebus* spp. were available for description, but the morphology of the deciduous dentition described here is based on an older infant.  $Di^1$  is broad with a lingual fossa and a slight lingual heel; the mesial margin is slightly raised as a ridge.  $Di^2$  is similar but smaller. Both incisors have nearly flat incisal margins and partially formed roots.  $Dc$  has a tall pointed cusp with a slight distal marginal ridge and a shallow lingual concavity. The distolingual part of the crown appears incomplete and the root is unmineralized.

$Dp^2$  has a pronounced paracone and a smaller but distinct protocone. Raised mesial and distal ridges help to define a shallow basin. On  $dp^3$ , the paracone and protocone are more close to equally sized, with the former being slightly larger. The basin is more expansive mesiodistally and there is a slight hypocone and indistinct metacone. Both  $dp^2$  and  $dp^4$  have small para- and distostyles.  $Dp^4$  is the largest deciduous premolar and is almost quadrate, with four cusps. A distinct crista obliqua is present, intersecting the metacone.

## Family Pitheciidae

*Pithecia pithecia*, neonate (Fig. 9)

$Di^1$  and  $di^2$  are broad at the crown apex, with roots beginning to mineralize.  $Di^1$  is far wider than  $di^2$  with a rounded incisal margin.  $Di^2$  has a pointed apex at the center of the incisal margin. The  $dc$  is conical except for a vertical ridge on the distolingual border; the base of the crown remains poorly mineralized at birth. All anterior teeth reach or exceed the 85th percentile of MHD,  $di^1$  at isolated points along the incisive margin,  $di^2$  at the central apex, and  $dc$  at the very tip of the cusp.

$Dp^2$  has an oval profile, elongated buccolingually, with a raised paracone bordered by mesial and distal ridges that lead to distinct para- and distostyles. Lingually is a diminutive protocone.  $Dp^3$  and especially  $dp^4$  are more quadrate in form.  $Dp^3$  has less distinct para- and distostyles than the other two premolars. A small tubercle on the postcingulum resembles the postprotostyle described on replacement premolars in *Pithecia* (Swindler, 2002). In  $dp^4$  the same features are present except a distinct metacone is seen, and a more prominent cusp is seen on the postcingulum, constituting a hypocone in our view. A crista obliqua is distinct near the base of the metacone and transects the common border of the trigon and talon basins, before diminishing to a low ridge near the protocone. Small para- and metastyles are visible. In all deciduous premolars, the paracone is the densest part of the crown, reaching or exceeding 85% MHD. In  $dp^3$  and  $dp^4$ , other cusps reach 50% MHD. The trigon basin of  $dp^3$  also reaches 50% MHD.  $M^1$  has four well-mineralized cusps and a trigon basin that has commenced mineralization and the talon is unmineralized. The paracone reaches 50% MHD, the protocone and metacone reach 25% MHD, while the hypocone and the periphery of the trigon basin are mineralized at <25% MHD.

The cusp tip of  $I^1$  has commenced mineralization.

*Callicebus cupreus*, neonate

$Di^1$  and  $di^2$  each have rounded incisal margins.  $Dc$  is broad with distinct mesial and distal marginal ridges.  $Di^1$  and  $di^2$  reach at least the 75<sup>th</sup> percentile of MHD along the incisal margin.  $Dc$  reaches or exceeds a MHD of 85%.

$Dp^2$  and  $dp^3$  both have a rounded shape in occlusal view with crests encircling the diameter. Each has a pronounced paracone; the lingual margin is raised with a small cusplets on  $dp^2$  and a protocone on  $dp^3$ .  $Dp^4$  is quadrate with three primary cusps; there is a widely flaring

distolingual cingulum, but no distinct hypocone. Transverse crests extend lingually from the paracone and metacone, dividing the occlusal surface into three fossae. The deciduous premolars all reach or exceed a MHD of 85% at the paracone.  $M^1$  is present and has four cusps mineralized, including just the tip of the hypocone. The basin of  $M^1$  has not yet mineralized.  $M^1$  reaches a MHD of 50% at the paracone, and reaches the 25<sup>th</sup> percentile at the protocone and metacone.

$I^1$  is located distolingual to  $di^1$ . Only the incisal margin is mineralized, reaching a MHD of 25% at a pointed apex.

#### *Aotus nancymaae*, neonate (Fig. 9)

$Di^1$  is apically broad with a slightly rounded incisal margin.  $Di^2$  is smaller than  $di^1$ , and has one small cusp in the center of an otherwise rounded incisal margin.  $Dc$  has a conical cusp; the crown base is as yet poorly mineralized but appears to have a parastyle.  $Di^1$  and  $dc$  each reach MHD at the 85<sup>th</sup> percentile or greater, while  $di^2$  varied in the two specimens examined for MHD (reaching the 50<sup>th</sup> percentile in one and exceeding the 85<sup>th</sup> percentile in a second specimen).

$Dp^2$  and  $dp^3$  are both broad with a prominent paracone, and smaller protocone; each has a deep basin between the cusps.  $Dp^4$  is quadrate with four primary cusps and a sharp crista obliqua demarcating the trigon basin. In one specimen the lingual cingulum is better developed, with a protostyle in addition to the hypocone. All deciduous premolars reach or exceed a MHD of 85% at the paracone.  $M^1$  is present with three primary cusps, but the basin of the tooth is not yet mineralized. This tooth reaches the 50<sup>th</sup> percentile of MHD.

No replacement teeth are mineralized at birth.

#### ***Mandibular dentition***

#### **Family Cebidae**

##### *Alouatta seniculus*, neonate (Fig. 10)

The incisal margin of  $di_1$  is nearly straight whereas it comes to a rounded tip in  $di_2$ , similar to *Alouatta palliata* (Swindler, 2002).  $Dc$  is broad-based; the crown is less erupted than

the incisors and only partially mineralized.  $Di_2$  and  $dc$  reach 85% (of peak density for all teeth; MHD), whereas  $di_1$  only reaches 75% MHD.

$Dp_2$  is nearly oval in occlusal profile, while  $dp_3$  and  $dp_4$  have a more quadrate shape.  $Dp_2$  has one cusp connected to a raised longitudinal ridge (the protocristid), which descends toward the lingual margin where a small tubercle might be regarded as a rudimentary metaconid. On either side of the protocristid, mesial and distal marginal ridges create distinct foveae. In *Alouatta palliatta*,  $dp_2$  is described as caniniform compared to the other dps (Swindler, 2002). In  $dp_3$  and  $dp_4$ , four cusps are present.  $Dp_4$  has more pronounced cusps compared to  $dp_3$ . The trigonid basin is larger than the talonid basin in  $dp_3$ , while this is reversed in  $dp_4$  (described similarly in *A. palliatta*). Swindler describes  $dp_3$  of *A. palliata* as relatively simple, in that it is bicuspid and lacks the cristid obliquid. In *A. seniculus*,  $dp_3$  and  $dp_4$  both have a cristid obliquid that connects to the protocristid near the protoconid. The mesial marginal ridge of  $dp_4$  ends in a small cusplet near the lingual border, followed by a slight depression. On the distal marginal ridge of  $dp_4$  there is a very small elevation that could be considered a rudimentary hypoconulid, which is rarely present in *Alouatta* according to Swindler (2002). The single prominent cusp in both  $dp_2$  and  $dp_3$  reaches 85% MHD, whereas  $dp_4$  has portions of two cusps that reach 85% MHD (metaconid and protoconid). Along the distal marginal ridge, the small cusplet (rudimentary hypoconulid?) corresponds to a small elevated MHD along this border.  $M_1$  has three mineralized cusps, each more prominent than in  $dp_4$ .  $M_2$  is not mineralized or present. The metaconid and protoconid cusps of  $M_1$  are the most mineralized, reaching 50% MHD.

No replacement teeth are mineralized at birth.

#### *Callithrix jacchus* and *Callithrix penicillata*, neonate

In both *Callithrix* spp., the anterior teeth are all buccolingually compressed; in this sense both dis are incisiform.  $Di_1$  has a rounded incisal margin that may reach a central point. Most have a broad cusp with an incisal ridge that comes to a point in the center.  $Di_2$  is narrower, though still buccolingually flattened, with a small distolingual heel.  $Dc$  also has a somewhat flattened apical cusp, with a sharper cusp tip, and a distolingual heel. Marginal ridges are not prominent in the anterior teeth. All anterior teeth reach or exceed a hydroxyapatite density of

85% MHD. The peak for  $di_1$  is more localized to the pointed center of the incisal ridge compared to  $di_2$ .

$Dp_2$  and  $dp_3$  each have a highly projecting protoconid that is connected to mesial and distal marginal ridges. Hershkovitz (1977) indicated distinct distolingual heels for  $dp_2$  and  $dp_3$ ; these are nearly mineralized in one of the two neonates examined here, and are only partially mineralized in another.  $Dp_4$  has four primary cusps and distinct basins. The trigonid basin is accentuated with a raised ridge along most of the perimeter; the talonid basin is completely or mostly mineralized at birth. It is distinctly more molariform than  $dp_3$  and  $dp_2$ . *C. jacchus* neonate.  $Dp_2$  and  $dp_3$  both reach a MHD of 75% at the cusp apex.  $Dp_4$  is less mineralized with a MHD of 50% in two of three specimens examined. Only the protoconid of  $M_1$  is mineralized in most neonates; the metaconid tip is also mineralized in one. The protoconid of  $M_1$  is at less than 25% of MHD in one specimen, but exceeds 25% MHD in two others.

No replacement teeth are mineralized at birth.

#### *Cebuella pygmaea*, neonate (Fig. 10)

$Di_1$  has a broad flattened cusp with a rounded incisal margin.  $Di_2$  is caniniform with a slightly curved cusp and, like the  $dc$ , possesses a distostyle.  $Dc$  has the same form but is more robust. It is a slight mesial swelling near the cusp base, but this is not a distinct projection (i.e., parastyle). Anterior teeth are more mineralized than the postcanine teeth. Both  $di_2$  and  $dc$  reach or exceed 85% of MHD at the cusp tip.  $Di_1$  reaches 75 to 85% MHD in the two newborns examined.

$Dp_2$  and  $dp_3$  are both mesiodistally narrow with a high protoconid.  $Dp_2$  resembles  $dc$  closely, but has a parastyle and a more projecting distostyle.  $Dp_3$  has a small metaconid.  $Dp_4$  is buccolingually broad with three to four prominent cusps mineralized at birth, and a cristid obliquid contacting the protocristid just buccal to the base of the protoconid. In one of the neonates the entoconid is as yet unmineralized. Mesially there is a pronounced paracristid that ends with a cusplet positionally consistent with a paraconid.  $Dp_2$  is the most mineralized, reaching or exceeding 85% MHD. The protoconid of  $dp_3$  and  $dp_4$  reaches 75% MHD.  $M_1$  is

mineralized at the mesial cusp pair and a small rim of the mesial margin. Anterior teeth have a more mineralized protoconid than the postcanine teeth.

$I_1$  and  $I_2$  have barely initiated mineralization (at < 25% MHD), at the cusp tips alone, in a day 5 newborn.

#### *Leontopithecus rosalia*, juvenile

The deciduous mandibular teeth of this species were briefly described and figured by Hershkovitz (1977, Fig. V.28). Deciduous incisors resemble those of other callitrichines.  $Dc$  is pictured as robust with a large distostyle/hypoconulid. Hershkovitz noted the conulids of  $dps$  were well developed in the single juvenile *Leontopithecus* he examined.

#### *Saguinus* spp., neonate

$Di_1$  and  $di_2$  each have three small swellings along the incisal margin, with  $di_1$  being more spatulate, and  $di_2$  have a sloping distal margin and a distostyle. Hershkovitz (1977) illustrated the same features in subadult *S. oedipus*, identifying the central cusp as protoconid, bracketed by the para- and distostyloid.  $Dc$  is conical and as yet lacks any features of the crown base. A lingual cingulum, shown in  $dc$  of *S. oedipus* by Hershkovitz (1977) is not yet mineralized. The anterior tooth crowns are more fully formed than the postcanine teeth (especially the incisors, and reach the 75<sup>th</sup> to 85<sup>th</sup> percentile of MHD ( $dc$ , reaching the higher level).

$Dp_2$  has one primary cusp.  $Dp_3$  has one to two primary cusps (protoconid, metaconid), a paracristid, and a protocristid, but it is incomplete lingually and distally. In an older (P30) *S. oedipus* infant there are two primary cusps, as indicated by Hershkovitz (1977). In a weanling *S. oedipus*, the protocristid is especially raised and divides two basins; a small hypoconid is present. Thus the degree of molarization of  $dp_3$  may vary.  $Dp_4$  has a cusplet at the end of the paracristid, in addition to the protoconid, metaconid and hypoconid. An entoconid is as yet unmineralized; it is present but minuscule in the P30 infant. The trigonid basin is completely or nearly mineralized, but the talonid basin is unmineralized as birth.  $Dp_4$  also has a cristid obliquid in a variable state of mineralization. In some newborns it is completely mineralized and intersects the protocristid buccal to the base of the protocone. The talonid basin is partially

mineralized in one newborn. In *S. midas* and *S. oedipus*,  $dp_2$  reaches the 75<sup>th</sup> percentile of MHD, whereas  $dp_3$  and  $dp_4$  only reach the 50<sup>th</sup> percentile. In *S. geoffroyi*,  $dp_2$  reaches the 85<sup>th</sup> percentile of MHD, and  $dp_3$  and  $dp_4$  reach the 75<sup>th</sup> percentile.  $M_1$  is not mineralized at birth in all but one newborn, a *S. geoffroyi* neonate, in which the protoconid is visible.

#### *Saimiri boliviensis*, neonate

$Di_1$  and  $di_2$  are both buccolingually flattened and slightly concave on the lingual side.  $Di_1$  has a narrow apex with a flat incisal margin, while  $di_2$  resembles the maxillary counterpart with its incisal border sloping distally.  $Dc$  is robust with a high cusp that tapers distally. A distolingual vertical ridge descends from the cusp to meet a pronounced lingual cingulum with a distostyliid. The crown base is slightly deficient in mineralization on the mesiolingual margin.

$Dp_2$  and  $dp_3$  are mesiodistally narrow.  $Dp_2$  is nearly caniniform, but with a less projecting protoconid; it possesses a transverse ridge (positionally the same as the distolingual vertical ridge of  $dc$ ) connecting the protoconid to a smaller metaconid.  $Dp_3$  is bicuspid with cusps of more equal size, and a distal ledge with a distostyliid.  $Dp_4$  is quadrate with four primary cusps. A cristid oblique connects to the protocristid to the base of the protoconid. A paracristid extends mesially and arcs to the buccal side, demarcating the trigonid mesially and lingually. The talonoid basin is incompletely mineralized in some newborns; in specimens where it is complete, a small hypoconulid is present.  $M_1$  is present with two to three primary cusps, but no mineralized ridges or basins.

#### *Cebus apella* (day 14)

$Di_1$  and  $di_2$  expand apically to broad incisal margins; each has partially mineralized roots.  $Di_2$  is larger with a more rounded apex and a more pronounced lingual heel.  $Di_2$  is more robust than  $di_1$ . There are no marginal ridges.  $Dc$  has a curved pointed cusp emanating from a broad base. There is a ridge on the lingual surface. The root is unmineralized.

$Dp_2$  and  $dp_3$  are nearly oval in occlusal profile, with two primary cusps (protoconid, metaconid) with a sharp, raised protocristid connecting them. The protocristid separates a broader mesial basin from a small distal basin. Small cusplets are found on the distobuccal side

of each deciduous premolar, and also on the mesiobuccal side of  $dp_2$ .  $Dp_4$  is quadrate in occlusal profile with four primary cusps, each pair parallel in mesiodistal position. The protoconid and metaconid are connected by a raised sharp crest, dividing a raised trigonid basin from a deeper talonid basin.  $M_1$  presents with a protoconid and metaconid connected by a sharp protocristid, which is not as raised as in  $dp_4$ . The trigonid basin is partially mineralized. The hypoconid is an isolated cusp tip and the entoconid is as yet, unmineralized.

## Family Pitheciidae

*Pithecia pithecia*, neonate (Fig. 10)

$Di_1$  and  $di_2$  each have straight incisal margins.  $Dc$  is conical with a sharp lingual crest projecting from tip toward the base of the crown. All anterior teeth reach or exceed the 85<sup>th</sup> percentile of MHD at the crown apex.

$Dp_2$  is bicuspid but with a weakly pronounced metaconid. The protoconid is prominent with a protocristid projecting partway toward a lingual shelf.  $Dp_3$  is bicuspid, although distally there is a minuscule pair of cusps (reduced hypoconid, entoconid). A distinct protocristid divides trigonid and talonid basins.  $Dp_4$  has four primary cusps, a small trigonid basin, and a broader talonid basin. In the  $dp_3$  and  $dp_4$ , the trigonid basin is slightly more elevated and more mineralized compared to the talonid basin. The protocristid is relatively pronounced in all deciduous premolars, resembling *Callicebus* (see below).  $Dp_2$  has the largest portion of 85% MHD compared to  $dp_3$  and  $dp_4$ , which only the very tip of the protoconid reaching 85% of MHD. Four cusps of  $M_1$  are present, but part of the talonid basin is unmineralized. Most of the cusps of  $M_1$  reach 25% of MHD, except for the hypoconid (< 25%). The protoconid of  $M_2$  is visible (25% MHD), the only portion of that tooth that is mineralized.

No replacement teeth are mineralized.

*Callicebus cupreus*, neonate

$Di_1$  is narrow with a straight incisal margin.  $Di_2$  is slightly broader than  $di_1$  with a marginally rounded distal margin.  $Dc$  has a conical cusp that leads to a sharp mesial ridge; there

is a flaring heel distolingually. Dc has the highest mineralization of each of the anterior teeth, reaching a MHD of 85%. Di<sub>1</sub> and di<sub>2</sub> reach a MHD of 50%.

Dp<sub>2</sub> and dp<sub>3</sub> are bicuspid and each have a prominent central crest running buccolingually, the protocristid; the metaconid is least pronounced in dp<sub>2</sub>. Dp<sub>4</sub> has four cusps, well mineralized basins, and a protocristid. The trigonid basin is elevated and bounded by raised marginal ridges; the talonid basin has deep grooves separating the distal cusp pair from the mesial pair. Distally the talonid basin lacks a marginal ridge; thus the talonid is “open” on all sides except for the protocristid on its mesial border. The protoconid of each deciduous premolar reaches or exceeds 85% MHD. On dp<sub>4</sub>, the metaconid reaches 85% MHD at its tip, the hypoconid reaches 75% MHD, and the entoconid reaches 50% MHD. Three cusps of M<sub>1</sub> are mineralized. The entoconid is not apparent. The three cusps are as yet unconnected; a small portion of the protocristid descends lingually from the protoconid. M<sub>1</sub> reaches 50% of MHD at the protoconid and 25% at the metaconid.

The edges of the incisive margins of I<sub>1</sub> and I<sub>2</sub> are mineralized, reaching < 25% MHD.

#### *Aotus nancymaae*, neonate (Fig. 10)

Di<sub>1</sub> and di<sub>2</sub> each are buccolingually flattened; di<sub>2</sub> is broader at its apex. The incisal margin of di<sub>1</sub> is straight and level, while in di<sub>2</sub> it slopes distally. Each may have mamelons. The deciduous incisors lack marginal or longitudinal ridges and are poorly mineralized near the crown base. The dc is a conical cusp with slight marginal ridges; it is likewise poorly mineralized at the crown base. All anterior teeth reach at least the 75<sup>th</sup> percentile of MHD. In one specimen di<sub>2</sub> reaches or exceeds the 85<sup>th</sup> percentile, while in another specimen both deciduous incisors exceed that.

Dp<sub>2</sub> and dp<sub>3</sub> are roughly ovoid in occlusal view, and have two cusps. The metaconid of dp<sub>2</sub> is small at best, and indistinct in one newborn. Each has an elevated shallow trigonid basin, and a small distal shelf in lieu of a talonid basin. Dp<sub>4</sub> is quadrate with four primary cusps, a small trigonid, and a larger and deeper talonid basin. There is a metastylid on two of four specimens examined. The crown base of dp<sub>3</sub> and dp<sub>4</sub> is better mineralized than that of dp<sub>2</sub>. Dp<sub>2</sub> reaches 85% MHD. Dp<sub>3</sub> reaches 75% MHD. Dp<sub>4</sub> varies from 75% to 85% MHD. In one specimen, the

protoconid of  $dp_4$  reaches or exceeds a MHD of 85%.  $M_1$  varies in its state of mineralization in newborns. In the least mineralized specimen, there are three isolated cusp tips. In another, there are four cusps and a protocristid. The protoconid and metaconid of  $M_1$  reaches a MHD of 50%; the hypoconid differs in the two specimens studied (reaching the 25<sup>th</sup> or 50th percentile of MHD).

No replacement teeth are mineralized at birth.

## **Morphology of the dentition in newborn tarsiers**

### ***General considerations***

Mineralization of permanent teeth is on an advanced schedule in tarsiers compared to nearly all other primates (Tables 1-3). Cusps are a particular focus of mineralization as opposed to crests. Tarsiers have an advanced mineralization schedule of replacement teeth. However,  $M^1/M_1$  is more advanced in mineralization than any deciduous or replacement tooth.

### ***Maxillary dentition***

*Tarsius syrichta*, neonate (Fig. 11)

$Di^1$  has a minute peg-shaped cusp and full root; although  $di^2$  is not visible in the reconstruction (Fig. 11), it was previously identified in the reconstruction of the contralateral side of this specimen (Smith et al., 2015).  $Dc$  has a conical cusp and a slight cingulum distolingually, with a partially resorbed root.

$Dp^2$  is absent, as reported for *T. bancanus* by Luckett and Maier (1982).  $Dp^3$  has one cusp with a pronounced cingulum on all sides. A parastyle is present and roots are nearly completely formed.  $Dp^4$  is triangular in occlusal profile, with a large paracone and smaller metacone and protocone; a parastyle is present. A sharp crest connects the buccal cusps. Roots are nearly completely formed.  $M^1$  is well mineralized at birth, although the cingulum is incompletely mineralized, and one newborn has a small gap in the center of the trigon basin.  $M^2$  has three mineralized cusps; the basin is unmineralized. The paracone of  $M^3$  is mineralized.

$I^1$ ,  $I^2$ ,  $P^2$ ,  $P^3$  and  $P^4$  are all partially mineralized at birth. Luckett and Maier (1982) note only  $I^1$ ,  $I^2$ , and  $P^2$  in a perinatal *T. bancanus*.

### ***Mandibular dentition***

*Tarsius syrichta*, neonate (Fig. 12)

$Di_1$  has a small rounded cusp and full root;  $di_2$  is absent or represented by a small vestigial fragment. The  $dc$  has a conical cusp, a lingual heel, and a nearly complete root.

$Dp_2$  is absent. Both  $dp_3$  and  $dp_4$  have highly projected protoconids.  $Dp_3$  is a single-rooted, caniniform tooth.  $Dp_4$  has one prominent cusp, no observable metaconid, and two stout roots.  $M_1$  is fully mineralized at birth except for parts of the cingulum. Part of the buccal cingulum is visible in a day 6 specimen.  $M_2$  is mineralized except for the middle of the talonid basin and the cingulum. The protoconid and metaconid of  $M_3$  are mineralized in two day 0 specimens. In a day 6 specimen, five primary cusps of  $M_3$  are mineralized (including the paraconid).

$I_1$ ,  $C$ ,  $P_2$ ,  $P_3$ , and  $P_4$  are partially mineralized at birth. The crowns and a portion of the roots of  $I_1$  and  $P_2$  are mineralized, in the remainder of the replacement teeth the base of the crown is poorly mineralized.

## **Morphology of the dentition in newborn lemuroid strepsirrhines**

### ***General considerations***

Lemurids stand apart from other strepsirrhines in having relatively less mineralized  $M^1/M_1$  at birth compared to other families, although there are variations among lemurids in the degree of mineralization of  $M^1/M_1$  and the replacement teeth at birth (Tables 1-3). Cheirogaleids and galagids have advanced mineralization of certain replacement teeth at birth. The single available lorisid has the most well mineralized replacement teeth of any primates aside from indriids and tarsiers.

In  $dp_4$ , strepsirrhines, like some cercopithecoids, possess a cusp on the leading edge of the paracristid - a possible paraconid. In no species is it as large as most of the other primary cusps. More work is needed to assess its degree of variation.

### ***Maxillary dentition***

#### **Family Cheirogaleidae**

##### *Cheirogaleus medius*, neonate

$Di^1$  and  $di^2$  are both small, especially the peg-like  $di^1$ .  $Dc$  is mesiodistally broad with a tall pointed cusp. Portions of the roots of all anterior teeth have begun to mineralize.  $Di^1$  and  $di^2$  both have a MHD reaching the 50th percentile.  $Dc$  reaches a MHD of 75%.

$Dp^2$  is caniniform but smaller than  $dc$ ; its root has initiated mineralization.  $Dp^3$  is broader than  $dp^3$  with a pyramidal cusp. Lingually there is a vertical ridge with a vertical groove on either side. There appears to be a parastyle present, but the base of the crown looks poorly mineralized as yet, rendering a complete description impossible.  $Dp^2$  reaches a MHD of 50% and  $dp^3$  reaches a MHD of 85% located at the cusp.  $Dp^4$  is triangular shaped with three primary cusps; the trigon basin is incompletely mineralized in both specimens examined and no trace of a cingulum can be seen, if present.  $Dp^4$  reaches a MHD of 85% in the paracone.  $M^1$  is present with three cusps and reaches a MHD of 50% at the paracone tip.

The tip of the  $I^1$  cusp is mineralized adjacent to  $di^1$ . As in *Microcebus*,  $I^2$  is distinctly less developed than  $I^1$ , showing no mineralization as yet (early bell stage).  $C$  is larger than  $I^1$  and is located lingually to  $dc$ . The mineralized part of  $P^2$  is larger than  $I^1$ , but smaller than  $C$ .  $I^1$ ,  $C$ , and  $P^2$  each reach a MHD of 25%.

##### *Microcebus murinus*, neonate (Fig. 13)

$Di^1$  and  $di^2$  are both small and narrow and rounded on their buccal sides.  $Dc$  is caniniform, yet buccolingually compressed. Whether there are marginal ridges on the anterior teeth is unclear, and this may owe to the limits of resolution with the small specimen. All anterior teeth are beginning to form roots.  $Di^1$  and  $di^2$  both reaching 50% of MHD.  $Dc$  reaches a MHD of 75%.

$Dp^2$  is larger than  $dp^3$ , but they both have a single, tall cusp.  $Dp^3$  is more triangular in profile (as noted by Tattersall and Schwartz, 1974) and yet appears partially unmineralized at the base of the crown. Because of this, the presence of stylar cusplets cannot be confirmed, although a parastyle has been attributed to  $dp^3$  in cheirogaleids (Tattersall and Schwartz, 1974). Both  $dp^4$  and  $M^1$  are represented by three cusps at birth; neither possesses a mineralized hypocone, as yet, which was noted in these teeth by Tattersall and Schwartz (1974). In  $dp^4$ , the entire trigon basin and the distal margin are unmineralized. In  $M^1$ , the three cusps are isolated..  $Dp^2$  and  $dp^3$  reach a MHD of 75%.  $Dp^4$  reaches or exceeds a MHD of 85% at the paracone. The metacone has a MHD of 50% and the protocone has a MHD of 25%. The paracone of  $M^1$  reaches a MHD of 50%, whereas the rest of the tooth has a MHD of at most 25%. The paracone of  $M^2$  is mineralized at the tip and reaches a MHD of less than 25%.

The apical part of C is mineralized, reaching 25% MHD at the tip. Although no other secondary teeth are shown in our reconstruction, histology of a specimen from the same litter reveals that  $I^1$  is at the late bell stage (whereas  $I^2$  is at the early bell stage). Regarding replacement premolars, histological observations show that  $P^2$  is the most advanced, but is only at the early bell stage at birth (Smith et al., 2015).

## Family Lemuridae

*Eulemur collaris* (Fig. 13), *E. mongoz* and *E. rubriventer*, neonate

$Di^1$  and  $di^2$  are small and buccolingually flat.  $Dc$  is broad and buccolingually compressed, with sharp mesial and distal margins. The roots of all anterior teeth have initiated mineralization in *E. mongoz*. In all newborns of *Eulemur* spp.,  $di^1$  and  $di^2$  reach the 50th percentile of MHD;  $dc$  reaches the 75th.

$Dp^2$  is small, caniniform, and buccolingually compressed, though not to the degree of  $dc$ .  $Dp^3$  is rounded buccally and has a lingual vertical ridge. Tattersall and Schwartz (1974), in describing *E. rubriventer*, noted the  $dp^3$  is “laterally compressed” like  $dp^2$ . This is not the case in any of our *Eulemur* infants.  $Dp^3$  is much larger and pyramidal, with a slightly concave distolingual surface. A comparison to older infants (P30 *E. collaris*, P24 *E. mongoz*) reveals that  $dp^2$  and  $dp^3$  have only partially mineralized crowns. The older infants have a cingulum on the

buccomesial and linguodistal border, and para- and distostyles.  $Dp^4$  is triangular in profile with three primary cusps. There is some variation in the smaller cusps of  $dp^4$ , which is difficult to attribute as species-specific based on the small samples. In *E. collaris*, a parastyle and smaller metastyle are present, as is a small paraconule (the latter is present in only two of the three neonates and also the older infant). The crista obliqua is incomplete; at P30 it only weakly connects to the metacone, near its base. Lingual to the protocone are two isolated cusplets, the incipient protostyle and hypocone. By P30 these can be visualized as projections from a lingual cingulum. In *E. mongoz*, a parastyle and a smaller metastyle are present. The crista obliqua is low and connects to the base of the metacone and bears a small metaconule. The trigon basin is unmineralized in the center at birth and fully mineralized by P24. In a single newborn *E. rubriventer*, a pronounced parastyle is present, as is a small paraconule. The crista obliqua is distinct (far more so than in *E. collaris*) and bears two metaconules. Distal to the protocone is a triangular shelf; because it is distinct from the partially mineralized lingual cingulum, and this specimen is different from the other *Eulemur* spp. in this respect. Such a cusp was called a “pseudohypocone” by Swindler (2002; but see Anemone et al., 2102 regarding the validity of this term). There are also two small cusps on an incipient lingual cingulum, the protostyle and a small true hypocone. The trigon basin is poorly mineralized. In representative specimens of all species,  $dp^2$  reaches a MHD of 75%.  $Dp^3$  and  $dp^4$  reach or exceed a MHD of 85% at the paracone.

$M^1$  is present with three cusp tips mineralized. In the P30 *E. collaris*, the crown of  $M^1$  is well-mineralized, and three cusps of  $M^2$  are mineralized. The basin of  $M^1$  remains unmineralized in the P24 *E. mongoz* and  $M^2$  is not yet apparent. The  $M^1$  paracone is the most mineralized (25<sup>th</sup> to 50th percentile MHD) and the metacone is the least mineralized cusp.

No portions of  $I^1$ ,  $I^2$ , or replacement premolars are mineralized at birth, and  $C$  is only beginning to mineralize in one newborn, *E. mongoz*, which reaches the 25<sup>th</sup> percentile of MHD. The cusp tip of  $C$  is also mineralized in a P30 *E. collaris*.

*Hapalemur griseus*, neonate

$Di^1$  is peg-like with a pronounced concavity lingually.  $Di^2$  is similar and more rounded on its buccal side than  $di^1$ . In the two specimens studied,  $di^1$  reaches a MHD of 25<sup>th</sup> and 75<sup>th</sup> percentile.  $Di^2$  reaches and MHD of 25 and 50%.  $Dc$  is broad-based, elongate mesiodistally, flattened buccolingually, and possesses a slight distal heel. Lingually it has a sharp vertical ridge that runs from the crown base to the tapered and distally curved cusp tip; distal and parallel to this ridge is a deep groove. In both specimens, the  $dc$  reaches a MHD of 85%.

$Dp^2$  is caniniform but more pyramidal in form than  $dc$ . Like  $dc$ , it has a vertical lingual ridge with a groove distal to it.  $Dp^3$  has a single cusp that connects to pronounced ridges mesially, distally, and lingually. In lingual view it resembles  $dp^2$ , with basin-like concavities that border the mesial ridge. The distolingual border is not completely mineralized.  $Dp^4$  is broad and triangular shaped with three prominent cusps, as seen in  $M^1$  (Swindler, 2002). Tattersall and Schwartz (1974) note that the metacone is the largest of the three cusps. This is true in our samples in terms of the cusp height, but in breadth it is nearly matched by the protocone. The trigon basin is shallow and a crista obliqua is lacking. Three stylar cusps are present along the buccal margin of  $dp^4$ ; a parastyle is visible on the first two dps, but the distal portion of these teeth is too poorly mineralized to detect a metastyle. The lingual cingulum is pronounced although the protostyle is quite small, and the hypocone is absent (as reported for  $M^1$  by Schwartz and Tattersall (1985) and Swindler (2002)). In one specimen, all deciduous premolars reach a MHD of 85%. In the other,  $dp^2$  reaches the 50th percentile while  $dp^3$  and  $dp^4$  reach the 75<sup>th</sup> percentile.  $Dp^2$  and  $dp^3$  each reach a MHD of 85%.  $Dp^4$  reaches a MHD of 85% that is predominantly observed in the paracone.  $M^1$  has three cusps and a mostly unmineralized basin, especially distally. At maximum,  $M^1$  reaches a MHD of 50% found at the paracone and metacone. In both  $dp^4$  and  $M^1$ , the buccal cusps are more mineralized (at higher MHD) or are more extensively mineralized than the protocone.

There are no replacement teeth mineralized at birth. In *Hapalemur* even the anterior maxillary teeth are less advanced (e.g., early bell stage) than in other lemurids (Smith et al., 2015).

$Di^1$  and  $di^2$  are both small with irregular incisal margins.  $Dc$  is buccolingually narrow and elongated. It is simple and blade-like compared to *Eulemur* or *Hapalemur*, lacking a pronounced lingual ridge, and having a very shallow lingual groove. In  $di^1$  and  $di^2$ , the crown has reached 50<sup>th</sup> and 25<sup>th</sup> percentile of MHD, respectively.  $Dc^1$  has a MHD of at least 85%.

$Dp^2$  and  $dp^3$  are both single-cusped, are rounded on buccal and lingual sides, and have sharp mesial and distal ridges; they. In the neonate, a parastyle can be seen on  $dp^2$  but not on  $dp^3$ . However, both  $dp^2$  and  $dp^3$  are as yet incompletely mineralized near the crown base. In an older infant (P28),  $dp^2$  and  $dp^3$  each have a parastyle and a small distostyle as well.  $Dp^4$  has three primary cusps, a parastyle, and a smaller metastyle. A portion of the trigon basin is unmineralized at birth, but fully mineralized in the P28 infant. The crista obliqua is not observed. The lingual cingulum is not mineralized in newborns, but is well-formed in the P28 infant. A protostyle is absent (as observed for  $M^1$  - Schwartz and Tattersall, 1985) and in the region of the hypocone, there is only a slight swelling Both of the  $dp^2$  and  $dp^3$  reach MHD of at least 85% at the cusp, more extensively so in  $dp^3$ . In  $dp^4$ , the most mineralized cusp being the paracone (85%), followed by the metacone, and then the protocone (each of the latter reaching 75% MHD).  $M^1$  has two mineralized cusps present. At P28, there is an isolated, spiky ossified element in the region of the lingual cingulum, as yet not bridged to the protocone. The paracone of  $M^1$  reaches 50% of MHD; the protocone and metacone of  $M^1$  reach a MHD of 25%.  $M^2$  is not mineralized at birth or at P28.

In the P28 infant, no replacement teeth are visible, but it is possible small cusp tips may be obscured by radio-opaque inclusions in incisor tooth crypts.

#### *Varecia* spp., neonate

At birth, the state of mineralization of the maxillary tooth row in *Varecia rubra* and *V. variegata* is nearly identical. At birth, *Varecia* species have the least mineralized teeth of any primate that we have examined, and this is especially true of postcanine teeth.

At birth the crown of  $di^1$  is visible, but only the apical part of the crown of  $di^2$  is mineralized. In an older infant (P25 *V. variegata*), the full crown of  $di^2$  is mineralized and it is more rounded and peg-like than  $di^1$ .  $Dc$  is mesiodistally elongated and buccolingually

compressed. There is no vertical lingual ridge (as in *Hapalemur*) and only a shallow vertical lingual groove (as in *Lemur*). A portion of the root of dc is seen at P25.

Only a small portion of the cusp of  $dp^2$  is mineralized in any of the newborns. A larger pyramidal portion of  $dp^3$ 's single cusp is mineralized, with a rounded buccal side, a more flattened mesiolingual side, and a concave distolingual side.  $Dp^4$  is visible as three isolated cusps; a portion of a parastyle may be connected to the paracone. The crown basin and lingual cingulum remain unmineralized. Form of the deciduous crowns is clear in the P25 infant. Both  $dp^2$  and  $dp^3$  have vertical ridges on the lingual surface.  $Dp^2$  is rounded mesial to this ridge and concave distal to this ridge. Much larger and broader than  $dp^2$ ,  $dp^3$  is now revealed to have a slight flaring of cingula on the buccal side. The basin and lingual cingulum of  $dp^4$  are fully mineralized in the P25 infant. The trigon basin is walled off mesially by a stout crest connecting the paracone and protocone. The basin is open distally. There is no crista obliqua. A small parastyle is present. A protostyle is lacking but there is a slight swelling consistent with a hypocone. Only the paracone of  $M^1$  is mineralized in newborns. However, in the P25 infant,  $M^1$  has three isolated mineralized cusps.

At P25, the apical part of the C cusp is mineralized.

### Family Lepilemuridae

In newborn *Lepilemur leucopus* (Fig. 13), one of the deciduous incisors is present. It is has a partial root and is further erupted than dc, possibly in the process of being shed. Dc reaches 50% MHD at the cusp tip; the di reaches the 25<sup>th</sup> percentile at the cusp.

All deciduous teeth have fully mineralized crowns and well-formed roots.  $Dp^2$  has one cusp; it is buccolingually compressed with a small parastyle. In  $dp^3$  there is one prominent cusp which leads to mesial and distal ridge; a parastyle is present. In  $dp^4$  three primary cusps are prominent; there is a parastyle and metastyle and a distinct lingual cingulum. The deciduous premolars are far less mineralized than permanent molars:  $dp^2$  reaches only the 25<sup>th</sup> percentile of MHD, and  $dp^3$  and  $dp^4$  reach 50% MHD. In both  $M^1$  and  $M^2$  the majority of the crown exceeds the 50<sup>th</sup> percentile of MHD and the three primary cusps all reach the 85<sup>th</sup> percentile of MHD. In

$M^3$  the paracone reaches the 85<sup>th</sup> percentile while the remaining cusps each reach the 75<sup>th</sup> percentile of MHD.

The cusp apices of C and the three replacement premolars are present, reaching 25% MHD.

### Family Indriidae

*Propithecus coquereli*, neonate (Fig. 13)

$Di^1$  and  $di^2$  are both small and buccolingually flat;  $di^1$  comes to a pointed apex and  $di^2$  has a more rounded incisal margin.  $Dc$  is broader and caniniform, with a slightly concave lingual surface and rounded buccal surface. However,  $dc$  is more buccolingually compressed than in other lemuroids, and seems proportionally far smaller. The deciduous anterior teeth reach a hydroxyapatite density of 50 to 75% MHD, the highest at  $dc$ .

$Dp^3$  is broad with one cusp that connects to mesial and distal marginal ridges; it is concave lingually.  $Dp^4$  is broad with two prominent buccal cusps, a paracone and a metacone. Lingually there is a distinct protocone as well as a hypocone that varies in prominence. As a result, the tooth may be triangular or trapezoidal in profile, depending on how pronounced the hypocone is. In any case, the paracone is displaced far mesially relative to the rest of the cusps. As described in  $M^1$  and  $M^2$  (Tattersall and Schwartz, 1974),  $dp^4$  possesses a well-developed buccal cingulum with three styles. The parastyle projects most prominently, while the metastyle is least prominent and is absent in some specimens. The contours of the crowns of  $M^1$  and  $M^2$  are nearly completely formed at birth. Moreover, the  $M^2$  crown is nearly as well mineralized at birth as in one-month-old specimens; the former showed only small poorly mineralized or thin basins compared to one-month-old specimens. Two isolated cusps of  $M^3$  are mineralized in one of the two newborns examined.  $Dp^3$  reaches the 50<sup>th</sup> percentile of MHD.  $Dp^4$  reaches or exceeds a MHD of 85% at the paracone.  $M^1$  reaches a MHD of 85% at the paracone and metacone.  $M^2$  has a MHD of 50 percent located in the paracone, metacone, and protocone.  $M^3$  has a MHD of 25% at the paracone.

$I^1$  is very well mineralized, already revealing its spatulate shape in newborns.  $I^2$  is as yet, unmineralized at birth. The cusp tip of C is present and lingual to  $dc$ . The paracone of  $P^4$  is more

advanced than  $P^3$ , and is already assuming a pyramidal shape and reaching a MHD of 50%.  $I^1$  is the most advanced in mineralization, reaching a MHD of 85% at the incisal margin. In a  $P32$  infant, the tip of  $I^2$  is now visible; thus all replacement teeth are mineralizing by one month of age.

### ***Mandibular dentition***

#### **Family Cheirogaleidae**

##### *Cheirogaleus medius*, neonate

$Di_1$  and  $di_2$  are narrow, pointed, and long with a longitudinal ridge running along the lingual side running from the tip toward a slight lingual heel.  $Dc$  is broader with a reduced longitudinal ridge, and a more flared lateral flange. Thus, the deciduous anterior teeth resemble the adult tooth comb, as described by Tattersall and Schwartz (1974). In two specimens examined, the anterior deciduous teeth each reach the 50th percentile of MHD.

$Dp_2$  is caniniform with a slight longitudinal ridge; the flanges are slightly larger than in the anterior teeth, and form marginal ridges.  $Dp_2$  reaches the 50th to 75th percentile of MHD at the cusp tip.  $Dp_3$  is narrower near its apex compared to  $dp_2$ , and has a more pronounced longitudinal ridge. Distal to this ridge, this tooth becomes concave, and appears to form part of a basin; however, the lingual margins are as yet poorly mineralized (or unmineralized) and the outer margins of this basin cannot be visualized in the reconstructions. A lingual cingulum, described in *C. major* by Tattersall and Schwartz (1974), is likewise not visible if present. The cusp tip of  $dp_3$  reaches the 50th percentile of MHD in one specimen and the 85th percentile the second specimen.  $Dp_4$  is broad and has a prominent protoconid, hypoconid, and entoconid; the metaconid is present, but only barely elevated above the level of the protocristid. A cristid obliquid, projecting mesially from the hypoconid, is well mineralized. This crest contacts the protocristid the base of the protoconid. A “paraconid shelf” projects mesially, without a distinct cusp on its leading edge; it is more pronounced than the same region of  $M_1$ . The trigonid basin is shallower, elevated and better mineralized than the talonid basin. There is a slight swelling on the crest forming the lingual margin of the talonid basin. This may be a metastylid, but detail is poor (perhaps due to limits of scan resolution in view of small tooth size). The protoconid of  $dp_4$

reaches the 85th percentile of MHD; the entoconid is the least mineralized cusp.  $M_1$  is represented by four cusps in one neonate. In a second neonate the entoconid is not yet mineralized. Similar to  $dp_4$ , the protoconid of  $M_1$  also has the highest MHD reaching the 50<sup>th</sup> to 75th percentile. One of the two mesial cusps of  $M_2$  are present. The MHD of the cusp present in  $M_2$  reaches 25% in one specimen.

The cusp tips of  $I_1$ ,  $I_2$ ,  $C$ , and  $P_2$  are mineralized. Of the replacement teeth,  $I_1$  is the most mineralized, reaching the 25<sup>th</sup> to 50<sup>th</sup> percentile of MHD.

#### *Microcebus murinus*, neonate (Fig. 14)

The deciduous anterior teeth resemble the adult tooth comb. Each of these teeth have a hydroxyapatite density reaching 50% of MHD.

$Dp_2$  is more robust than the  $dc$  and is caniniform with a pronounced lingual heel.  $Dp_2$  reaches a MHD of 75%.  $Dp_3$  is smaller than  $dp_2$  with a prominent protoconid that leans distally; a vertical lingual ridge is present.  $Dp_4$  has four primary cusps, and a deep talonid basin that is incompletely mineralized. A cristid obliquid intersects the protocristid near the protoconid. A small cusplet is present on the distal margin adjacent to the hypoconid. The protoconid of  $dp_3$  and  $dp_4$  reach a MHD of 85%. The entoconid of  $dp_4$  is the least mineralized cusp.  $M_1$  is present with three cusps, and a mineralized tip of the entoconid. The protoconid of  $M_2$  is mineralized. Similar to  $dp_3$  and  $dp_4$ , the protoconid is most mineralized (75%) cusp and the entoconid is least mineralized (25%) cusp on  $M_1$ . The protoconid of  $M_2$  is mineralized at 25% MHD.

The cusp tips of  $I_1$ ,  $I_2$ , and  $C$  are mineralized.  $I_1$  has the highest mineralization as 25% MHD.

#### *Mirza coquereli*, neonate

The deciduous anterior teeth resemble an adult strepsirrhine tooth comb.  $Di_1$  reaches the 75th percentile of MHD.  $Di_2$  and  $dc$  reach a MHD of 85%.

$Dp_2$  is caniniform but more robust than the anterior teeth. The base of its crown is poorly mineralized lingually and the distal side.  $Dp_4$  is larger than  $dp_2$  and  $dp_3$  with three well mineralized cusps and the cusp tip of the entoconid. A cristid obliquid is mineralized and connects low on the protocristid. The trigonid basin is raised and with the mesial limit on the buccal side; the talonid basin is at yet unmineralized at birth. No smaller cusplets are evident. Three cusps of  $M_1$  are mineralized, excluding the entoconoid.  $Dp_2$  and the protoconid of  $dp_4$  reaches or exceeds a MHD of 85%.  $Dp_3$  reaches a MHD of 75%.  $M_1$  reaches a MHD of 50%.

The cusp tips of  $I_1$  and  $I_2$  have begun to mineralize. They are at a MHD of < 20%.

### Family Lemuridae

*Eulemur collaris* (Fig. 14), *E. mongoz* and *E. rubriventer*, neonate

$Di_1$  to  $dc$  resemble the adult tooth comb of *Eulemur* spp. The deciduous anterior teeth reach at least the 50th percentile of MHD. In one *E. collaris*,  $di_2$  and  $dc$  reach a MHD of 75% at their caniniform cusp tips.

$Dp_2$  is caniniform. A distal marginal ridge and a smaller mesial marginal ridge are present. At its base  $dp_2$  is triangular in shape; lingually there is an angular ridge creating fossae on either side. In some specimens the distolingual margin is incompletely mineralized. At birth,  $dp_3$  has a single primary cusp, but with a broader base. However, a comparison to an older (P30) *E. collaris* specimen reveals that in both  $dp_2$  and  $dp_3$ , the crown is only partially mineralized in each of three newborns examined.  $Dp_2$  expands mesially and distally into a buccolingually compressed, peg-like tooth.  $Dp_3$  is more molariform in a P30 *E. collaris*, since the distal portion is mineralized as an elongated shelf in this older infant. The distal concave surface is expanded to a talonid basin. The mesial surface expands to form a shallow trigonid basin. In the P30 infant,  $dp_3$  has a protoconid, metaconid, and hypoconid. A small paraconid is present.

$Dp_4$  is the most molariform deciduous tooth, with multiple cusps, and some variation among specimens. In *E. collaris*, the protoconid and hypoconid are prominent. On the lingual margin there are multiple cusps, including a small cusplet on the mesiolingual corner near the end of the paracristid, after a small gap. Distal to this small cusp is a deep groove, such that the

trigonid basin is open lingually. A cristid obliquid intersects the protocristid centrally between the mesial cusp pair. The number of small cusps lingual to the talonid varies from one to two. Distal to the metaconid is a small cusplet, and even more distally is a metastylid (the first of these is conspicuously missing in one of the three neonates). Distal to the metastylid is a deep groove, such that the talonid basin, too, is open lingually. Further distally on the lingual side of the talonid is another small cusp, which we consider a small entoconid, but it is not equally pronounced in all specimens. On the distal margin of the talonid basin is a final small cusp, perhaps the hypoconulid. In the P30 infant, there is a slight buccal cingulum on  $dp_4$ , not as pronounced as that of  $M_1$ . A neonatal and infant (P24) *E. mongoz*, are similar to the description above except neither of them has secondary cusps. In an *E. rubriventer* neonate, there are multiple cusps and smaller cusplets in addition to four primary cusps. One small cusplet on the mesiolingual margin. It is near the end of the paracristid, after a small gap. The paracristid is relatively elevated, with two small cusplets at the mesial apex, one of which may be a paraconid. There is no cusplet closely opposed to the metaconid, as observed in other *Eulemur* spp. There are two cusplets mesial to the small entoconid on the crest bordering the lingual side of the talonid basin. No clear hypoconulid is visible. A small cusplet is present on the cristid obliquid, which meets the protocristid between the mesial cusp pair.

In newborn *Eulemur*,  $M_1$  has three pyramidal primary cusps plus the entoconid tip. Additional small cusplet tips are visible in the newborn *E. collaris*. The crown of  $M_1$  is entirely mineralized in the P30 *E. collaris* infant.

The protoconid is the most mineralized cusp in all dps (reaching 85% MHD in *E. collaris* and *E. rubriventer*). The entoconid is the least mineralized of the primary cusps. Smaller cusplets on  $dp_4$ , such as the tuberculum intermedium and metastylid (if present) can be focal points of MHD, each reaching 50% while adjacent part of the lingual ridge are less dense. The trigonid basin is better mineralized than the talonid basin, reaching a MHD as high as 75% near the margins. The MHD of  $M_1$  follows an identical pattern at the cusps, though lagging behind  $dp_4$ .

In *E. collaris* and *E. mongoz*, the cusp tips of  $I_1$ ,  $I_2$  and  $C_2$  are mineralized at birth. In the older infant, each of these teeth is further mineralized and are beginning to form a longitudinal ridge and flanges. In the newborn *E. rubriventer*, only the cusp tip of  $C$  is mineralized.

*Hapalemur griseus*, neonate

The deciduous anterior teeth resemble the adult tooth comb. In both specimens studied for hydroxyapatite density, the dc exceeds that of the deciduous incisors (although in one specimen, di1 has not scanned). In the specimen with all anterior teeth available, di1 and di2 reach a MHD of 50 percent, while the dc reaches 75 % MHD.

Dp<sub>2</sub> and dp<sub>3</sub> are buccolingually compressed with only one distinct cusp. Dp<sub>2</sub> shares some similarities to the dc, but is more robust and has a less distinct longitudinal ridge, creating a shallow mesolingual depression and a deeper and broader buccolingual depression on either side. In dp<sub>3</sub> there is a distinct protocristid passing mesially from the protoconid, but lingually the metaconid is indistinct. Mesial to the protocristid is a descending triangular plane; distally is a shallow depression within a raised heel. No distinct anterior stylids, as mentioned by Tattersall and Schwartz (1974) could be detected. Dp<sub>4</sub> is extremely robust with prominent crests, a cristid obliquid and four primary cusps. Like dp<sub>4</sub>, M<sub>1</sub> is also present with four cusps – with the protoconid being the most mineralized and the entoconid being the least mineralized. Mesially the dp<sub>4</sub> trigonid slopes distinctly upward to a pointed tip, consistent with a paraconid, as suggested by Tattersall and Schwartz (1974). There are multiple cusplets in both neonates; all are on the lingual side of dp<sub>4</sub>. One is just distal to the metaconid (resembles the tuberculum intermedium described on P<sub>4</sub> and M<sub>1</sub> by Swindler). Distally to this cusplet is a smaller one, what might be called a metastylid along the lingual marginal crest bordering the talonid. Distal to the metastylid is a distinct notch, so that the basin is open lingually (as also true of M<sub>1</sub> - Tattersall and Schwartz, 1974). Along the distolingual boundary, there is a pair of distinct cusps in both dp<sub>4</sub> and M<sub>1</sub>. Observing these in M<sub>1</sub>, Schwartz and Tattersall (1985) considered the more distal of the two to be a rather distended entoconid, whereas Swindler (2002) appeared to be referring to the same structure as a hypoconulid. Here, we can observe that the more distal of the two has greater HA density, suggesting it may have formed first (in both dp<sub>4</sub> and M<sub>1</sub>). All deciduous premolars reach a MHD of 85%. Dp<sub>4</sub> has a MHD of 85%, which mostly present in the cristids of the tooth.

The cusp tips of I<sub>1</sub>, I<sub>2</sub>, and C are mineralized.

*Lemur catta*, neonate

The deciduous anterior teeth resemble the adult tooth comb. The anterior teeth reached at least the 75th percentile of MHD near the apex. In one of the two specimens studied, di2 and dc have small foci that have reached the 85<sup>th</sup> percentile of MHD.

Dp<sub>2</sub> and dp<sub>3</sub> both have one cusp that connects to mesial and distal ridges. Lingually, there is slight vertical swelling with a slight groove mesial and distal to it. A comparison to an older infant (P28) reveals that the base of the crown is partially unmineralized at birth in both dp<sub>2</sub> and dp<sub>3</sub> (especially, the latter). Dp<sub>4</sub> has four primary cusps, including the protoconid, metaconid, hypoconid and a slightly smaller cusp on the distal side of the talonid basin. This cusp may correspond to what Swindler (2002) interprets as a hypoconulid on M<sub>1</sub>. There is no clear entoconid; instead there is a slight depression at the distolingual margin, such that the talonid basin is open lingually. Two smaller cusps are present. A metastylid is distinct on the lingual border of the talonid basin. Mesially, there is a small cusplet at the end of a distinct, arcing paracristid. Tattersall and Schwartz (1974) interpreted this as a paraconid. This cusp and the paracristid are notably more elevated in dp<sub>4</sub> compared to M<sub>1</sub>, in which the trigonid slopes downward. A buccal cingulum is present on dp<sub>4</sub>. M<sub>1</sub> has three cusps, the largest being the protoconid. A less mineralized, smaller cusp is present on the lingual side, the presumptive metastylid. No mineralization occurs distally as yet; neither the floor of the talonid basin nor the hypoconulid of M<sub>1</sub> are mineralized in P4 and P8 infants. The hypoconulid is present at P28 and the talonid basin is mineralized except at the center. The buccal cingulum of M<sub>1</sub> is beginning to mineralize at P28. Postcanine deciduous teeth are more mineralized than anterior teeth. The paracones of all deciduous premolars reach 85% of MHD at the cusp tip. On dp<sub>4</sub>, the tip of the metaconid also reaches or exceeds 85% of MHD; the hypoconid reaches 75% of MHD. The hypoconulid reaches 50% MHD; in one of the two specimens examined for hydroxyapatite density, it is an isolated focus of MHD relative to the adjacent crown. The trigonid basin is better mineralized (50 to 75% MHD) compared to the talonid basin (reaching a MHD of 25%). M<sub>1</sub> reaches a maximum of 50% MHD at the protoconid, and in one of the two specimens, also the metaconid.

No replacement teeth are mineralized at birth. In the P28 infant, I<sub>1</sub> and I<sub>2</sub> cusp tips are mineralized.

*Varecia rubra* and *V. variegata* neonate

At birth, the state of mineralization of the mandibular tooth row in *Varecia rubra* and *V. variegata* is nearly identical. The species are described together. The morphology of the deciduous teeth is described based on an older infant *V. variegata*.

The deciduous anterior tooth resemble the adult tooth comb. In an older infant (P25 *V. variegata*) each of the anterior teeth has initiated root formation.

The  $dp_2$  and  $dp_3$  are each more robust than  $dc$  but are similarly rounded buccally and somewhat curved toward the lingual side. Each of them has a vertical lingual ridge; distolingually to the ridge there is a concavity (these are less pronounced in  $dp_2$ ).  $Dp_4$  is much broader and more molariform than  $dp_2$  and  $dp_3$ , with  $dp_4$  having three primary cusps but no mineralization of the talonid basin or the distolingual margin. The trigonid basin is only partially mineralized, but already walled off buccomesially with a distinct paracristid. At the mesial end of the paracristid is a small cusplet. Only the protoconid of  $M_1$  is mineralized. In the P25 infant,  $dp_2$  is revealed to be more caniniform than  $dp_3$ . A small heel is seen distolingually. In  $dp_3$  the distolingual concavity now has the appearance of a shallow basin. Three primary cusps are present on  $dp_4$ ; a distinct entoconid is not present. The scan resolution for the infant was lower than for the newborn, perhaps preventing clear visualization of these small cusps. Distolingually, there is a slight groove, opening the talonid basin, as described in  $M_1$  (Tattersall and Schwartz, 1974). As in the newborn, a small cusplet is seen at the mesial end of the trigonid basin. This might be interpreted as a paraconid. The protoconid and metaconid are closer to one another (thus a shorter protocristid) compared to  $M_1$ . The cristid obliqua tapers toward the crown base as it approaches the protoconid, and never meets the protocristid. In  $M_1$ , there are four mineralized cusps in the P25 infant. The protocristid and part of the talonid basin are mineralized; the latter is far less raised than in  $dp_4$ . The presumptive entoconid is small but distinctly mineralized. It is clearly delayed relative to the other three cusps, and it might be noted that there is little difference between this cusp and the metastylids seen in other lemurids. It thus seems possible that *Varecia* lacks entoconids on  $dp_4$  and  $M_1$ , as described in *Lemur* (Tattersall and Schwartz, 1974). In another subadult (day 140 *V. rubra*), scanned at the highest resolution,  $dp_4$  bears no

entoconid, nor any raised cusplet lingual to the talonid basin. There was a small elevated cusplet on  $M_1$  lingual to the talonid.

No replacement teeth are mineralized at birth.  $I_1$ ,  $I_2$ ,  $C_1$ , and  $P_2$  have all initiated mineralization, but  $P_2$  is only mineralized at the very apex of the cusp.

### Family Lepilemuridae

In newborn *Lepilemur leucopus* (Fig. 14), the deciduous anterior teeth resemble an adult tooth comb, and each cusp reaches the 25<sup>th</sup> percentile of MHD. The roots have initiated mineralization.

$Dp_2$  has one buccolingually compressed cusp. In  $dp_3$  there is one prominent cusp which leads to mesial and distal ridge that end in small cusps; there is a distal heel. In  $dp_4$  three primary cusps are prominent, but there is no entoconid. The cristid obliqua is pronounced and intersects the protocristid at its center.  $M_1$  and  $M_2$  are both well mineralized, including the basins, with pronounced cusps.  $M_3$  is also well-mineralized, except for the distolingual border where the entoconid is not yet apparent. Deciduous premolars reach only the 50<sup>th</sup> percentile of MHD. In both  $M_1$  and  $M_2$  the majority of the crown exceeds the 50<sup>th</sup> percentile of MHD and all primary cusps reach the 85<sup>th</sup> percentile of MHD. In  $M_3$ , only the protoconid reaches the 85<sup>th</sup> percentile of MHD.

$I_1$  and  $I_2$  and  $C$  are all partially mineralized, reaching 50% MHD. The permanent premolars have initiated mineralization,  $P_2$  and  $P_4$  are more mineralized than  $P_3$ , reaching the 25<sup>th</sup> and 50<sup>th</sup> percentile of MHD, respectively.

### Family Indriidae

*Propithecus coquereli*, neonate (Fig. 14)

$Di_1$  and  $di_2$  are narrow and possess a very subtle lingual longitudinal ridge that is only apparent in the upper half of the crown. The mesial and distal ridges are likewise only apparent along the more apical portion of the crown. The dc is far smaller than the deciduous incisors and peg-like.  $Di_1$  and dc reach a MHD of 50 to 75% and  $di_2$  reaches a MHD of 85%.

D<sub>p2</sub> is has one cusp and mesial and distal marginal ridges; the cusp is triangular in buccal profile. D<sub>p3</sub> is smaller with a slight lingual concavity. Both d<sub>p2</sub> and d<sub>p3</sub> reach 50% MHD at the cusp tip. D<sub>p4</sub> is elongated with four primary cusps, a long shallow trigonid basin, and a deeper talonid basin. The cristid obliquid is pronounced and intersects the protocristid at its center. D<sub>p4</sub> reaches a MHD of 50% on all four cusps and the paracristid; the talonid basin is better mineralized than the trigonid basin. M<sub>1</sub> and M<sub>2</sub> are both very well mineralized, including the basins, and have far more pronounced cusps compared to the deciduous premolars. M<sub>1</sub> has a low curved protocristid, with the cristid obliquid intersecting it in the middle. The protocristid is lower still on M<sub>2</sub>. M<sub>1</sub> reaches a MHD of 85% and is located in the metaconid and protoconid. M<sub>2</sub> has a MHD of 50% located in each of the cusps, but predominantly in the metaconid and protoconid. Three cusps of M<sub>3</sub> are mineralized at birth and the entoconid is not yet apparent. At this point, M<sub>3</sub> reaches a MHD of 25%. In one-month-old *Propithecus* the entire M<sub>3</sub> crown is mineralized but the protocristid is absent

The crowns of I<sub>1</sub> and I<sub>2</sub> are advanced in mineralization, and exceed their deciduous counterparts in MHD. P<sub>2</sub> and P<sub>4</sub> are mineralized although only at the tip of the protoconid.

## Morphology of the dentition in newborn lorisoid primates

### Family Galagidae

#### *Maxillary dentition*

*Otolemur crassicaudatus* (Fig. 15) and *O. garnettii*

In both species, d<sub>i1</sub><sup>1</sup> and d<sub>i2</sub><sup>2</sup> are both peg-like and slightly concave ventrally. D<sub>c</sub> is much larger and broader with sharp mesial and distal marginal ridges. Lingually there is a broad, rounded longitudinal ridge with concave depressions on either side; buccally d<sub>c</sub> is convex. D<sub>i1</sub><sup>1</sup> and d<sub>i2</sub><sup>2</sup> both reach a MHD of 75%. D<sub>c</sub> reaches a MHD of 85%. In an older (one-month-old) *O. crassicaudatus*, the roots of d<sub>i1</sub><sup>1</sup> and d<sub>i2</sub><sup>2</sup> are nearly complete; d<sub>c</sub> has two roots.

$Dp^2$  is smaller than  $dc$ , with a buccolingually compressed plate leading to a single cusp. Distolingually, there is a small projecting stylar cusp.  $Dp^3$  is triangular in occlusal profile. Part of the crown appears to be, as yet, unmineralized, although a small parastyle is present.  $Dp^4$  is very large and has three primary cusps and an incompletely mineralized basin; a parastyle and metastyle are evident in all specimens. In addition, a paraconule is visible in our single specimen of *O. garnettii*. The tip of the hypocone is mineralized, but as yet unconnected to the rest of  $dp^4$ .  $Dp^2$  and  $dp^3$  both reach a MHD of 85%.  $Dp^4$  reaches a MHD of 85% at the buccal cusps in a newborn *O. crassicaudatus*, most broadly on the paracone; in *O. garnettii* the paracone alone reaches the 85<sup>th</sup> percentile. The hypocone has commenced mineralization in the newborn *O. garnettii*.  $M^1$  has three mineralized cusps. In  $M^1$  of *O. crassicaudatus*, the paracone reaches a MHD of 50%, while the metacone and protocone reach the 25th percentile. Only the tip of the paracone of  $M^2$  is mineralized at < 25%. In *O. garnettii*, two cusps of  $M^1$  are mineralized and  $M^2$  is not yet apparent. However, based on histology Smith et al. (2015) observed  $M^2$  had reached the late bell stage in a newborn *O. garnettii*.

In the older (P26) *O. crassicaudatus* infant, the root of  $dp^2$  has started to form.  $Dp^3$  is revealed to have a broad base and a wide lingual cingulum, still incomplete distolingually; a para- and distostyle are present. The trigon basin and hypocone are fully mineralized in  $dp^4$  and a small parastyle is present. The crown of  $M^1$  appears fully mineralized;  $M^2$  now presents with three isolated mineralized cusps.

The apical cusp of C is mineralized at birth. The cusp reaches the 25<sup>th</sup> percentile of MHD in both *Otolemur* specimens. The tip of the cusp of  $P^2$  is also present in a newborn *O. garnettii*. In the older infant *O. crassicaudatus*,  $I^1$ ,  $I^2$ , and  $P^2$  are mineralized, in addition to C.

#### *Galago moholi* and *Galago senegalensis*

In both species,  $di^1$  and  $di^2$  are small and peglike.  $Dc$  is caniniform and broad. The deciduous incisors reach a MHD of 25%. The cusp of  $dc$  reaches 75% MHD.

$Dp^2$  is similarly shaped to  $dc$  but smaller. There is a small gap between  $dp^2$  and  $dp^3$ .  $Dp^3$  has one cusp and para- and distostyles.  $Dp^4$  has four cusps; the hypocone is mineralized at the cusp tip; a parastyle and metastyle are present. A paraconule is present in *G. moholi*, but was not

observed in *G. senegalensis*. The trigon basin is well mineralized except at the center.  $M^1$  has three cusps; the hypocone is not yet mineralized. The paracone of  $M^2$  is present. In a P30 *G. moholi* infant,  $dp^3$  has a broader base of the crown. The lingual cingulum of  $dp^4$  is now more expansive and the hypocone appears more prominent.  $M^1$  has a greatly expanded mineralization in the P30 infant. The entire trigon basin is mineralized as is the lingual cingulum and hypocone. In the P30 infant,  $M^2$  is also advanced, with three primary cusps, the paraconule, and an isolated cusp tip of the hypocone. The paracone of  $dp^2$  and  $dp^3$  reach a MHD of 50%.  $Dp^4$  reaches a MHD of 85% (at the protocone in one *G. moholi* examined for hydroxyapatite density) or the 75<sup>th</sup> percentile (the paracone, protocone, and metacone). The hypocone is the least mineralized at 25 % MHD.  $M^1$  reaches a MHD of 75% in *G. moholi* and 85% in *G. senegalensis*, in both cases at the paracone. The paracone of  $M^2$  reaches less than 25% of MHD in *G. moholi* and <25% in *G. senegalensis*

The apical part of the cusp of C is present, reaching 25% MHD. A smaller mineralized portion of  $P^2$  is also present at birth. In the P30 *G. moholi* infant,  $I^1$  and  $I^2$  are now mineralizing, and the mineralized parts of C and  $P^2$  are nearing the size of their deciduous precursors.

## Family Lorisidae

*Nycticebus pygmaeus* (Fig. 15)

$Di^1$  and  $di^2$  are small, peglike teeth.  $Dc$  is larger and cylindrical except for a tapering, triangular tip. The deciduous incisors reach a MHD of 25%, and the  $dc$  reaches the 50<sup>th</sup> percentile at the cusp tip.

$Dp^2$  has a single cusp with short mesial and distal ridges emanating away from the tip; it is rounded buccally and more flattened lingually.  $Dp^2$  reaches a MHD of 50 percent MHD.  $Dp^3$  has a conical paracone with an adjacent parastyle. Since both are only partially mineralized, it is impossible to say whether either has cingula except for the buccal cingulum that supports the parastyle of  $dp^3$ .  $Dp^4$  is a triangular shaped mass with three primary cusps, all merged. The trigon basin is unmineralized in the center and the hypocone is an isolated cusp, unsupported as yet by mineralized cingulum. A parastyle is present, as well as a prominent paraconule. A crista obliqua is not apparent, as yet, if there is one.  $Dp^3$  and  $dp^4$  reach a MHD of 85% at the paracone

(and metacone of  $dp^4$ ).  $M^1$  is represented by three cusps and the tip of the paraconule. Neither the parastyle nor the hypocone has started to mineralize. The three cusps of  $M^1$  reach MHD of 50% (buccal cusps) and 25% (protocone). *N. coucang* is reported to have a metastyle and distinct buccal cingulum on  $M^1$  (Swindler, 2002), and these are not present (or not mineralized) on  $dp^4$  or  $M^1$  of the newborn *N. pygmaeus*. Conversely, the distinct paracone of  $dp^4$  and  $M^1$  was not reported or illustrated on *N. coucang* by Swindler (2002).

Four replacement teeth are mineralized,  $I^1$ ,  $I^2$ ,  $C^1$ , and  $P^2$ . Only the tip of the cusp of  $P^2$  is seen. The anterior replacement teeth are far larger and better mineralized than their precursors: the incisors reach the 50<sup>th</sup> percentile and the  $C$  reaches the 85<sup>th</sup> percentile of MHD.  $P^2$  appears to have just initiated mineralization, reaching 25% MHD.

#### *Perodicticus potto*, infant

Specimen #CM69182 is a skeletonized skull in the collection of the Carnegie Museum, Section of Mammals. Obtained from the Pittsburgh Zoo, the specimen is of unrecorded precise age. Dentally, it is considerably more mature than the day 0 newborn lorisoids described above. It is very comparable with the P26 infant *Otolemur crassicaudatus* described above in possessing completely mineralized  $M^1$  crown. This specimen, an older infant, is used only to describe deciduous tooth morphology.

The crowns of  $di^1$  and  $di^2$  are lingually flat, with rounded buccal surfaces; incisal margins are rounded. The  $dc$  resembles that of other lorisoids, possessing a buccolingually flattened single cusp.

$Dp^2$  is caniniform, resembling  $dc$ , except with distinct para- and distostyles.  $Dp^3$  has a conical paracone bracketed by para- and distostyles. It has a pronounced lingual cingulum with a slight swelling as a hypocone. Since both are only partially mineralized, it is impossible to say whether either has cingula except for the buccal cingulum that supports the parastyle of  $dp^3$ .  $Dp^4$  is a triangular shaped mass with three primary cusps; there is a small cingulum flaring distolingually, but no hypocone.  $M^1$  is fully mineralized.  $M^2$  is not visible, but may well have mineralized cusps that are separated from the skull, as the last developing molars in sequence form in advance of an osseous crypt.

Two replacement teeth are clearly visible: C and P<sup>2</sup>. I<sup>1</sup> and I<sup>2</sup> are not visible but are presumably in crypts hidden by the palate (premaxillary portion). A crypt for P<sup>3</sup> is visible, but small with no cusp within. There is no evidence of cusps for P<sup>3</sup> or P<sup>4</sup>.

### ***Mandibular dentition***

#### **Family Galagidae**

*Otolemur crassicaudatus* (Fig. 16) and *Otolemur garnettii*

The deciduous anterior tooth resemble the adult tooth comb. Di<sub>1</sub> and di<sub>2</sub> reach a MHD of 57 (*O. crassicaudatus*) to 85% (*O. garnettii*). Dc reaches a MHD of 75% at the apex of the tooth.

Dp<sub>2</sub> is also long and caniniform, but more robust than dc. Dp<sub>3</sub> is less mineralized than adjacent premolars, especially distolingually. The two mesial cusps are present. In an older (P26) *O. crassicaudatus*, the distal crown is mineralized as an extended shelf, including a hypoconid. At birth, dp<sub>3</sub> appears obliquely oriented in the tooth row. This may be a transient condition due to crowding because in the P26 specimen, the axis is more in line with other postcanine teeth. Dp<sub>4</sub> has four primary cusps and two small cusplets along the paracristid ridge. The talonid basin is deep and poorly mineralized in the center; the trigonid is shallow and elevated by comparison. The paracristid arcs sharply to the buccal side where it ends at a moderately-sized cusp. Dp<sub>4</sub> resembles M<sub>1</sub> closely, except that in the latter there is no cusp at the leading edge of the paracristid. M<sub>2</sub> has two mineralized cusps. In the newborn *O. crassicaudatus*, Dp<sub>2</sub> reaches a MHD of 85%, whereas dp<sub>3</sub> reaches a MHD of 75%. Dp<sub>4</sub> reaches a MHD of 85% predominantly located in the protoconid and metaconid. M<sub>1</sub> reaches a MHD of 75% at the metaconid. M<sub>2</sub> reaches a MHD of 25%. The newborn *O. garnettii* follows a similar pattern but since di<sub>1</sub> was absent, it is not precisely comparable. By one month of age, the crown of M<sub>1</sub> appears fully mineralized. M<sub>2</sub> is mineralized except for the center of the talonid basin. M<sub>3</sub> has two mineralized cusps.

I<sub>1</sub>, I<sub>2</sub>, and C are all small and located lingually to di<sub>1</sub>, di<sub>2</sub>, and dc respectively. The tip of the protoconid of P<sub>2</sub> is also mineralized. The deciduous anterior teeth reach the 25<sup>th</sup> percentile of MHD.

### *Galago moholi* and *G. senegalensis*

$Di_1$ ,  $di_2$ , and  $dc$  form the tooth comb, and closely resemble the replacement teeth. The roots of the anterior teeth are barely mineralized at birth, but have started to extend in an older *G. moholi* infant (P30). The deciduous incisors reach a MHD of 25%. In the newborn, all have deciduous teeth have a MHD reaching 50%.

$Dp_2$  is caniniform but broader than  $dc$  with a distal heel.  $Dp_3$  has a maximum of three cusps at birth. The largest, the protoconid, is rotated relative to its position in  $dp_4$ ; the metaconid is present but far smaller. In both *Galago* species, a large cusp mesial to the protoconid resembles a paraconid. In the P30 infant,  $dp_3$  is revealed to have an elongated crown, with a now extended distal surface leading to a distolingual heel.  $Dp_4$  is far larger and more molariform than  $dp_2$  and  $dp_3$ , with four primary cusps, as well as a mesiobuccal cusp at the leading edge of the trigonid basin.  $M_1$  is present with four cusps. Unlike  $dp_4$ , the trigonid basin slopes down toward the base of the crown. The talonid basin is poorly mineralized.  $M_2$  is present with only the protoconid mineralized. In the P30 infant,  $M_1$  is fully mineralized and  $M_2$  is mineralized except for the floor of the talonid basin; the protoconid and metaconid of  $M_3$  are mineralized as isolated cusps. At birth,  $dp_2$  reaches a MHD of 75%. Both  $dp_3$  and  $dp_4$  have a MHD of 85% (the latter at both mesial cusps). Similar to  $dp_4$ ,  $M_1$  has a MHD of 85% localized at the tip of the protoconid and metaconid.  $M_2$  protoconid is mineralized to 25% MHD.

The toothcomb teeth have permanent counterparts ( $I_1$ ,  $I_2$ , and  $C$ ). A small part of the cusp of  $P_2$  is present in a newborn *G. moholi*.  $I_1$ ,  $I_2$ , and  $C_1$  reach 25% MHD in *G. moholi*; they are at <25% MHD in *G. senegalensis*. The P30 infant possesses the same replacement teeth with more of the crowns mineralized.

### Family Lorisidae

#### *Nycticebus pygmaeus* (Fig. 16)

$Di_1$ ,  $di_2$ , and  $dc$  are all conical in shape. The  $dc$  is more robust than the incisors. The deciduous incisors each have a lingual longitudinal ridge and flanges flaring mesially and distally. The flanges are not clearly evident on  $dc$ , nor on  $C$ . Although this might be due to the

limits of resolution, it is noteworthy that the crowns are not fully mineralized, Dc and C may simply have marginal ridges closer to the crown base, as illustrated in *N. coucang* (see Fig 5.13, in Swindler, 2002). Each of those teeth has a hydroxyapatite density reaching 50% MHD.

Dp<sub>2</sub> is caniniform and broader than dc with a slight lingual heel. Dp<sub>3</sub> has one cusp, the protoconid, and a smaller mesial cusp that could be a paraconid. Both dp<sub>2</sub> and dp<sub>3</sub> crowns are incompletely mineralized – the dp<sub>2</sub> reaches a MHD of 75% whereas the dp<sub>3</sub> reaches a MHD of 85%. Dp<sub>4</sub> and M<sub>1</sub> are quadrate shaped with four cusps. Dp<sub>4</sub> has a small cusplet between the protoconid and metaconid; the talonid basin is incompletely mineralized. In M<sub>1</sub>, the two mesial cusps are mineralized and joined by a protocristid. However, the hypoconid and entoconid are isolated cusps as yet, since the adjacent basin is not mineralized. In *N. coucang*, a buccal cingulid is described in M<sub>1</sub> (Swindler, 2002). If present, it is not mineralized in newborn *N. pygmaeus*. In M<sub>1</sub>, the two mesial cusps are better mineralized than the distal pair (75 and 50% MHD for the protoconid and metaconid, respectively); only a small portion of the entoconid reaches the 25<sup>th</sup> percentile of MHD. One of the two newborns (sibling pair) is better developed than the other, and has three cusps of M<sub>2</sub> mineralized (no entoconid), while in the other, only the protoconid is mineralized.

Most of the crown of I<sub>1</sub>, I<sub>2</sub>, C, and P<sub>2</sub> are mineralized at birth. The anterior replacement teeth are far larger and better mineralized than their precursors: all reach or exceed the 85<sup>th</sup> percentile of MHD. P<sub>2</sub> reaches 50% MHD.

#### *Perodicticus potto*, infant

The anterior teeth resemble an adult tooth comb.

Dp<sub>2</sub> looks similar to dc, but more robust. Dp<sub>3</sub> has a flattened, sharp protoconid; a large heel projects from the base of the crown distolingually. Dp<sub>4</sub> has four primary cusps; the paracristid is obscured by the more fully erupted dp<sub>3</sub>. A cristid oblique intersects the protocristid close to the metaconid. The crown of M<sub>1</sub> appears fully mineralized.

Among replacement teeth, C and P<sub>2</sub> are partially mineralized; the permanent canine is more fully erupted. I<sub>1</sub> and I<sub>2</sub> are not visible. Small crypts for P<sub>3</sub> and P<sub>4</sub> are present with no cusps visible within.

## Hydroxyapatite density of mandibular tooth rows

### *Maximum Hydroxyapatite Density of crowns in perinatal or older infant specimens: no correlations with duration of fixation*

To ascertain whether prolonged fixation in formalin may demineralize the developing dentition, MHD measurement on sixty-six prosimian primates were plotted against the duration of fixation based on records of the Duke Lemur Center, or recorded transfer of frozen specimens to formalin fixation by the authors. MHD measurements were highly variable. The correlations were weak and non-significant for two mandibular teeth measured, including  $dp_4$  ( $r= 0.16$ ) and  $M_1$  ( $r= -0.08$ ). The range of fixation was quite broad, from 9 to 13,822 days. Scatterplots indicate no apparent downward trend in MHD based on increasing duration of fixation, as might be hypothesized based on acidification of formalin over time. Instead, the minimum to maximum MHD is similar at both ends of the range of fixation duration (Fig. 17).

### *Crown Hydroxyapatite Density in newborn specimens: phylogenetic patterns*

Mean mandibular MHD measurements for 40 primate species (20 haplorhines; 20 strepsirrhines; Table 4) and *Tupaia* are plotted against cranial length in Figures 31A and 31B. *Tupaia belangeri* scales far below all primates in MHD of  $dp_4$  and below strepsirrhines (with smaller anthropoids) for MHD of  $M_1$  (Fig. 18). For both teeth, MHD of *Tarsius syrichta* scales to cranial length similarly to strepsirrhines of comparable head size. Scaling patterns differ strikingly between anthropoid monkeys and strepsirrhines (Fig. 18). For both teeth, MHD of strepsirrhines is significantly and negatively correlated to cranial length ( $dp_4$ ,  $r = -0.39$ ;  $M_1$ ,  $r = -0.57$ ). In contrast,  $dp_4$  of anthropoids bears no significant correlation to cranial length, while  $M_1$  is positively correlated ( $r= 0.51$ ) with cranial length. In the case of  $M_1$ , there are clear outliers for each group. If the folivorous *Lepilemur* and *Propithecus* are excluded, the  $M_1$  of strepsirrhines has a stronger correlation of  $r = -0.72$ . Among anthropoids, the  $M_1$  of two tamarins (*Leontopithecus rosalia*, *Saguinus geoffroyi*) is of notably low MHD for their head size. Once tamarins are excluded, the correlation reaches 0.81.

Overall patterns of crown hydroxyapatite density reveal that the crowns with the densest hydroxyapatite are within the postcanine teeth of strepsirrhines; in most species MHD is located at the protoconid of  $dp_4$  (Fig. 19). The protoconid of  $dp_3$  may reach a similar range of density. In two strepsirrhines, *Propithecus coquereli* and *Lepilemur leucopus*,  $M_1$  has the densest crown (Fig. 18); this also describes *Tarsius syrichta* (Fig. 20). In contrast to strepsirrhines and tarsiers, in anthropoids the MHD of the anterior teeth may rival or exceed that of postcanine teeth (Fig. 20).

Certain phylogenetic patterns are evident. For example, even though cheirogaleids have a relatively high MHD of postcanine teeth (Fig. 18) much of the crown remains comparably poorly mineralized at birth. The most folivorous strepsirrhines do not consistently scale as having a higher or lower MHD than other strepsirrhines. The highest range of hydroxyapatite density (e.g., > 50% MHD) is localized at the cusps, whereas the basins and the base of the crowns is < 25% MHD (Fig. 18). *Varecia* spp. exhibit the same pattern (Figs. 19, 21), but they are aberrant among the large-bodied lemuroids. In lemurids, mineralization of most postcanine tooth crowns is more advanced in the basins and crown base compared to cheirogaleids. Exceptions include the talonid basin of  $dp_4$ , the crown base of  $dp_3$ , and  $M_1$ , each of which may be unmineralized or less mineralized than the rest of the crown. Newborn lorisoids have highly localized MHD at cusps of deciduous postcanine teeth, and tend to have poorly mineralized talonid basins. Cheirogaleids and lorisoids have advanced mineralization of replacement teeth, and in newborn *Nycticebus* the MHD of anterior replacement teeth actually exceeds that of their precursors (Fig. 19).

Anthropoids have distinctive family- or subfamily-level patterns in crown mineralization. Callitrichines are distinguished by advanced mineralization of the deciduous incisors at birth (Fig. 20). The crowns of these teeth are entirely mineralized, and the roots are more advanced in mineralization compared to other anthropoids. In contrast, the remaining teeth have completely unmineralized crown bases, and in  $dp_4$  the talonid basin is partially or completely unmineralized in all callitrichines except *Cebuella* (Figs. 10, 20). Delayed mineralization of  $dp_4$  is especially notable in newborn tamarins, in which the entoconid may be unmineralized as well. Aside from callitrichines, in most cebids the degree of mineralization appears to be more evenly advanced throughout the crown, with the entire crown of each deciduous tooth reaching at least 25% MHD.

All cercopithecoids have a distinctly less mineralized  $dp_4$  compared to more anterior teeth (Figs. 7, 8, 20).

In the most molariform teeth, the protoconid is typically the locus of MHD, followed by the metaconid; the entoconid is at the lowest hydroxyapatite density of all primary cusps. This is the case in nearly all primates. One exception is a day 6 *Tarsius*, in which the paraconid of  $M_1$  is the cusp at maximum density. However, in both  $M_2$  and  $M_3$  the protoconid is the site of MHD. In a day 0 *Tarsius*, both the protoconid and metaconid exceed the paraconid in MHD.

### ***Progression of crown mineralization: cross-sectional age samples***

Several cross-sectional age samples that bracket the newborn stage are shown in Figure 21. At the earliest time point examined (late fetal stage), both lemuroids have more advanced mineralization of the anterior teeth and  $dp_2$  relative to more posterior postcanine teeth. Specifically, MHD of all mandibular teeth is found within the former group of teeth; in contrast, a greater proportion of the crown of  $dp_3$  and  $dp_4$  remains unmineralized (Fig. 21). In the *Lemur* fetus (possessing a cranial length at 80% of that for average neonatal cranial length), the two mesial cusps of  $M_1$  are mineralized. In *Varecia*, which may be somewhat less advanced (at 73% of neonatal cranial length), only the protoconid of  $M_1$  is visible. The fetal *Propithecus*, which appeared close to neonatal size (cranial length is unavailable, but palatal length is 87% of that for known neonates), has fully formed deciduous crowns. The crown of  $dp_4$  (arrowheads) is the most uniformly well-mineralized of all deciduous teeth. The  $M_1$  crown (open arrows) is nearly fully formed, but aside from cusp tips, the hydroxyapatite density is less than that in  $dp_4$ .

Our cross-sectional age samples indicate different postnatal progression of cusp mineralization. In *Lemur*, newborns have a more mineralized  $dp_4$  relative to more anterior teeth, suggesting the former accelerates its rate of mineralization perinatally. *Varecia* also exhibits the same change, but it occurs later. At birth, and even at day 12,  $dp_4$  still has an incomplete crown, unlike newborn lemurids (Fig. 21). The crown of  $dp_4$  in our day 25 *Varecia* is at a stage comparable to similarly aged *Lemur* (Fig. 21) and *Eulemur* spp. (not shown). In contrast to the lemurids, all deciduous teeth of *Propithecus* become *relatively* less mineralized postnatally. That is, the range of HA density in permanent teeth reaches the highest parts of the overall range in

HA density (75 to 85% MHD at the cusp tips and some crests), while in deciduous teeth the entire crowns are < 50% of the overall range. In contrast,  $M_1$  is less mineralized compared to deciduous teeth in all specimens aged 0 to 25 days in *Lemur* and *Varecia*. In our sample, the protoconid of  $M_1$  overlaps the HA density of  $dp_4$  in a P28 *Lemur*, but not in a P25 *Varecia*. The wide disparity of crown mineralization rates among large-bodied lemurs is perhaps best emphasized in a comparison of a day 140 *Varecia* (a possible weaning age) with one-month-old *Propithecus*. In the *Varecia*, only  $M_1$  and  $M_2$  are mineralized as yet, and neither are in occlusion. In the much younger *Propithecus*,  $M_1$  is in occlusion already, and all permanent molar crowns are fully formed (Fig. 21).

## DISCUSSION

Knowledge of primate dental development has expanded considerably in the past several decades. In particular, observations on dental development (e.g., tooth eruption) have grown to encompass representatives of nearly all extant primate families (Smith et al., 1994; Godfrey et al., 2001; Smith et al., 2015). Increased resolution of  $\mu$ -CT in recent decades now provides a nondestructive means of expanding our knowledge of crown morphology and mineralization patterns.

### Methodological Considerations

***Maximum Hydroxapatite Density of teeth at pre-eruptive or late bell stages are unaffected by lengthy fixation in formalin***

We evaluated MHD measurements in two teeth that are in very different stages of ontogeny. The well-formed crowns of  $dp^4$  are advanced to a pre-eruptive stage in most newborn or older infant primates, meaning the enamel is fully formed in most species (see Smith et al., 2015). In contrast,  $M^1$  varies from a similar stage of maturity in highly folivorous species, to those that have just commenced the late bell stage (e.g., most callitrichines). Correlations reveal

no significant influence of lengthy formalin fixation on MHD on these teeth. This may indicate that the densest regions of the crown are unlikely to be demineralized and softened, even by decades of storage in formalin. In contrast, bone is documented to lose fracture resistance after prolonged fixation in formalin (e.g., Kikugawa and Asaka, 2004), suggesting bone demineralization occurs. We cannot discount the possibility that enamel is unaffected whereas the less hard dentin and cementin are more affected. It is also possible that the thinner periphery of enamel and dentin (e.g., nearer the crown cervix) are more affected than the densest core of the cusp tip. However, our findings on a large sample of subadult prosimians suggest that MHD is a reliable indicator of the extent of mineralization in developing crowns, especially within the densely mineralized cusp and crests. Selected specimens were stored in ethanol, some for decades. Although our sample of ethanol-stored specimens was far smaller, these data points did not differ noticeably from formalin-stored specimens at the species level.

### ***Micro-Computed Tomography parameters***

Numerous parameters affect radiographic visualization of mineralized tissues. Here we chose to standardize two variables: voxel size and energy levels. The majority of our volumes were reconstructed using 20.5  $\mu\text{m}$  cubic voxels. Our voxel size range is within the range used recently to morphometrically study the teeth of adult *Tupaia* spp. (Selig et al., 2019), mammals whose tooth crowns are similarly-sized to those of the smallest primates. That said, the unmineralized portions of some tooth crowns at birth prevent us from definitively determining presence or absence of some smaller cusps, especially those projecting from the cingula/cingulids.

Hydroxyapatite density of human teeth, including deciduous premolars, has been assessed at 70 kVp (He et al., 2011; Elfrink et al., 2013). Our efforts to differentiate surfaces of crowns using different energy levels (Fig. 3) strongly suggest that our highest energy level of 70 kVp offered the best possible fidelity of the crown surface in subadults; an added benefit is that it also allows a comparison of hydroxyapatite density in human teeth to our data on nonhuman primates.

## Newborn primate dentition: Morphology of deciduous teeth

Previous work on deciduous teeth has provided much detail on catarrhine primates (e.g., Swindler and McCoy, 1964; Siebert and Swindler, 1991; Winkler et al., 1991; Swarts, 1988), very limited morphological detail on platyrhines (Tarrant and Swindler, 1973; Hershkovitz, 1977), and only one detailed study on strepsirrhines (Tattersall and Schwartz, 1977).

Our results agree with previous findings, summarized in Swindler (2002) on morphology of the deciduous dentition in Old World monkeys. Of the two deciduous incisors, the  $di_1$  of each jaw possesses a rounded or flattened incisal margin, while the  $di_2$  has a more pointed cusp margin (caniniform). There is consistency of results at the genus level, e.g., our description of deciduous incisors of *T. francoisi* is similar to that figured for *T. cristata* by Swindler (2002; see Fig. 4.4 therein). Some details may vary. For example, Swindler also described mesial and distal ridges on  $di_1$  and  $di_2$  in some cercopithecines, but these are not apparent in the *Allenopithecus* specimen described here. Reconciling descriptions of the deciduous canines is made difficult since the crown base of the canine is typically still mineralizing at birth. As in permanent molars, the deciduous premolars are each bilophodont, with transverse crests connecting mesial and distal cusp pairs. The crowns appear complete at birth, although mineralization patterns suggest  $dp_3$  of the upper and lower jaws has undergone further matrix maturation than  $dp_4$  (see below). They each have four primary cusps; this excludes a putative paraconid of  $dp_4$ , which will be discussed further below. Mandibular  $dp_3$  is notably different than  $dp_4$  in that the mesial cusp pair is more closely opposed than the distal cusp pair. Swindler noted that stylar cusps are rare on upper deciduous premolars of Old World monkeys, but noted cusplets that are positionally consistent with parastyles in at least one of the premolars of *Trachypithecus cristata* and *Cercocebus torquata*. Our findings concur on the absence of meso- and metastyles, but we observed parastyles in all but one (*Colobus guereza*) of the six species we studied. It is of note that Swindler's samples for descriptive study (2002) were of mixed age subadults; it is possible smaller secondary cusps were subject to more wear than other crown structures. In the broad context provided by this study in combination with previous work on hominoids (e.g., Swarts, 1988), the close similarity in size of deciduous premolars is distinctive in catarrhines among all primates.

Our descriptions of deciduous teeth in platyrhines must be considered incomplete in some cases. For example, callitrichines have notably undermineralized dps at birth, preventing definitive assessment of cingula/cingulids, and small associated secondary cusps. Except for *Cebuella*, for which we possess a broader range of subadult ages, we exclude callitrichines from our summary of accessory cusps (Table 2). However, readers are referred to Hershkovitz (1977, Fig. V.28 therein), who indicated numerous deciduous teeth with stylar cusps, illustrating parastyles/metastyles on  $di^2$ , dc and the deciduous premolars. His illustration also indicates metastyles on  $di^2$  and  $dp^4$  (but not clearly shown on  $dp^2$ ,  $dp^3$ ).

Broadly, the platyrhines described here have caniniform  $di^2$  in contrast to the rounded or flat incisal margin of  $di^1$ . Deciduous canines of both jaws are poorly mineralized at the crown base in newborns, and are thus poor subjects for morphological description. We confirm the abrupt transition from caniniform  $dp^2$  and  $dp^3$  to highly molariform  $dp^4$  in callitrichines, as observed by Hershkovitz (1977). However, it can also be generalized that in all platyrhines,  $dp^4$  is distinct from other deciduous premolars in its close morphological similarity to  $M^1$ . The same is observed for the lower premolars. Thus, no platyrhines has the near size parity of deciduous premolars observed for catarrhines. With the exception of *Aotus* and *Callicebus*, stylar cusps are far more common in the platyrhines we studied compared to catarrhines (Table 2).

The present study examines the broadest sampling of strepsirrhines confirmed at newborn age to date. Here, we can confirm that  $dp^4$  of both jaws is abruptly more molariform and robust compared to more anterior premolars (an exception is *Propithecus* and *Lepilemur*, in which  $dp^4$  is much smaller than  $M^1$ , though still more molariform than  $dp^3$ ). A raised mesial shelf is also visible in most mandibular  $dp^4$ s, and may possess a putative paraconid. The presence of accessory cusps can be confirmed in some species (Table 2), but in cheirogaleids the crown bases are too poorly mineralized to confirm presence or absence. The readers are referred to Tattersall and Schwartz (1974), who noted that *C. major* was the only cheirogaleid in their sample that lacked a parastyle on  $dp^4$ .

A final consideration is the putative paraconid. Swindler (2002) discussed a mesial cusp, at the leading edge of the paracristid in some catarrhines. He noted that paraconid is present 80% of the time on  $dp^3$  of colobines, and that it was previously described in some cercopithecines. Tattersall and Schwartz (1977) described a paraconid in some strepsirrhines (e.g., *Hapalemur*),

and similar cusps are visible on numerous strepsirrhine described here. We do not make a claim here of homology to the clear and pronounced paraconid observable in tarsiers. Yet, it is noteworthy that this cusp was at least weakly pronounced in most of the catarrhines examined here. Moreover, it is positionally similar to a small cusp in some other primates, as described below. The cusp is more buccally positioned than the paraconid of  $M_1$  in tarsiers (as is the entire paracristid). A critical difference between  $M_1$  and  $dp_4$  of all extant primates described to date (except tarsiers) is the raised mesial edge of the latter, producing a mesial “shelf” that is lacking in  $M_1$ . This creates a vexing dilemma: any cusplet that forms at the leading edge of this shelf, regardless of homology, projects upward similarly to a paraconid. As there is a distinct concentration of hydroxyapatite density at birth may support homology, but further cross-sectional age studies are needed for confirmation.

### **Sequence of crown mineralization in the perinatal period**

The process of dental crown formation has been well studied in humans (e.g., Kraus and Jordan, 1965) and several anthropoid species have been studied in some depth (Swindler and McCoy, 1964; Swindler et al., 1968; Tarrant and Swindler, 1973). Swindler (2002) described the pattern of cusp mineralization for both upper and lower molariform teeth in a common pattern: beginning with the buccomesial cusp (e.g., paracone), mineralization proceeds lingually, (protocone), then buccodistally, and finally distolingually. He emphasized some variation in the transition to the second and third cusps (e.g., whether protocone or hypocone mineralizes first).

Swindler’s observations were based on a number of catarrhines and one platyrhine. With the large sample examined here, this pattern appears to hold for primates broadly. Several observations support this. First, in cross-sectional age samples, if only one cusp of a molariform tooth is mineralized at a given age, it is invariably the buccomesial cusp (Fig. 21). If only two cusps are mineralized, it is typically the two mesial cusps. If only one cusp remains unmineralized in mandibular molariform teeth, it is the distolingual cusp in all cases. Our samples also confirm some variation. For example, in one *Varecia* newborn the two buccal cusps are mineralized while both lingual cusps are not (Fig. 21). A second line of evidence may be gleaned from hydroxyapatite densities observed in subadult crowns. The same patterns are

observed: the greatest hydroxyapatite density is found buccomesially (or mesially, when both mesial cusps presumably have reached a similar density range), and then density is sequentially lower in the same sequence that cusps appear. This is likely only typical at early ages. Kraus and Jordan (1965) maintained that the rate of mineralization among cusps changes postnatally across human development. Supporting this, Kono et al. (2002) found that enamel thickness of the hypoconulid was greater than that of the protoconid in the human  $M_1$ .

## Phylogenetic patterns of crown mineralization

### ***Molariform teeth***

Using histological material, the state of mineralization of the maxillary teeth at birth was recently discussed by Smith et al. (2015).  $Dp^4$  is well mineralized in most primates, except in most neonatal callitrichines and *Varecia*.  $M^1$  of galagids, indriids and tarsiers is at a more advanced state of mineralization than lemurids or anthropoids (see also Godfrey et al., 2004);  $M^1$  is more mineralized in catarrhines than in most platyrhines. Given that these teeth are equally molariform in primates and functionally similar, these observations illustrate that primates have different strategies in transitioning the role of  $dp^4$  toward its successor.

Our new observations on mandibular tooth crowns agree with our previous histological work, but the present report expands observations to a broader array of primates. In nearly all primate genera studied, at least some neonates have initiated mineralization of  $M_1$  (Fig. 22). *Leontopithecus* was an exception, however, only one specimen was examined. Given that at least some newborns have  $M^1$  commencing the late bell stage (Smith et al., 2015), we expect that may be the case for the mandibular counterpart. Our finding also put the more commonly studied hominid teeth in a broader perspective. In great apes and humans (Kraus and Jordan, 1965; Siebert and Swindler, 1991; Winkler et al., 1991),  $dp_4$  is well mineralized but may have an unmineralized central basin or an isolated hypoconid, and  $M_1$  is represented only by isolated cusps. In contrast, in all cercopithecoids the central basin and primary cusps have merged at birth, and in many newborns the two mesial cusps of  $M_1$  are connected by a mineralized protocristid (Fig. 22). In this manner, well-described hominids (noting that newborn *Gorilla* remains poorly investigated) are less advanced in mineralization of both of these teeth at birth. Platyrhines vary

more than catarrhines. *Callithrix* and all tamarins have the least complex dp4 and M1 crowns among all anthropoids. *Cebuella* and most platyrhines have complete, or nearly complete dp4 crowns at birth, and M<sub>1</sub> is represented by two to three isolated cusps; in some cases the mesial cusp pair are bridged. Among platyrhines we have examined, *Pithecia pithecia* has the most advanced development of M<sub>1</sub>, with mineralization of the central basin underway (Fig. 22).

Mineralization of permanent molars at birth in *Tarsius syrichta* is entirely similar to *T. bancanus* (Luckett and Maier, 1982). M<sub>2</sub> is fully formed except for the center of the talonid basin; M<sub>3</sub> already has two mineralized cusps. No extant anthropoid that has been studied approaches this degree of advanced mineralization. Among strepsirrhines, there is an even starker disparity. *Varecia* spp. have the least mineralized crowns of all primates. On the other hand, lorisoids, indriids (see also Godfrey et al., 2004), and *Lepilemur* have more advanced permanent molar mineralization than any primate (Table 5, Fig. 22).

### ***Replacement teeth***

Extant anthropoids are revealed to have a unified tendency to delay mineralization of replacement teeth. Only *Callicebus*, *Pithecia*, and *Cebuella* possessed any mineralized portions of replacement teeth. As with the upper jaw (Smith et al., 2007), mineralization of replacement teeth in *Cebuella* is not observed in all newborns. Moreover, our previous histological work on maxillary teeth revealed that among all anthropoids, only callitrichines possess replacement tooth germs that were more advanced than the cap stage. Thus, we would generalize that 1) mineralization of replacement teeth is uncommon at birth in anthropoids broadly, 2) few anthropoids invest at all in prenatal mineralization of these teeth, and 3) only anterior replacement teeth, if any, may be mineralized at birth.

Strepsirrhines vary far more in the development of replacement teeth. Although teeth of *Varecia* spp. are undermineralized compared to all other true lemurs, it may be generalized that all lemurids delay mineralization of replacement teeth relative to other strepsirrhines. Only *Eulemur* spp. commonly (not always) have mineralized replacement teeth, and if so, only the cusp tips of the anterior teeth are seen. The anterior teeth are more advanced in mineralization in

all lorisoids; *Nycticebus* is the only strepsirrhine in our sample with a premolar mineralization ( $P_3$ ). *Lepilemur* and *Propithecus* have initiated  $P_4$  mineralization as well.

### **Degree of crown mineralization: Patterns of hydroxyapatite density in newborn crowns**

Anthropoids have a general pattern that distinguishes them from all other extant primates. Their anterior teeth and first deciduous premolar (upper and lower  $dp_2$  or  $dp_3$ ) have the most surface area of relatively dense crown (as estimated by distribution of hydroxyapatite density – Fig. 20) and are often the locus of MHD within the tooth row. In tarsiers and strepsirrhines, both anterior and postcanine teeth tend to have extensive parts of the crown at > 50% MHD for the mandibular tooth row (Figs. 19-20). In other words, the overall hydroxyapatite density is more evenly distributed among teeth in strepsirrhines (and also tarsiers) compared to anthropoids. In addition, the MHD among mandibular teeth most frequently occurs at the protoconid of  $dp_4$ , or more rarely at  $M_1$  (*Propithecus*, *Lepilemur*, and some galagids).

Our preliminary comparison of MHD measurements in primate mandibular teeth shows that strepsirrhines, and especially small-bodied species, have higher  $dp_4$  and  $M_1$  MHD at birth than anthropoids. It remains of great interest how these data compare in an analysis that controls for phylogeny and body size. However, our results support a previous assertion based on maxillary tooth germs (Smith et al., 2017). Since  $M_1$  volume is positively correlated with cranial length in all strepsirrhines, our finding of a *negative* correlation of MHD with cranial length supports our conclusion that tooth germ size and degree of mineralization at birth are highly independent, and that growth and mineralization proceed at different rate across gestational time.

Hominoid newborn samples remain unavailable to us at this time, and the relationship of their data to other primates remains of great interest. Still, we can at least assess peak densities newly reported here to previous work on humans using the same CT energy parameters. In human children of 4 to 5.8 years,  $dp_4$  was reported to range from 1345 to 2077 mg/cc (Elfrink et al., 2013). Among strepsirrhines, specimens of several species (*Microcebus*, *Nycticebus*, *Lemur*) exhibit a MHD of  $dp_4$  exceeding 1500 mg/cc. In anthropoid monkeys studied here, no newborns exceed that density, and only one specimen (*Saimiri*) exceeds 1400 mg/cc. The MHD of  $M_1$  in humans from 18-25 years ranges from 2006.5-2281.8 mg/cc (He et al., 2011). The densest foci of

$M_1$  crowns measured here are observed in *Tarsius* and *Nycticebus* (both  $> 1500$  mg/cc), and *Propithecus* ( $> 1400$  mg/cc). In contrast, only one anthropoid measured here exceeds a MHD 800 mg/MHD. Of course, the published human data are from ontogenetically disparate samples. We may expect that MHD measured in the humans does not reveal true peaks, since some of the denser apical enamel likely wore away. Most certainly, most if not all primates studied here are still undergoing maturation of enamel. However, this comparison enables us to see that broadly, newborn anthropoids have lesser MHD of  $dp_4$  and especially  $M_1$  compared to the fully formed homologues in human children. In newborn strepsirrhines,  $dp_4$  already falls within the range observed for the  $M_1$  of young adult humans.

### ***Early postnatal rates of mineralization***

Our small cross-sectional age samples suggest that mineralization rate shifts within the mandibular tooth row during early ontogeny. In the late fetal lemurids in our sample, MHD is located in more anterior deciduous teeth than at birth. MHD is found in  $d_1$  to  $dc$  in fetal *Lemur* and *Varecia*, and shifts posteriorly in newborns. In *Varecia* this shift occurs over a longer time span (day 0 to 12) than in *Lemur* (by day 0). A similar transition occurs in *Propithecus*, but the MHD and overall crown density increase in the permanent molars rather than  $dps$  (Fig. 21). This indicates shifting rates of mineralization. Initially, MHD likely reflects the timing at which teeth enter the later bell stage, occurring in an anterior to posterior direction. A shift in MHD to teeth with greater importance in crushing food begins perinatally.

In galagids, as in lemurids, maps of HA density indicate a likely shift in mineralization rates. Maximum HA density is initially centered on cusps of  $dp_3$  and  $dp_4$ . By one month of age, maximum HA density is centered at the protoconid of  $M_1$ , suggesting an acceleration of mineralization in permanent molars.

Among anthropoids, there is a more limited representation of different age stages in our sample, however *Cebuella* and *Saguinus oedipus* provide useful contrasts to show the extent of variability. In newborn *Cebuella*,  $M_1$  is more mineralized than in other callitrichines, and the cusp tips of two replacement teeth ( $I_1$ ,  $I_2$ ) are present. In an infant specimen (which resembles a specimen recorded at one-month-old)  $P_2$  and  $P_4$  have initiated mineralization. In *Saguinus* at one

month of age,  $M_1$  is still incompletely mineralized (lacks an entoconid) and only the very tip of  $I_1$  is mineralized. In a specimen 117 days old, only the cusp tips of the three anterior replacement teeth are mineralized.

Our findings comparing MHD among species at age-matched time points reveals variation in postnatal rate of mineralization between and within primate suborders (Table 7). In the case of the most molariform teeth ( $dp_4$  and  $M_1$ ), only *Cebuella* is known to be as precocious as most strepsirrhines in terms of age at crown completion. Among anthropoids and strepsirrhines, catarrhines and *Lemur*, respectively, stand out in having early completion of  $dp_4$  crown.

There is perhaps a greater range in timing of replacement teeth. As expected based on observations of maxillary cusp mineralization in newborns (Smith et al., 2015), cheirogaleids, indriids and galagids have more rapid mineralization of the first permanent molar and the first permanent incisor (the first replacement tooth to mineralize) compared to all other primates except tarsiers. Lemurids are delayed by comparison, but still may well reach these two dental milestones before weaning (Table 7).

Simply looking at newborns alone, it is apparent that strepsirrhines exhibit vastly different rates of mineralization of mandibular teeth, as reported for eruption rates. There appear to be strongly phylogenetic patterns as discussed above (Fig. 19), and as recently discussed for eruption sequences (López-Torres et al., 2015; Monson et al., 2019). But it may also be the case that other factors may influence variation within families. In addition, the influence on primate social behaviors and group size are worth consideration. Primates with later weaning appear to be particularly variable in the rate of at which molariform crowns are completed (Table 6), and in which replacement teeth begin to mineralize (Table 7). Among strepsirrhines, those primates that are left in nests and/or “parked” while the mother forages tend to have advanced mineralization of replacement teeth at birth. In contrast, those that cling and then ride the mothers may or may not have mineralized replacement teeth at birth (Fig. 23); what factors influence these patterns is a matter a future interest.

## Conclusions

### ***Phylogenetic implications***

Because deciduous teeth were previously described in far fewer taxa relative to permanent teeth, their phylogenetic and functional importance has been rarely discussed. The findings herein may provide a better context to comparative and paleontological studies. While individual fossil deciduous teeth will continue to be described with regularity, we await opportunities to see more subadults with fully preserved deciduous dentition (e.g., Bloch et al., 2002; Franzen et al., 2009). Although it is difficult to assign precise ages to such fossils, and newborns are less likely to be well preserved than older subadults, knowing variability in the mineralization and eruption rates in extant primates provides a valuable comparative lens with which to view these fossils.

Of great interest in future studies is the antiquity of anthropoid patterns of dental development. Nearly all extant anthropoids have pronounced delays in mineralization of replacement teeth, especially premolars. Knowing the origin of these delays offers clues to life history characteristics of extinct relatives.

Lemurids require further exploration for similar reasons. The greater abundance of subfossil material may be of great comparative value to understand the deferred investment in mineralization of replacement teeth by lemurids.

In fossil primates, deciduous teeth have been used to infer relationships of extant species. Benefit (1994) compared deciduous premolars of extant cercopithecoids to a fossil cercopithecine, *Victoriapithecus*. The latter lacked distinct crests associated with bilophodont teeth; such observations have implication for the relationships of extant cercopithecoids to fossil species. The primitive dental eruption sequence for Primates is of great interest. Fossils of primates and other euarchontans may allow us to further explore how various factors influence developmental pacing of dental maturation and eruption (Smith, 2000; Bloch et al., 2002; Gingerich and Smith, 2010; López-Torres et al., 2015; Monson and Hlusko, 2018).

### ***Patterns of dental development***

Strepsirrhines and anthropoids have clear differences in the relationship of MHD to cranial length. The relatively strong correlation of  $dp_4$  and  $M_1$  MHD in strepsirrhines is striking in several ways. First of all, dental germ volume of all strepsirrhines (and all primates) is positively correlated with head size (unsurprisingly, in absolute size, larger heads house larger teeth). This relationship is negative regarding MHD, suggesting that smaller species may be accelerating tooth mineralization. Secondly, this relationship in strepsirrhines contrasts clearly with anthropoids. Anthropoids show no clear pattern at all in MHD of  $dp_4$ , but have a strong *positive* correlation of  $M_1$  MHD to cranial length. To the extent that cranial length includes both a neurocranial and midfacial component, it is presently difficult to explain this dichotomy. However, the positive relationship of anthropoid  $M_1$ , but not  $dp_4$ , to cranial length recalls that among all teeth,  $M_1$  development bears a strong correlation to brain growth (Smith et al., 1994; Godfrey et al., 2001). A future study is needed to isolate the specific relationship of neonatal MHD to neurocranial measurements (e.g., endocranial volume). Finally, the findings on MHD confirm our previous conclusion, based on qualitative observations, that dental mineralization and dental germ growth do not closely covary (Smith et al., 2017).

For now, we interpret the MHD data with caution as they may only measure how densely HA is deposited in cusps and crest of teeth, the portions of teeth that mineralize first (Tarrant and Swindler, 1973). We do not yet know whether the overall extent of mineralization at birth also differs, and this might best be assessed by measuring crown volumes relative to fully mineralized crowns of older specimens. Analysis of these two measurements in concert could elucidate whether primates vary in the pace of tooth maturation or simply in the pattern by which they mineralize.

### ***Factors influencing dental development***

Diet, life history, and phylogeny have been discussed as the biggest factors in the pace of dental eruption (e.g., Smith et al., 1994; Godfrey et al., 2001; Smith et al., 2017; Monson and Hlusko, 2018). If defined based on dental eruption schedules, ontogenetic stages such as “infancy” do not always follow a similar duration across species, even in species of similar lifespans (Smith, 1994; Godfrey et al., 2001). Some primates are especially precocious in

development of the permanent teeth, in some cases forecasting their dietary specialization (Godfrey et al., 2004). But life history traits such as the duration of gestation have complex relationships with dental growth, and these affect development of the deciduous and permanent teeth differently. For example, relative deciduous premolar volume scales negatively with relative gestation length in strepsirrhines at birth, whereas  $M^1$  scales positively (Smith et al., 2017). The convergence of dietary specialization adds additional complexity. Folivorous species are outliers with larger than predicted  $dp_4$  (*Hapalemur*) or  $M_1$  (*Propithecus*) volume when plotted against relative gestation length (Smith et al., 2017). Dental maturity during infancy reflects adaptation, even prior to use in mastication.

Our observations on the extent of crown mineralization and MHD do not reveal consistent patterns reflecting diet. The three highly folivorous strepsirrhines studied here (*Lepilemur*, *Propithecus*, and *Hapalemur*) are notable in the relative completeness of the  $M_1$  crown (Fig. 22). *Lepilemur* and *Propithecus* have notably high MHD in  $M_1$  at birth (relative to cranial length), but this is not apparent in *Hapalemur*. Among anthropoids, the seed-eating *Pithecia* is notable for the degree of completeness of its  $M_1$  crown, but *Colobus*, *Trachypithecus* and *Alouatta* are not more advanced in  $M_1$  crown formation than most non-folivores (Fig. 22). MHD of  $M_1$  in highly folivorous anthropoids does not appear notably higher than non-folivores, relative to body size. However, all folivorous anthropoid species are only available to us as single specimens at this time.

The influence of life history variables such as gestation length and weaning age on dental mineralization in primates has not been studied. Generally, monkeys have a more prolonged process of dental mineralization that begins with non-grinding teeth, while mineralization of postcanine teeth, especially  $M_1$ , is delayed until after birth. This may in part be a result of relatively later weaning in most anthropoid primates. However, it is also striking that in some strepsirrhines the crowns of  $dp_4$  and  $M_1$  are poorly mineralized; an altricial state similar to hominoids. The departure of lemurids from the overall trend in strepsirrhines, of relatively well-developed crowns at birth, suggests additional factors have an influence. Whether this is explained purely by phylogeny, life history, or perhaps infant care strategies requires a future phylogenetically-controlled quantitative study.

## **Acknowledgements**

Our study is supported in part by grant number P51 OD011132 to Yerkes Center. This project also used biological materials collected at SNPRC and funded by the Office of Research Infrastructure Programs/ OD P51 OD011133. Specimens were also obtained through the Duke Lemur Center's Director's Fund. We also thank A.M. Burrows and L.T. Nash for providing selected samples. Thank you to E. Hoeger and N. Duncan for providing access to specimens from the AMNH. This is DLC publication # 1443.

## REFERENCES

Ahrens H. 1913. Die Entwicklung der menschlichen Zähne. *Anat Hefte* 48:169–257.

Anemone RL, Mooney MP, Siegel MI. 1996. Longitudinal study of dental development in chimpanzees of known chronological age: Implications for understanding age at death of Plio-Pleistocene hominids. *Am J Phys Anthropol* 99:119-133.

Anemone RL, Skinner MM, Dirks W. 2012. Are there two distinct types of hypocone in Eocene primates? The ‘pseudohypocone’ of notharctines revisited. *Paleontol Electron* 15, Issue 3;26A.

Avery JK. 2002. Oral development and histology. 3<sup>rd</sup> ed. New York: Thieme Medical Publishers.

Benefit BR. 1994. Phylogenetic, paleodemographic, and taphonomic implications of *Victoriapithecus* deciduous teeth from Maboko, Kenya. *Am J Phys Anthropol* 95:277-331.

Blechschmidt E. 1954. Rekonstruktionsverfahren mit Verwendung von Kunststoffen. Ein Verfahren zur Ermittlung und Rekonstruktion von Entwicklungsbewegungen. *Z Anat EntwicklGesch* 118:170–174.

Bloch JI, Boyer DM, Gingerich PD, Gunnell GF. 2002. New primitive paromomyid from the Clarkforkian of Wyoming and dental eruption in plesiadapiformes. *J Vert Paleontol* 22:366-379.

Bouxsein MJ, Boyd SK, Christiansen BA, Guldborg RE, Jepsen KJ, Muller R. 2010. Guideline for assessment of bone microstructure in rodents using micro-computed tomography *J Bone Min Res* 25:1468-1486.

DeLeon VB, and TD Smith. 2014. Mapping the nasal airways: using histology to enhance CT-based three-dimensional reconstruction. *Anat Rec* 297:2113-2120.

Elfrink MEC, ten Cate JM, van Ruijven LJ, Veerkamp JSJ. 2013. Mineral content in teeth with deciduous molar hypomineralisation (DMH). *J Dentistry* 41:974-978.

Fleagle JG. 2013. Primate adaptation and evolution. New York: Academic Press.

Franzen JL, Gingerich PD, Habersetzer J, Hurum JH, von Koenigswald W, Smith BH. 2009. Complete primate skeleton from the Middle Eocene of Messel in Germany: morphology and paleobiology. *PLoS One* 4(5): e5723.

Garn SM, Lewis AB, Polacheck DL. 1959. Variability of tooth formation. *J Dent Res* 38:135–148.

Gingerich PD, Smith BH. 2010. Premolar development and eruption in the early Eocene adapoids *Cantius ralstoni* and *Cantius abditus* (Mammalia, Primates). *Contrib Mus Paleontol, Univ Mich* 3241-47.

Godfrey LR, Samonds KE, Jungers WL, Sutherland MR. 2001. Teeth, brains, and primate life histories. *Am J Phys Anthropol* 114:192-214.

Godfrey LR, Samonds KE, Jungers WJ, Sutherland MR, Irwin MT. 2004. Ontogenetic correlates of diet in Malagasy lemurs. *Am J Phys Anthropol* 123: 250-276.

He B, Huang S, Zhang C, Jing J, Hao Y, Xiao L, Zhou X. 2011. Mineral densities and elemental content in different layers of healthy human enamel with varying teeth age. *Arch Oral Biol* 56:997-1004.

Hershkovitz P. 1977. Living New World monkeys (Platyrrhini). Vol. 1. Chicago: University of Chicago Press.

Jernvall J, Kettunen P, Karavanova I, Martin LB, Thesleff I. 1994. Evidence for the role of the enamel knot as a control center in mammalian tooth cusp formation: non-dividing cells express growth stimulating Fgf-4 gene. *Int J Dev Biol* 38: 463-469.

Kappeler PM, Pereira ME. 2003. Primate life histories and socioecology. Chicago: University of Chicago Press.

Kikugawa H, Asaka T. 2004. Effect of long-term formalin preservation on bending properties and fracture toughness of bovine compact bone. *Mater Trans JIM* 45:3060–3064.

Kono RT, Suwa G, Tanijiri T. 2002. A three-dimensional analysis of enamel distribution patterns in human permanent first molars. *Arch Oral Biol* 47:867-875.

Kraus BS, Jordan R. 1965. The human dentition before birth. Philadelphia: Lea and Febiger.

López-Torres S, Schillaci MA, Silcox MT. 2015. Life history of the most complete fossil primate skeleton: Exploring growth models for *Darwinius*. *Royal Soc Open Sci* 2:1-15.

Luckett WP, Maier W. 1982. Development of deciduous and permanent dentition in *Tarsius* and its phylogenetic significance. *Folia Primatol* 37:1-36.

Macchiarelli R, Bondioli L, Debénath A, Mazurier A, Tournepiche J-F, Birch W, Dean C. 2006. How Neanderthal molar teeth grew. *Nature* 444: 748-751.

Mann A. 1988. The nature of Taung dental maturation. *Nature* 333:123.

Monson TA, Hlusko LJ. 2018. Breaking the rules: Phylogeny, not life history, explains dental eruptionsequence in primates. *Am J Phys Anthropol* 167: 217-233.

Monson TA, Coleman JL, Hlusko LJ. 2019. Craniodental allometry, prenatal growth rates, and the evolutionary loss of the third molars in New World monkeys. *Anat Rec* 302:1419-1433.

Nanci A. 2007. Ten Cate's oral histology: development, structure, and function. 9<sup>th</sup> Ed. St. Louis: Elsevier.

Oka SW, Kraus BS. 1969. The circumnatal status of molar crown maturation among the Hominoidea. *Archives Oral Biol* 14: 639-659.

Ooë T. 1979. Development of human first and second permanent molar, with special reference to the distal portion of the dental lamina. *Anat Embryol* 155:221–240.

Radlanski RJ. Morphogenesis of human tooth primordia: the importance of 3D computer-assisted reconstruction. *Int J Dev Biol* 1995;39:249–256.

Reinholt LE, Burrows AM, Eiting TP, Dumont ER, Smith TD. 2009. Brief communication: Histology and microCT as methods for assessing facial suture patency. *American Journal of Physical Anthropology*, 138:499-506.

Rosenberger AL. 2011. Evolutionary morphology, platyrhine evolution, and systematics. *Anat Rec* 294:1955–1974.

Schwartz JH. 2007. *Skeleton Keys*. New York: Oxford University Press.

Selig KR, Sargis EKJ, Silcox MT. 2019. Three-dimensional geometric morphometric analysis of treeshrew (Scandentia) lower molars: insight into dental variation and systematics. *Anat Rec* (in press).

Seibert JR, Swindler DR. 1991. Perinatal dental development in the chimpanzee (*Pan troglodytes*). *Am J Phys Anthropol* 86: 287-294.

Sirianni JE, Swindler DR. 1985. Growth and development of the pigtailed macaque. Boca Raton:CRC Press.

Smith BH. 1994. Patterns of dental development in *Homo*, *Australopithecus*, *Pan*, and *Gorilla*. *Am J Phys Anthropol* 94: 307-325.

Smith BH, Crummett, Brandt KL. 1994. Ages of eruption of primate teeth: A compendium foraging individuals and comparing life histories. *Yrbk Phys Anthropol* 37:177-231.

Smith BH. 2000. 'Schultz's Rule' and the evolution of tooth emergence and replacement patterns in primates and ungulates. In: Teaford M, Smith MM, Ferguson MWJ, editors. *Development, Function and Evolution of Teeth*. Cambridge: Cambridge University Press. p. 218-228.

Smith TD, DeLeon VB, Vinyard, CJ, Young JW. In press. *Skeletal anatomy of the newborn primate*. Cambridge: Cambridge University Press.

Smith TD, Jankord KD, Progar AJ, Bonar CJ, Evans S, Williams L, Vinyard CJ, DeLeon VB. 2015. Dental maturation, eruption, and gingival emergence in the upper jaw of newborn primates. *Anat Rec*, 298:2098–2131.

Smith TD, Muchlinski MN, Bucher WR, Vinyard CJ, Bonar CJ, Evans S, Williams L, DeLeon VB. 2017. Relative tooth size at birth in primates: Life history correlates. *Amer J Phys Anthropol*, 164:623-634.

Smith TD, Rossie JB, Cooper GM, Carmody KA, Schmieg RM, Bonar CJ, Mooney MP, Siegel MI. 2011. Comparative micro CT and histological study of maxillary pneumatization in four species of New World monkeys: The perinatal period. *Am J Phys Anthropol* 144:392-410.

Swarts JD. 1988. Deciduous dentition: Implications for hominoid phylogeny. In: JH Schwatz (ed.), *Orang-utan Biology*. New York: Oxford University Press. Pp 263-270.

Swindler DR. 2002. Primate dentition. An introduction to the teeth of non-human primates. New York: Cambridge University Press.

Swindler DR, McCoy HA. 1964. Calcification of deciduous teeth in rhesus monkeys. *Science* 144:1243-1244.

Swindler DR, Orlosky FJ, Hendrickx AG. 1968. Calcification of the deciduous molars in baboons (*Papio anubis*) and other primates. *J Dent Res* 47:167-170.

Swindler DR, Beynon AD. 1993. The development and microstructure of the dentition in *Theropithecus*. In: Jablonski NG (ed.), *Theropithecus*: The rise and fall of a primate genus. Cambridge: Cambridge University Press. Pp. 351-381.

Tarrant LH, Swindler DR. 1973. Prenatal dental development in the black howler monkey (*Alouatta caraya*). *Am J Phys Anthropol* 38:255–260.

Tattersall I, Schwartz JH. 1974. Craniodental morphology and the systematics of the Malagasy lemurs (Primates, Prosimii). *Anthrop. Papers Amer Mus Nat Hist* 52:139-192.

Winkler LA, Schwartz JH, Swindler DR. 1991. Aspects of dental development in the orangutan prior to eruption of the permanent dentition. *Am J Phys Anthropol* 86:255-271.

Zehr SM, Roach RG, Haring D, Taylor J, Cameron FH, and Yoder AD. 2014. Life history profiles for 27 strepsirrhine primate taxa generated using captive data from the Duke Lemur Center. *Scientific Data* 1, Article number: 140019.

FIGURES:

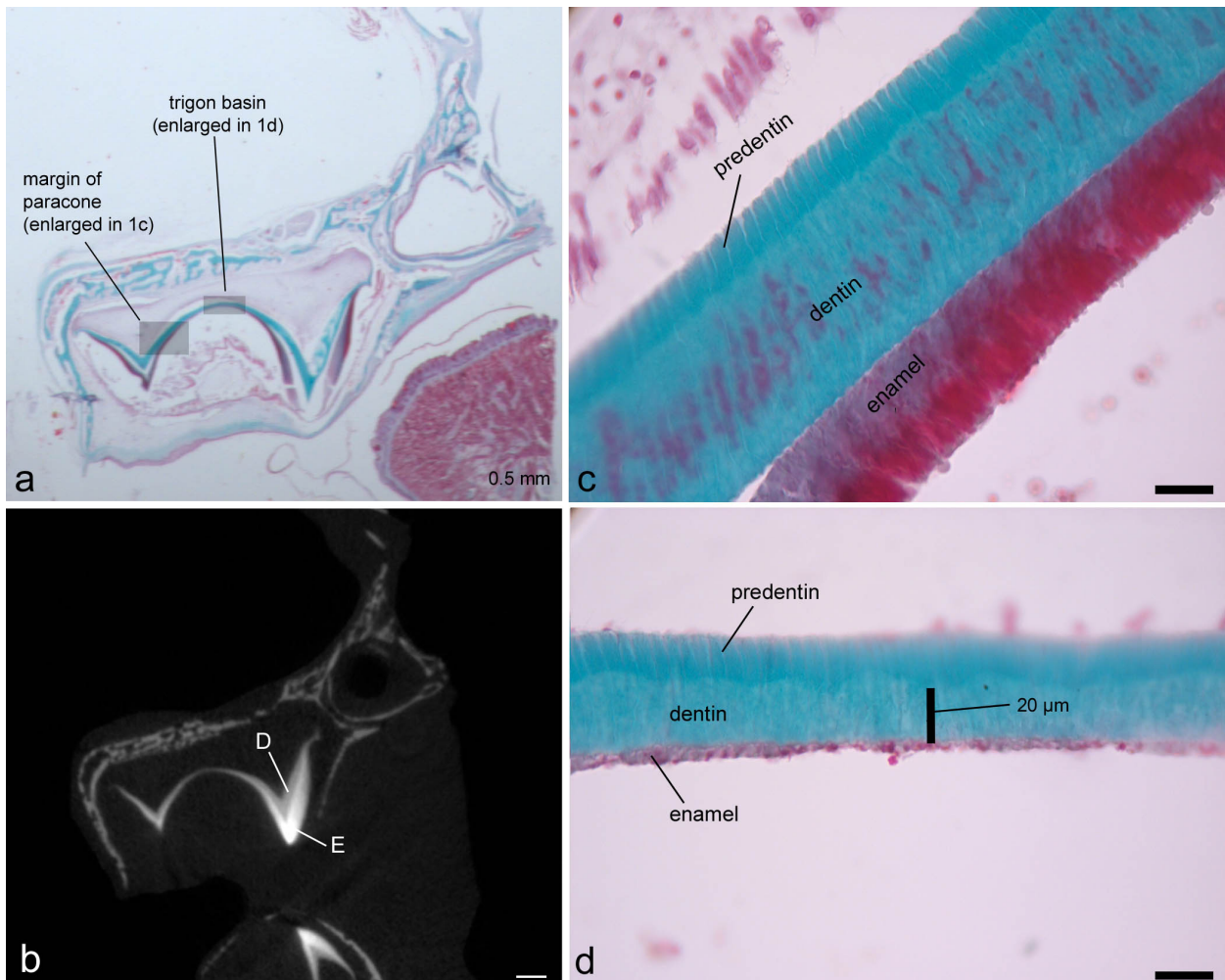


Figure 1: Matching histology and  $\mu$ -CT slices, following alignment (a, b), showing  $M^1$  of *Tarsius syrichta*. Boxes indicate site of enlarged views (c, d). Enamel (E) and dentin (D) are distinct at the cusp tip (e.g., protocone shown in 1b). However, near the base of the cusps (e.g., paracone, 1c), or in the basins (1d) microCT cannot distinguish enamel and dentin. Scale bars: a,b, 0.5mm; c,d 20  $\mu$ m.

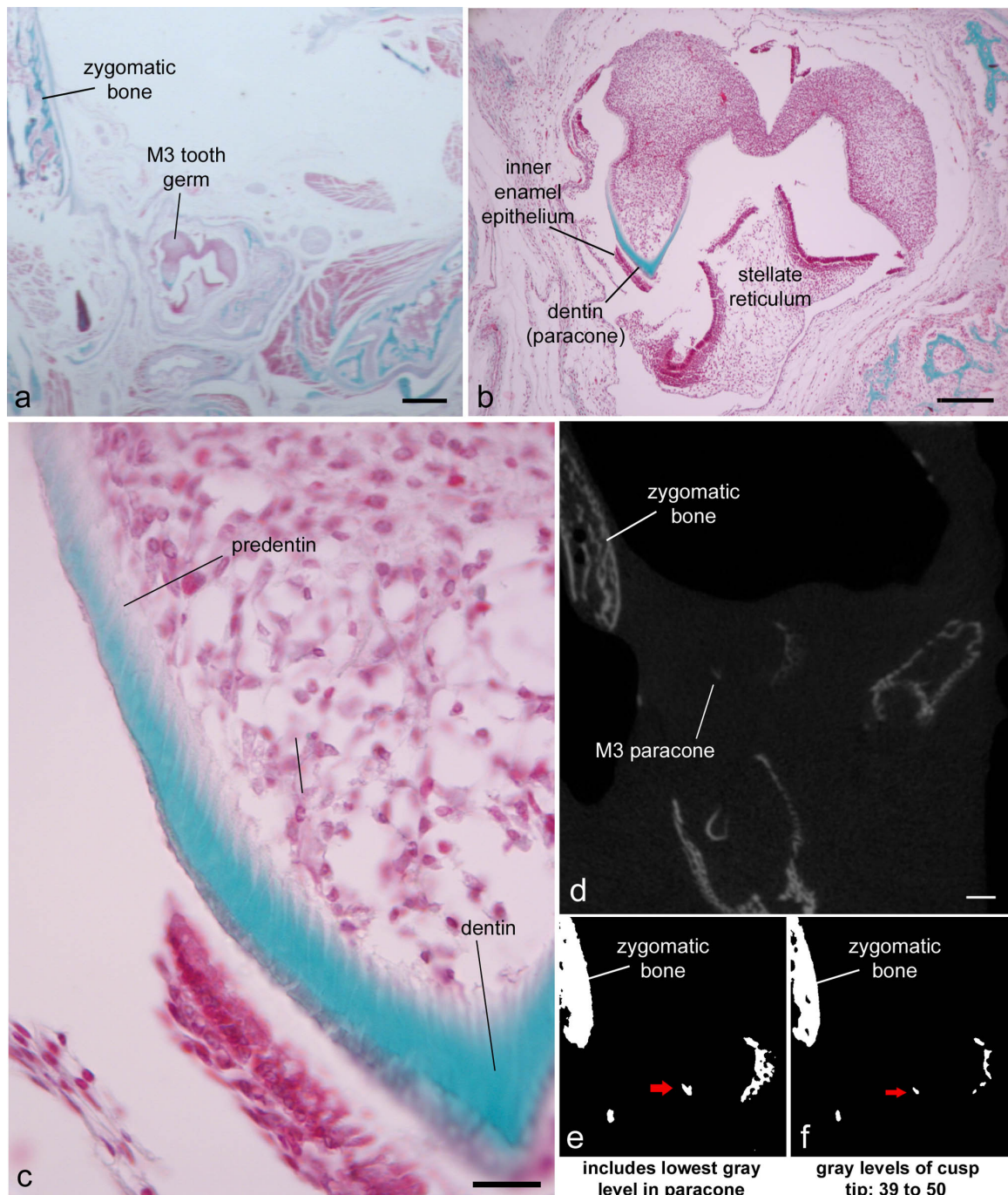


Figure 2: a, b) The  $M^3$  tooth germ of *T. syrichta* has a mineralized paracone only. Histology confirms that the tip of the cusp is mature dentin, but tapers to only predentin approaching the base of the cusp (Fig. 2c). The cusp tip is easily detected via  $\mu$ -CT (2d). The cusp itself is barely thicker than voxel size. Low ranges of thresholds may detect less mineralized dentin (2e), but may exaggerate the thickness of the cusp tip, which is identified by a narrower threshold range (2f). Scale bars: a, 0.5mm; b, 150  $\mu$ m; c, 20  $\mu$ m; d, 0.5mm.

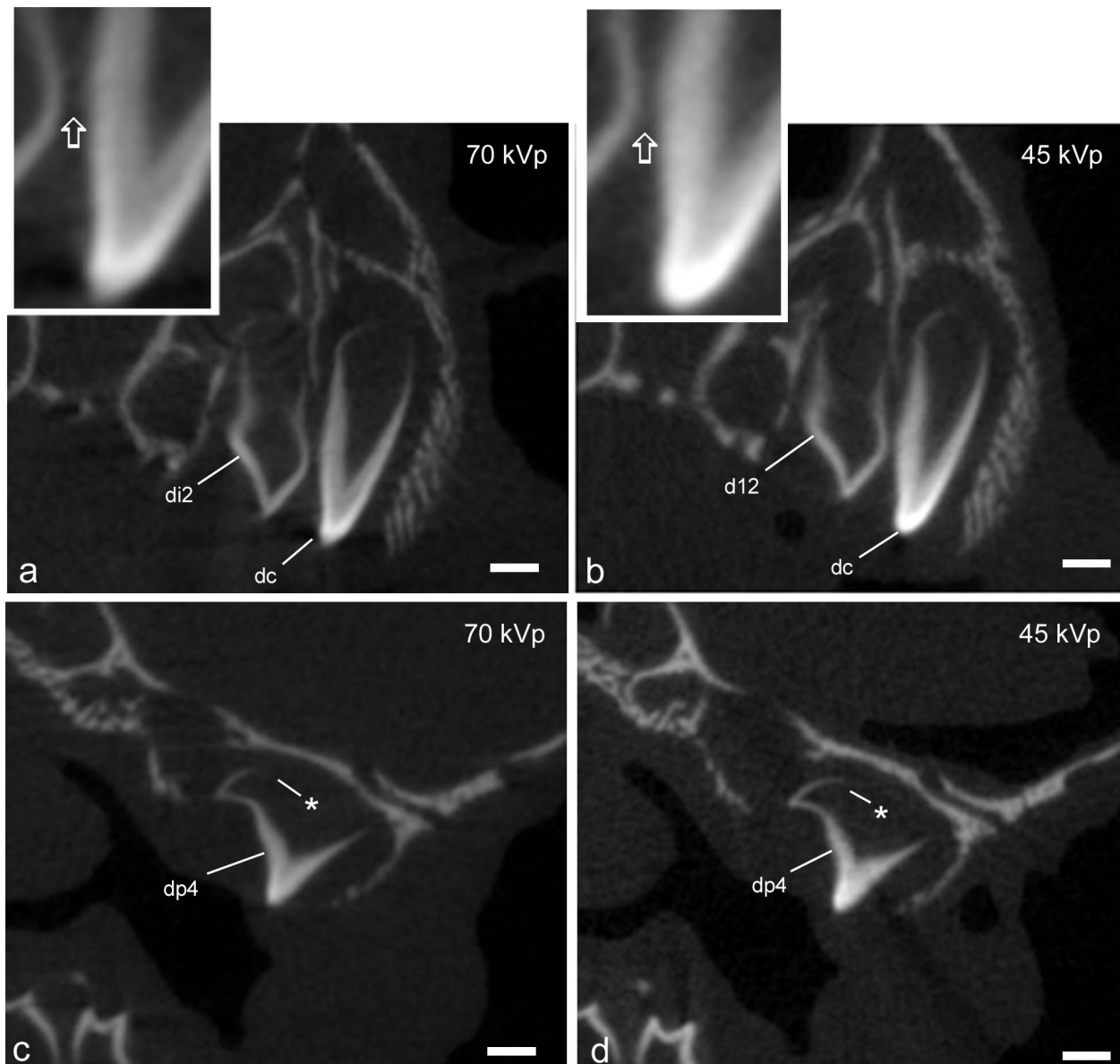


Figure 3.  $\mu$ -CT slices showing similar cross-sectional levels of deciduous anterior teeth (a,b,) and  $dp^4$  (c,d) in a newborn *Callithrix jacchus* scanned using different energy levels. On the left side are slices with the head scanned at 70 kVp (a,c); on the right are slices with the head scanned at 45 kVp (b,d). The 70 kVp reveals a sharper boundary between adjacent teeth (see open arrow inset, a) compared to the 45 kVp scan (inset, b). Conversely, the 45 kVp was more effective at revealing the cervical region of the crown (c, d: \*), where the cusp was least mineralized.

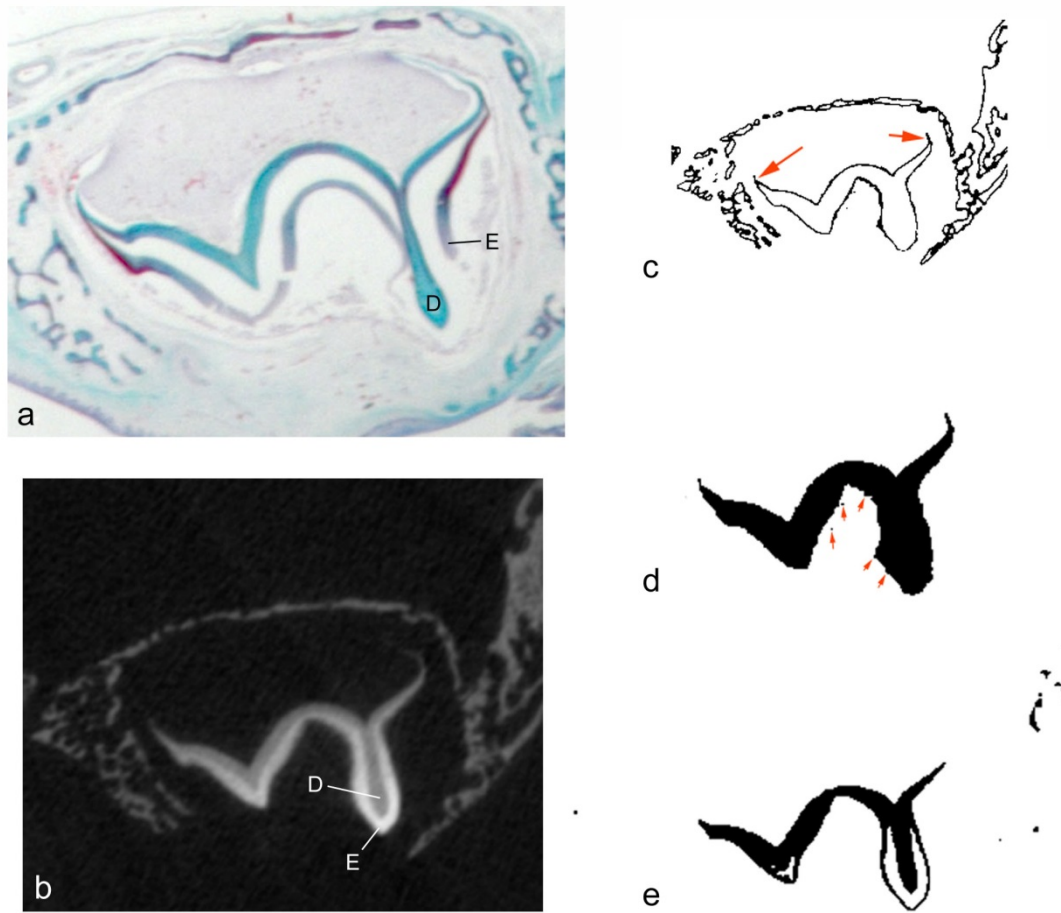


Figure 4: a) Histological section of  $dp^4$  in a newborn squirrel monkey (*Saimiri*), showing the maxillary  $dp^4$  in the region of the paracone. Note that enamel (E) is present, though fragmented near the cusp tip (D = dentin). b) The same specimen shown as a  $\mu$ -CT slice aligned to histology; enamel is distinctly more radio-opaque than the dentin, especially along the cusps. A low threshold range, such as that shown in plate c (46 to 70 gray level range) is required to capture the least mineralized dentin found closest to the cervical region (red arrows). However, this range also captures a halo of noise surrounding the crown, including the occlusal surface. As a result, a slice segmented with a threshold that captures all gray levels above that which captures the least mineralized dentin results in a rough cusp surface, with artifactual complexity (red arrows). e) A more limited grayscale range of 99 to 174 captures a specific deeper part of the crown, but appears to exclude the densest enamel. Also, a comparison to the matching level of histology (right) suggests this threshold range isolates the full depth of dentin in the paracone.

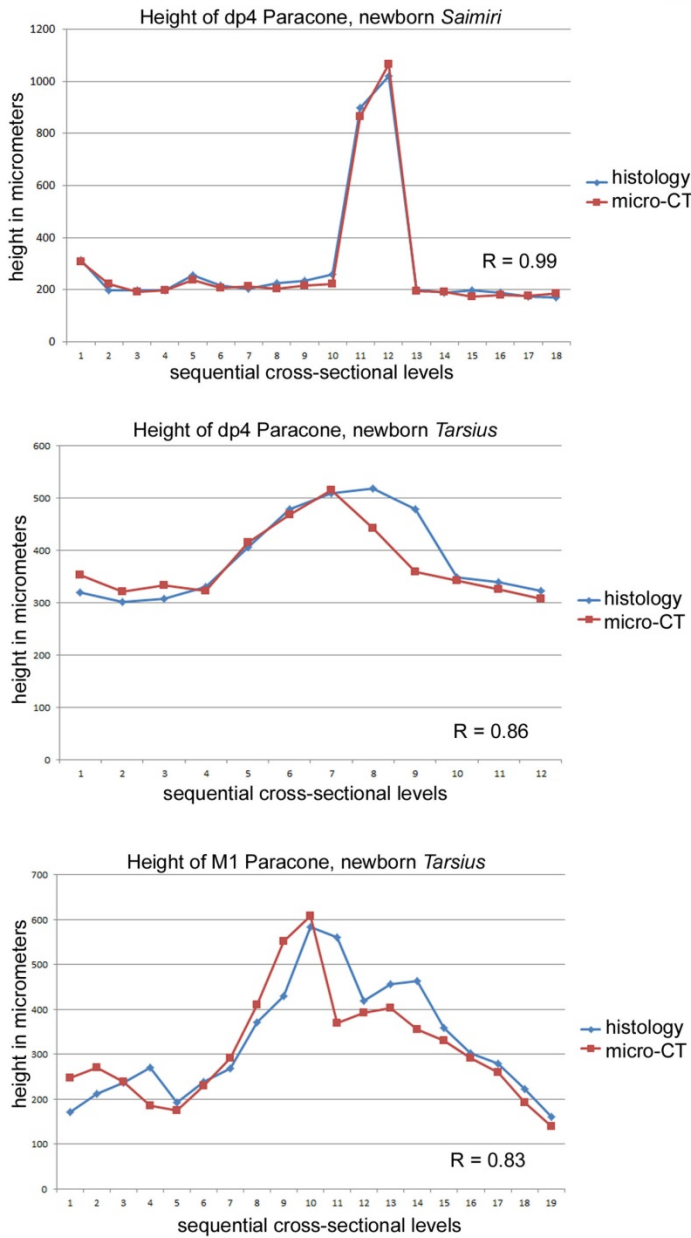


Figure 5: Histology versus  $\mu$ -CT-derived measurements. Graphs show measurements “height” (maximum apical-basal thickness) of dentin in the paracone of  $dp^4$  or  $M^1$ , as measured using histology and  $\mu$ -CT. In these specimens (newborn *Saimiri boliviensis* and *Tarsius syrichta*), the  $\mu$ -CT scan volumes were aligned so that serial slices matched the same plan as histological sections of the same heads. Matching levels of histology and  $\mu$ -CT slices were used for these measurements. Correlation coefficient for a comparison between methods is shown in the bottom right of each graph.

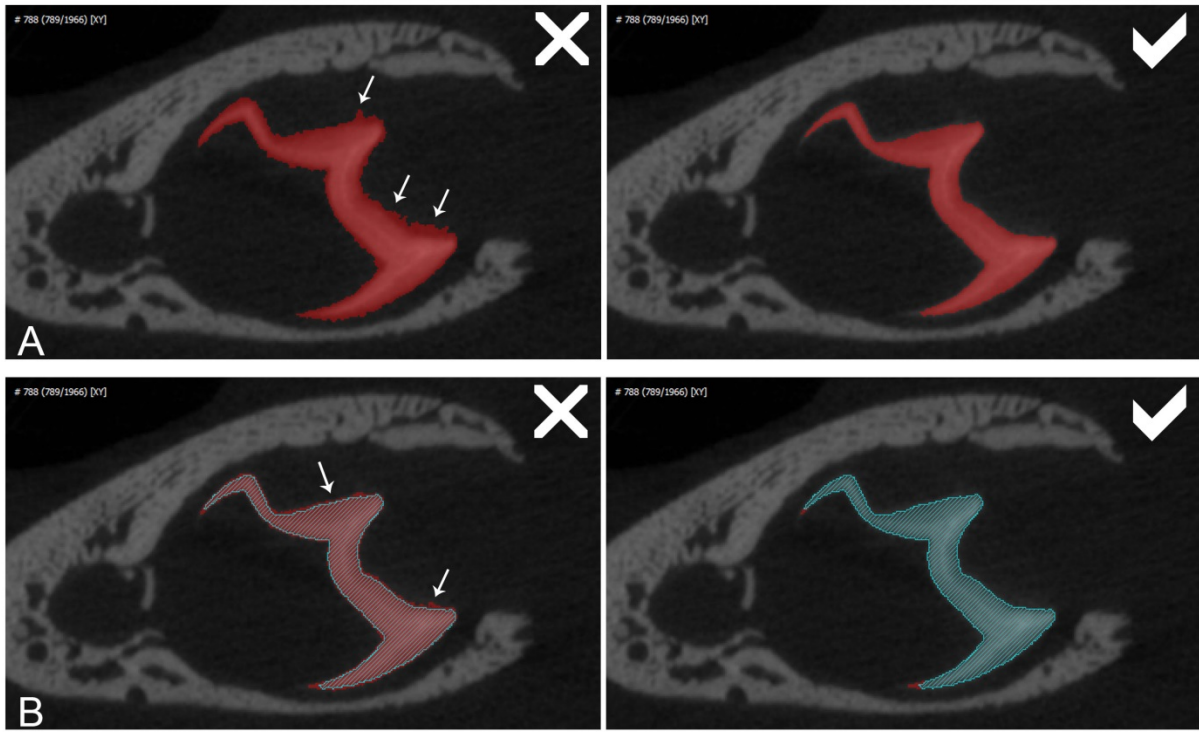


Figure 6: Stepwise method of crown segmentation. In initial phases of segmentation (A), the range of gray levels is carefully selected to establish a relatively smooth occlusal surface (see right side image), and to avoid capturing artefactual “stray” voxels (left side, arrows). Subsequent phases of segmentation are similarly conducted by establishing incrementally lower ranges of gray levels (B), being careful not to allow captured ranges of voxels to “bleed” out onto the occlusal surface (left side, arrows), while adding more of the crown in less-mineralized areas (right side).

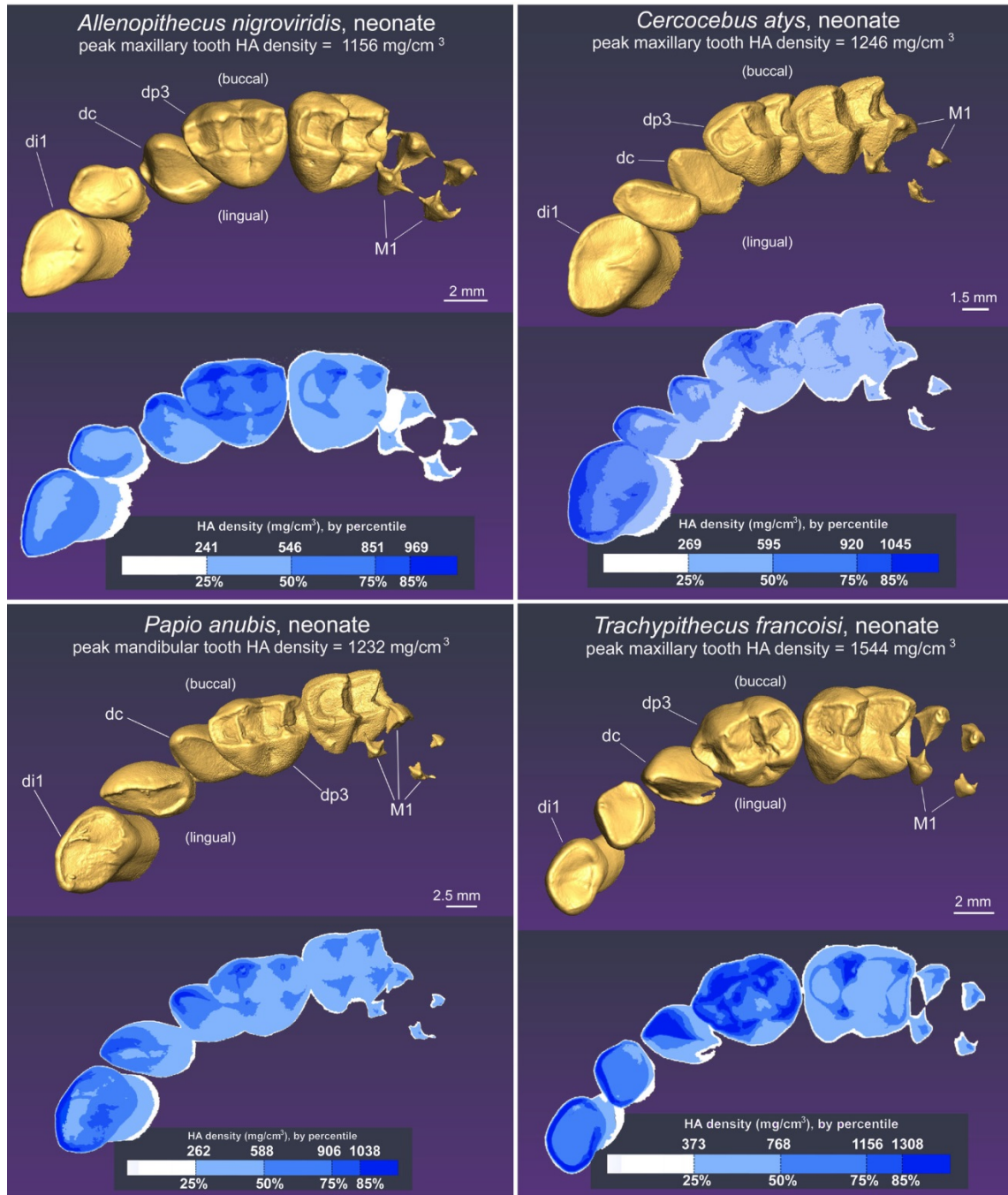


Figure 7: Morphology and hydroxyapatite density in maxillary tooth crowns at birth in *Allenopithecus nigroviridis*, *Cerocebus atys*, *Papio anubis*, and *Trachypithecus francoisi*. In *Allenopithecus* and *Trachypithecus*, the right jaw is shown (inverted to facilitate comparison to other species) and the left jaw is shown in the other species. At the top of each image, the peak (or maximum) hydroxyapatite density for the pictured specimen is indicated.

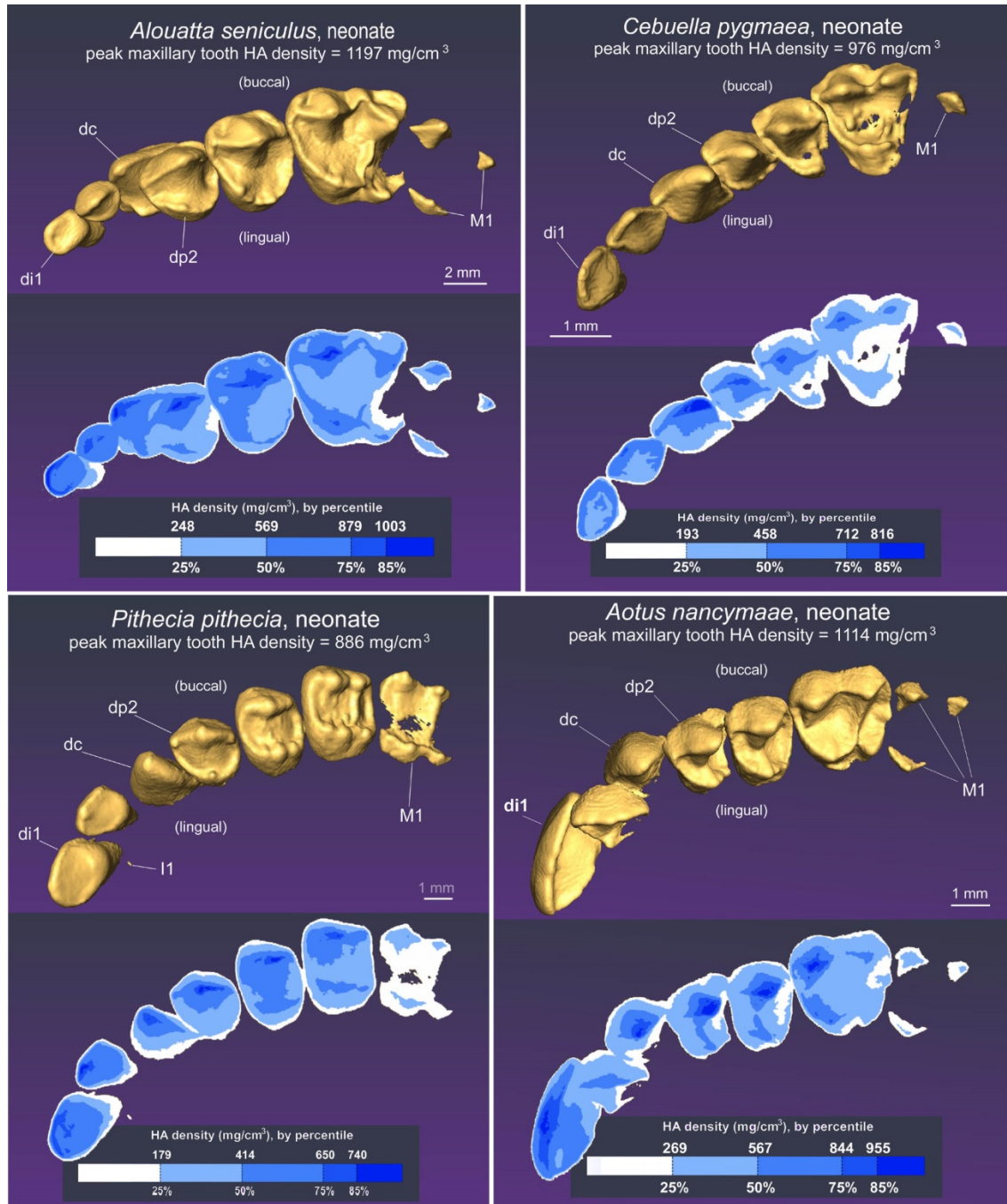


Figure 8: Morphology and hydroxyapatite density in mandibular tooth crowns at birth in *Allenopithecus nigroviridis*, *Cercocebus atys*, *Papio anubis*, and *Trachypithecus francoisi*. In

*Allenopithecus* and *Trachypithecus*, the right jaw is shown (inverted to facilitate comparison to other species) and the left jaw is shown in the other species.

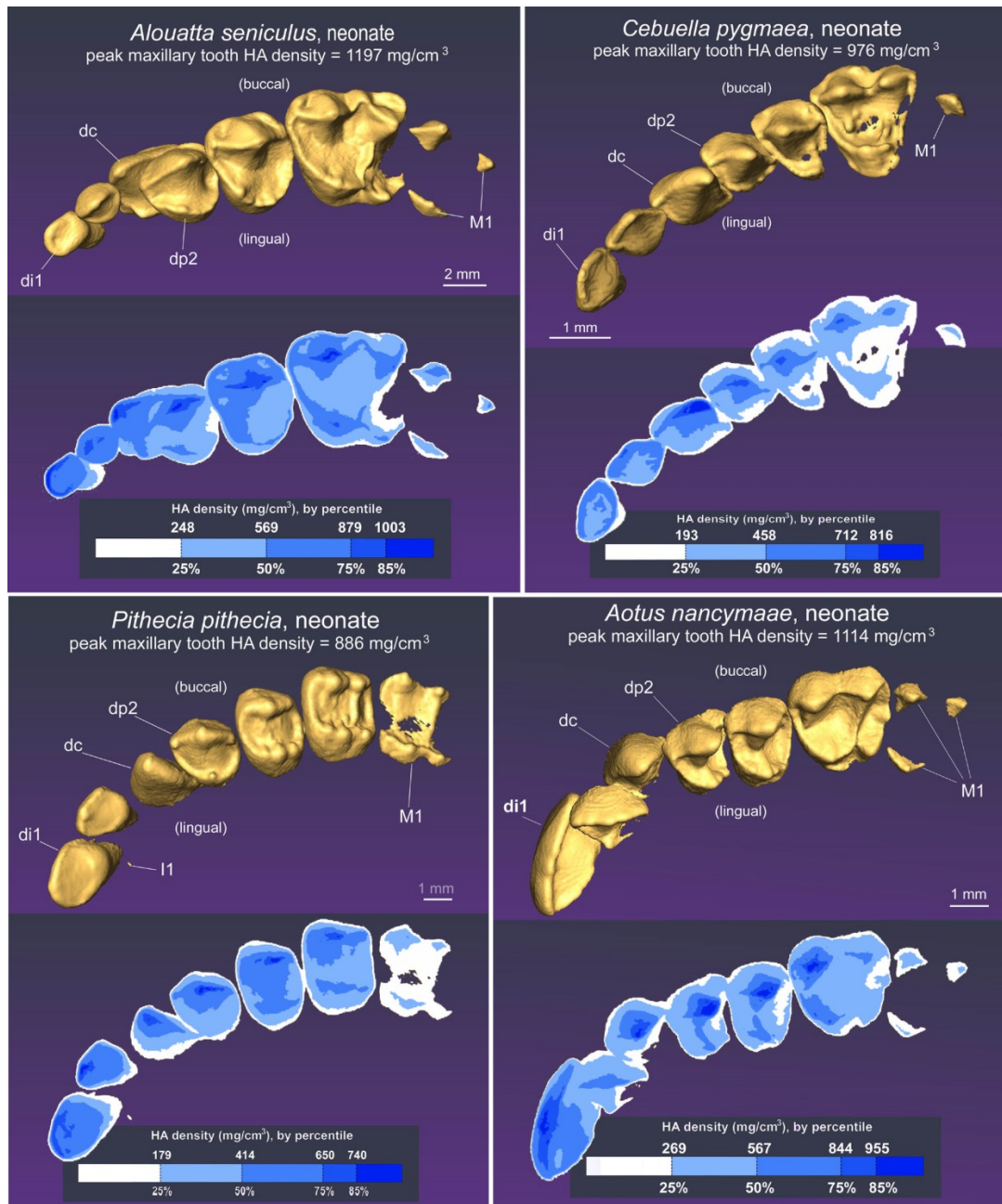


Figure 9: Morphology and hydroxyapatite density in left maxillary tooth crowns at birth in *Alouatta seniculus*, *Cebuella pygmaea*, *Pithecia pithecia*, and *Aotus nancymaae*.

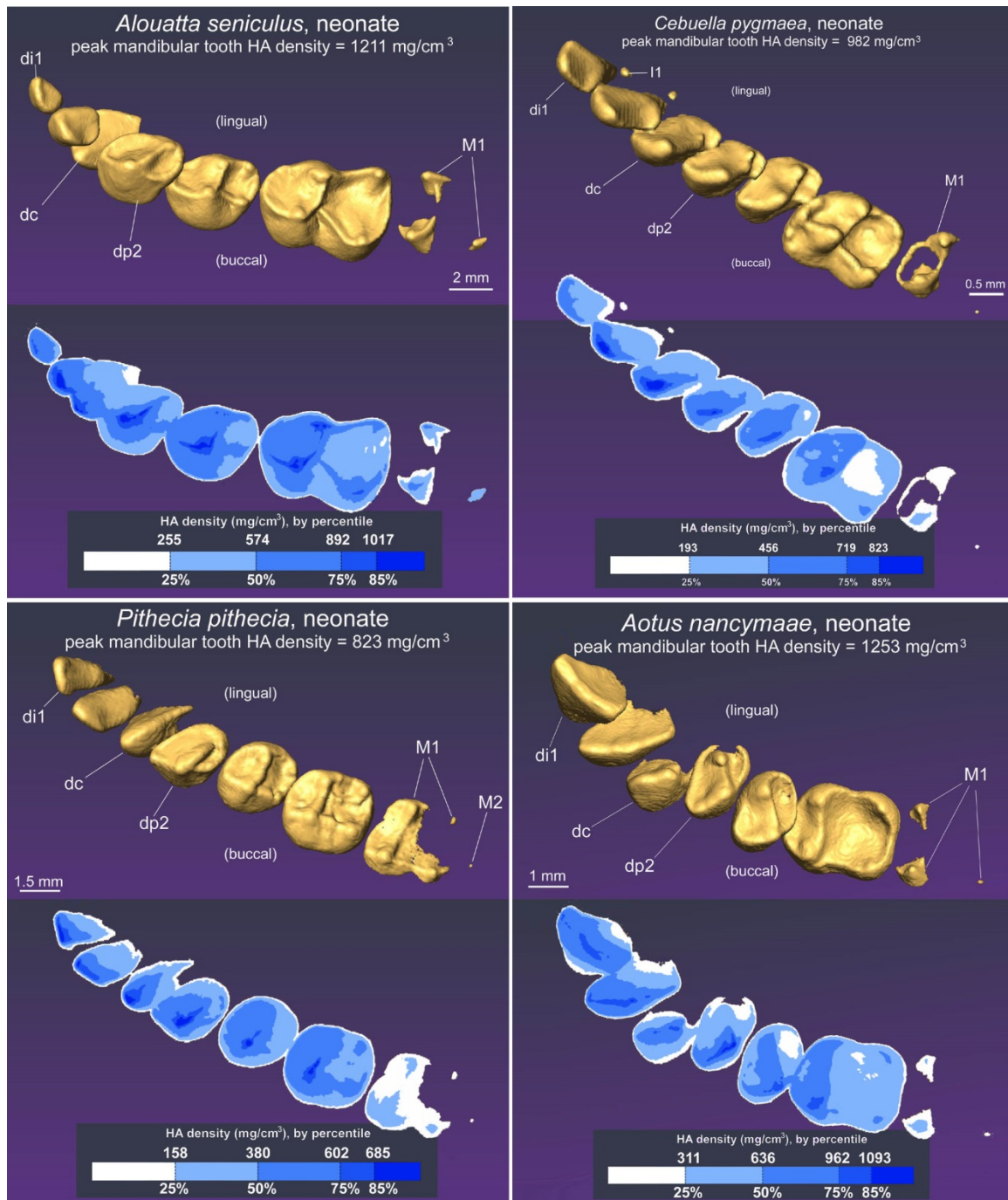


Figure 10: Morphology and hydroxyapatite density in left mandibular tooth crowns at birth in *Alouatta seniculus*, *Cebuella pygmaea*, *Pithecia pithecia*, and *Aotus nancymaae*.

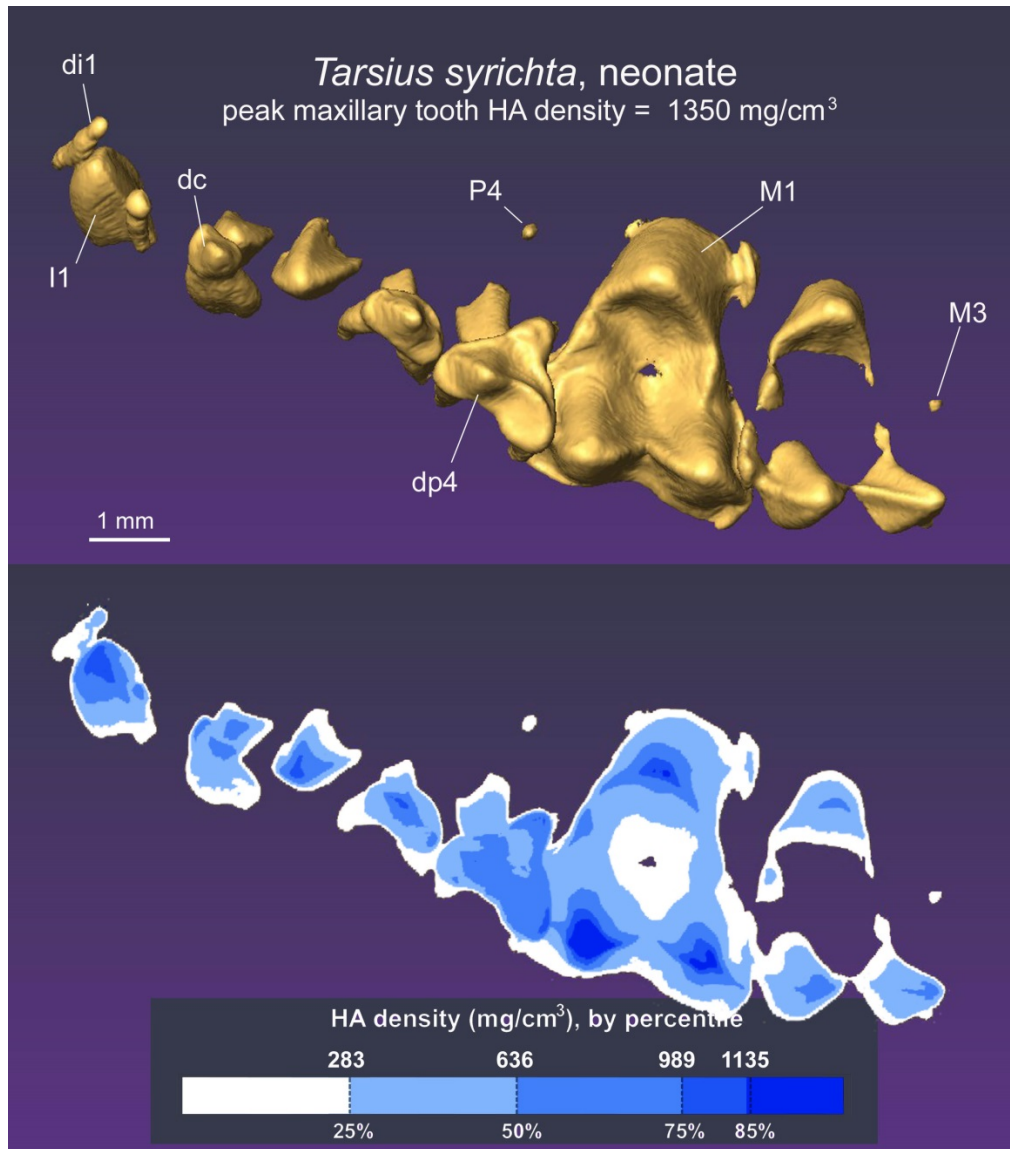


Figure 11: Morphology and hydroxyapatite density in maxillary tooth crowns at birth in *Tarsius syrichta*. A day 0 newborn is shown using the right jaw (image inverted to facilitate comparison to other species).

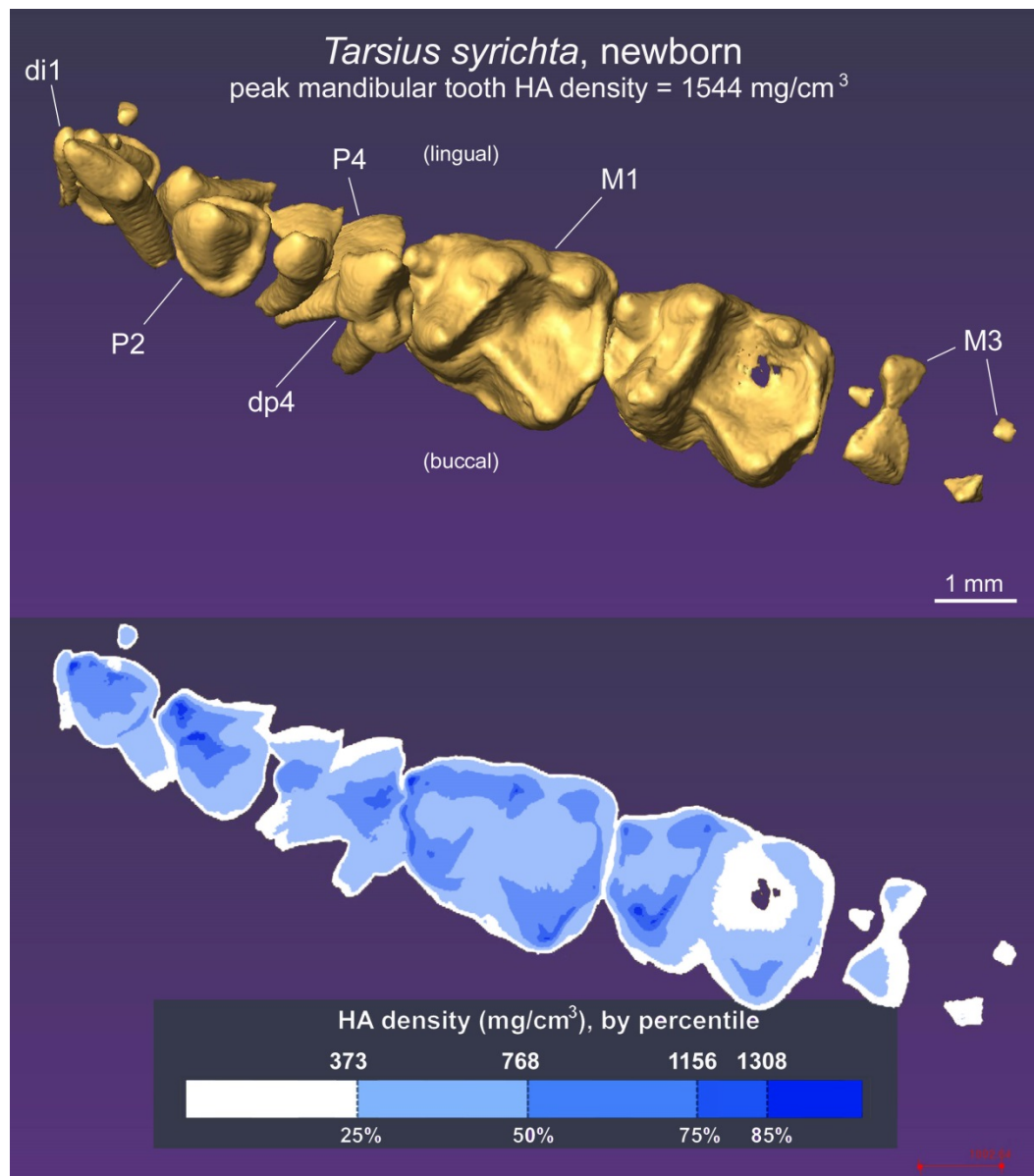


Figure 12: Morphology and hydroxyapatite density in left mandibular tooth crowns at birth in *Tarsius syrichta*. A day 6 newborn is shown.

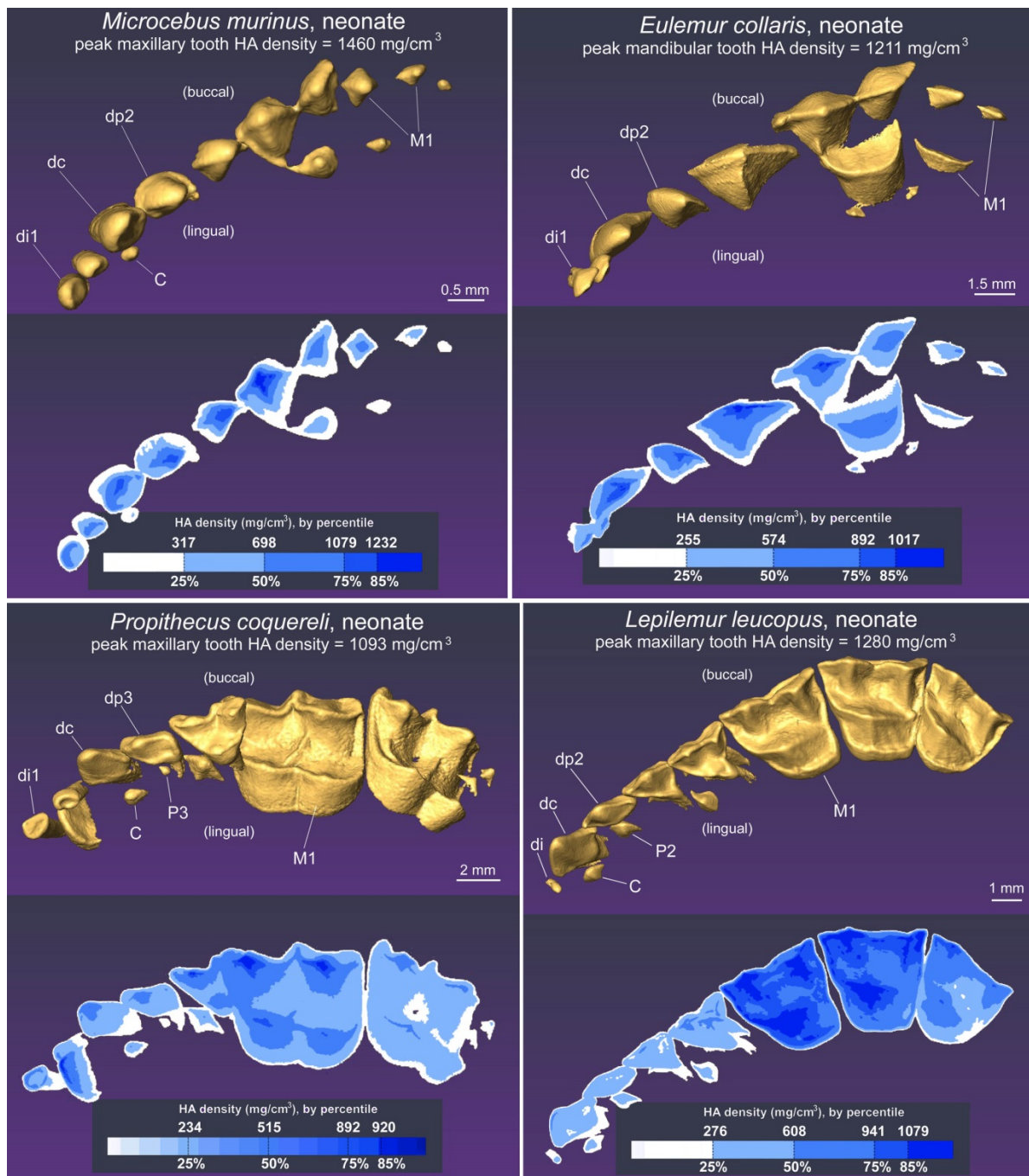


Figure 13: Morphology and hydroxyapatite density in left maxillary tooth crowns at birth in *Microcebus murinus*, *Eulemur collaris*, *Propithecus coquereli*, and *Lepilemur leucopus*.

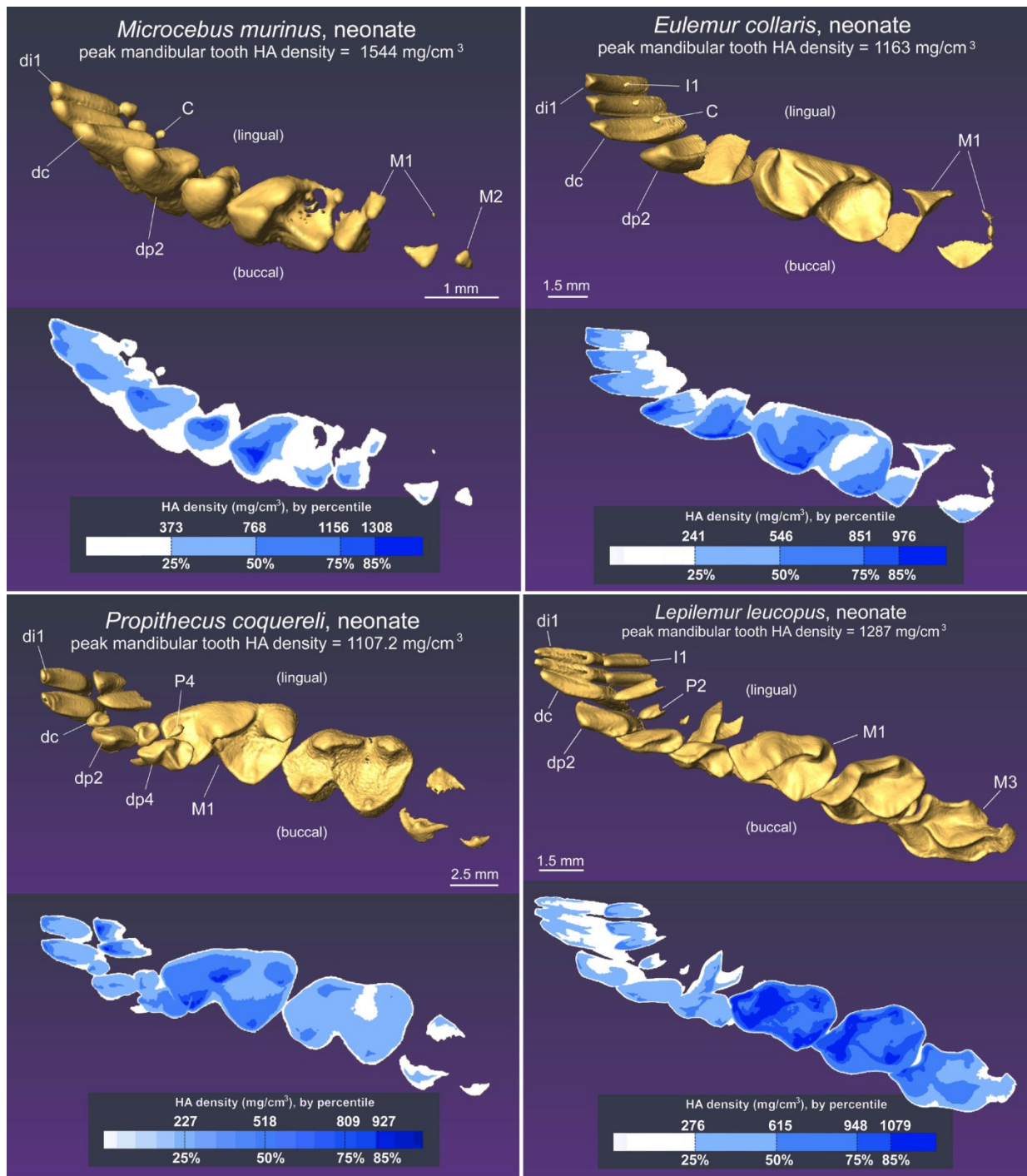


Figure 14: Morphology and hydroxyapatite density in left mandibular tooth crowns at birth in *Microcebus murinus*, *Eulemur collaris*, *Propithecus coquereli*, and *Lepilemur leucopus*.

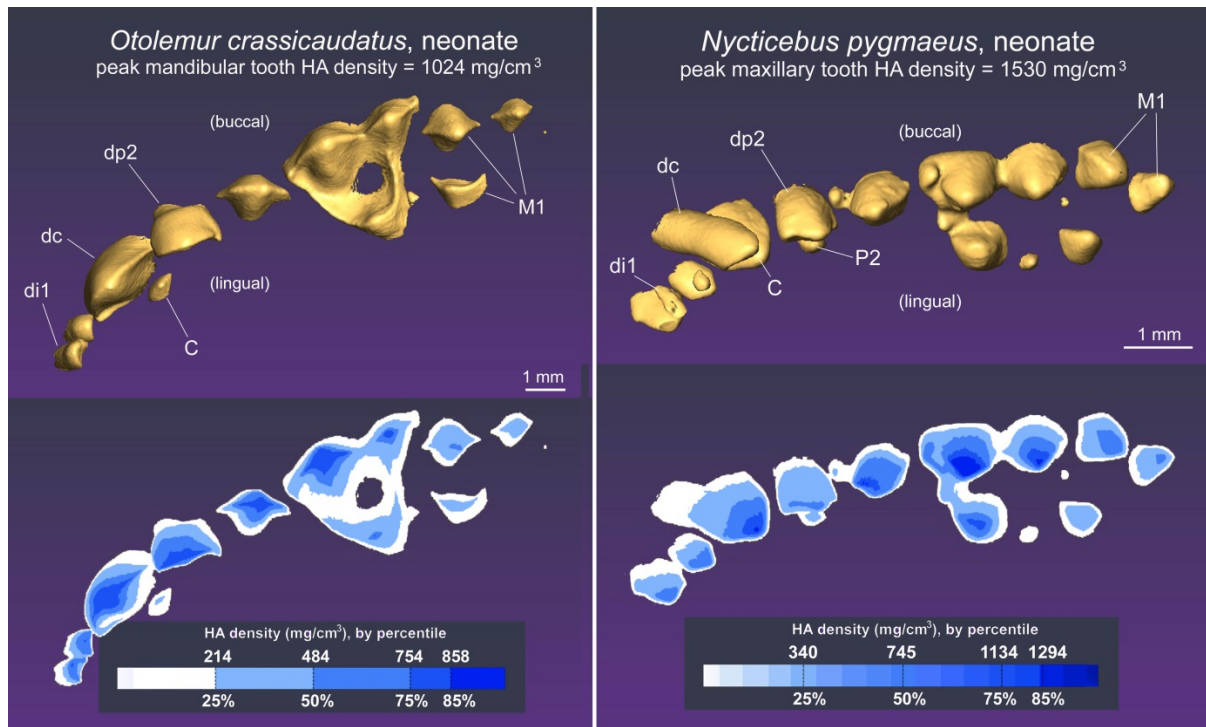


Figure 15: Morphology and hydroxyapatite density in maxillary tooth crowns at birth in *Otolemur crassicaudatus* and *Nycticebus pygmaeus*. In *Otolemur crassicaudatus*, the right jaw is shown (inverted to facilitate comparison to other species) and the left jaw is shown in *Nycticebus pygmaeus*.

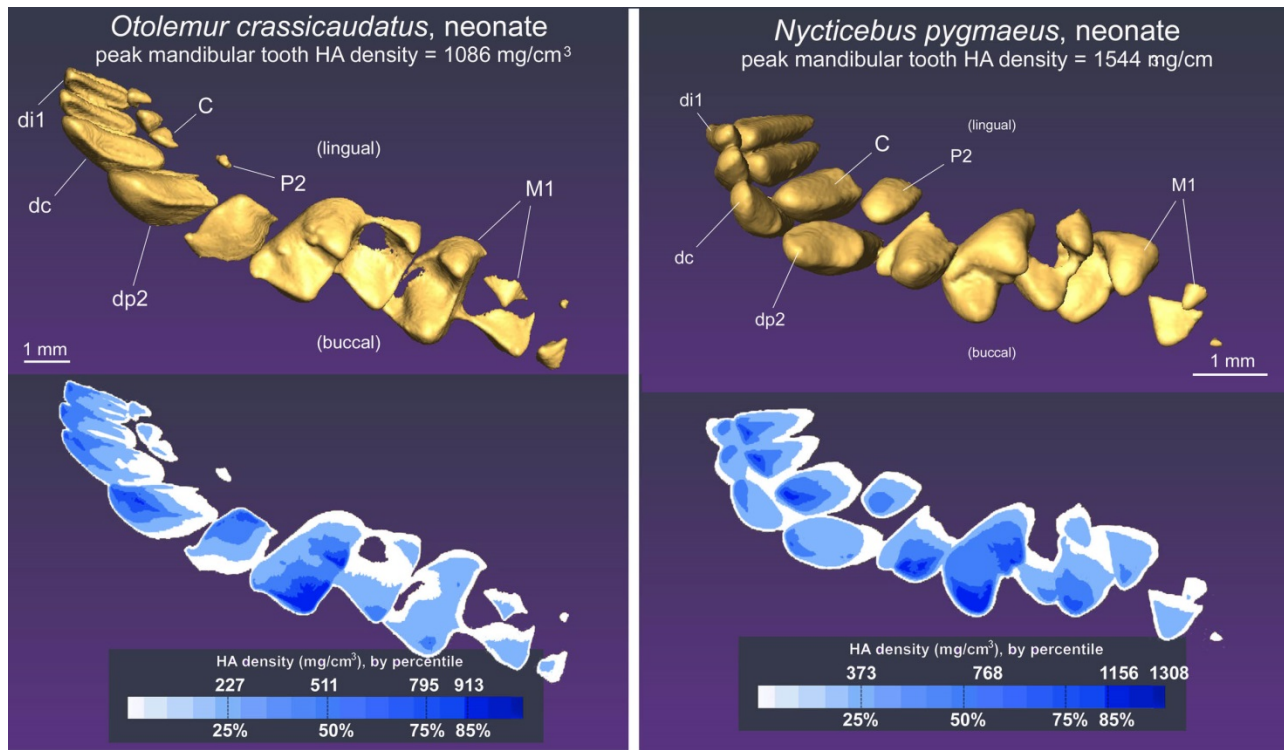


Figure 16: Morphology and hydroxyapatite density in mandibular tooth crowns at birth in *Otolemur crassicaudatus* and *Nycticebus pygmaeus*. In *Otolemur crassicaudatus*, the right jaw is shown (inverted to facilitate comparison to other species) and the left jaw is shown in *Nycticebus pygmaeus*.

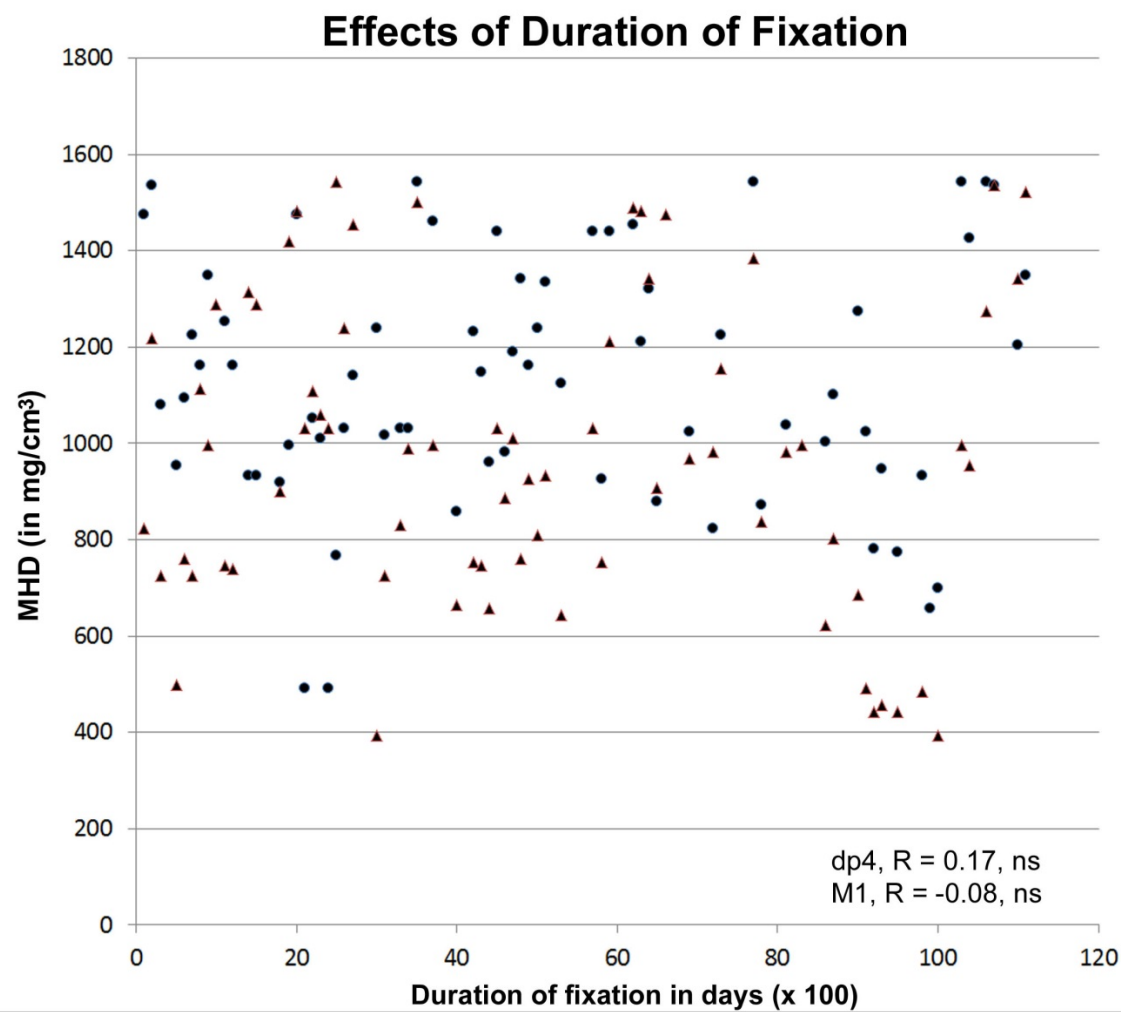


Figure 17: Maximum hydroxyapatite density (MHD) of the last mandibular deciduous premolar (circles) and the first mandibular permanent molar (triangles) plotted against duration of fixation in formalin. All specimens are from the Duke Lemur Center.

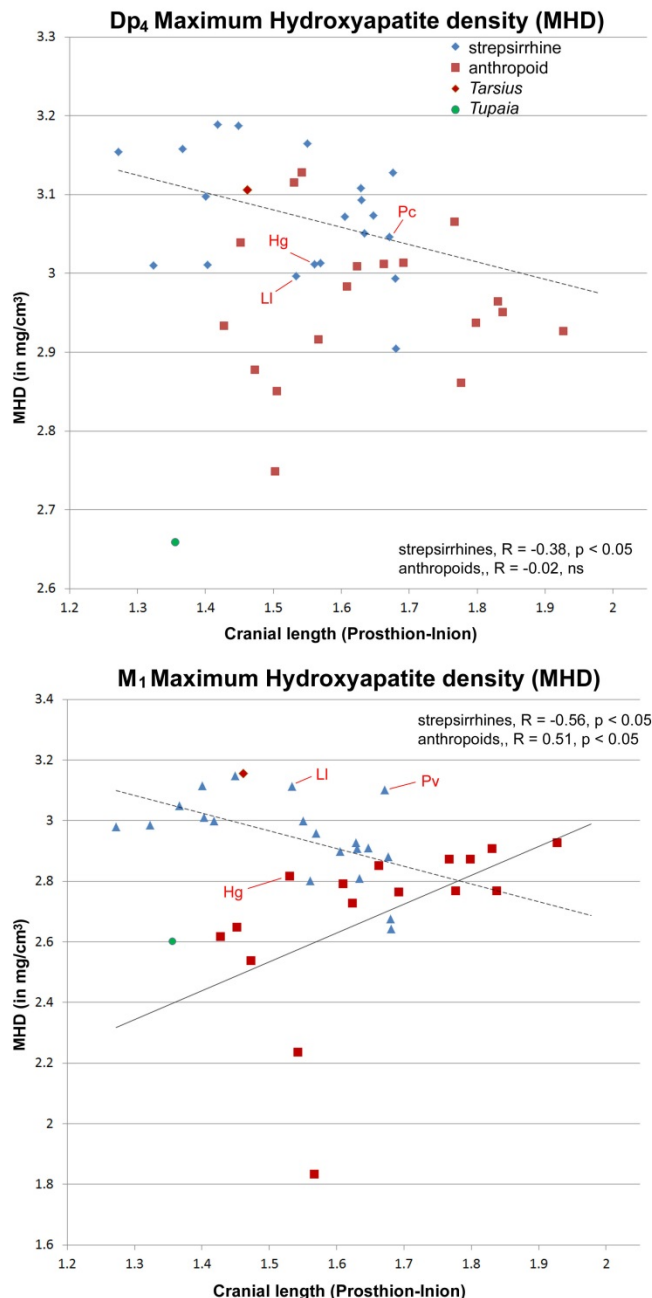


Figure 18: Top) MHD of dp<sub>4</sub> plotted against cranial length. The dashed line illustrates the negative slope for the significant correlation of dp<sub>4</sub> in strepsirrhines. Bottom) MHD of M<sub>1</sub> plotted against cranial length. The dashed line illustrates the negative slope for the significant correlation of M<sub>1</sub> in strepsirrhines; the solid line illustrates the positive slope for the significant correlation of M<sub>1</sub> in Old and New World monkeys. Hg, *Hapalemur griseus*; LI, *Lepilemur leucopus*; Pc, *Propithecus coquereli*.

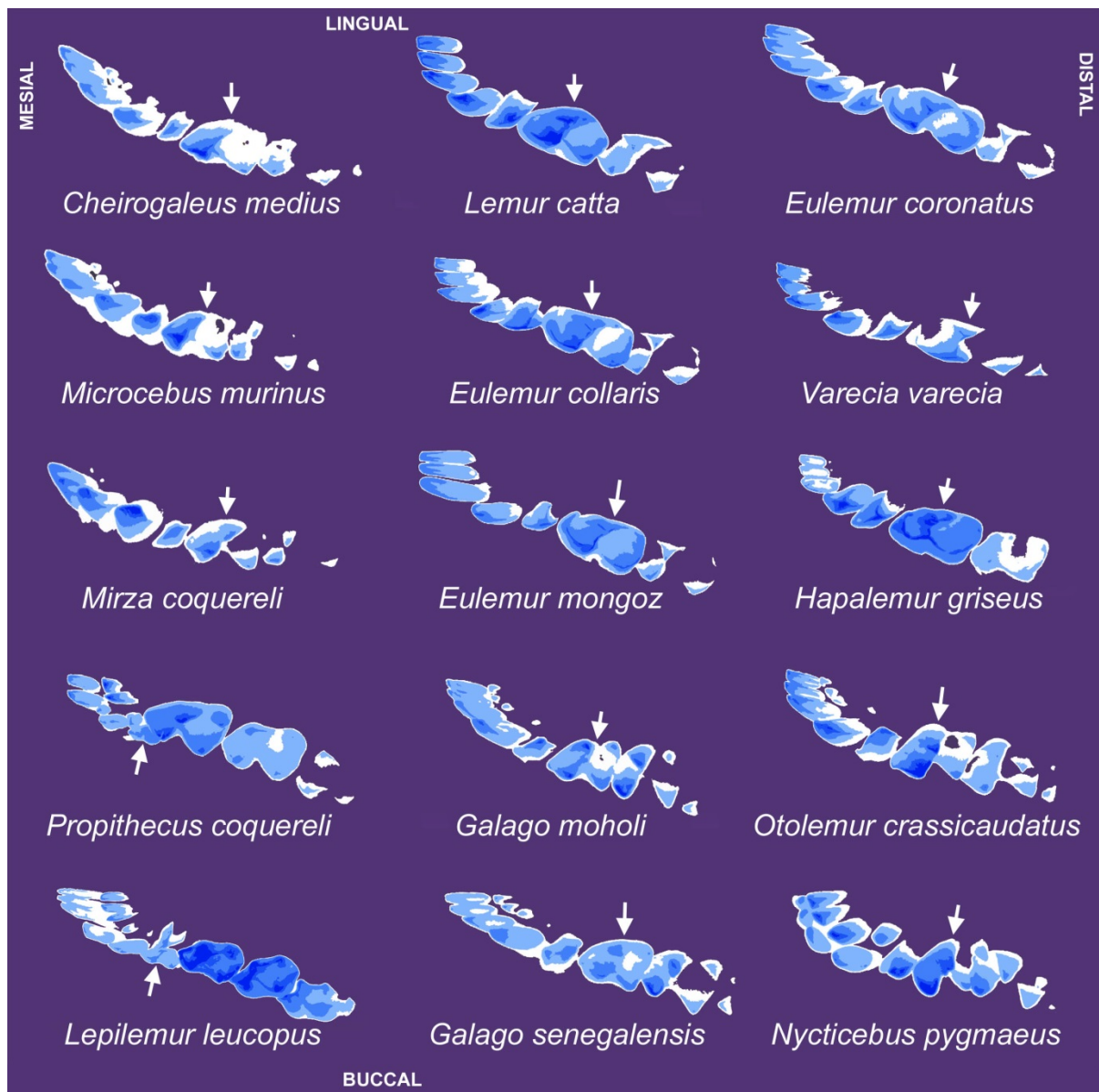


Figure 19: Survey of hydroxyapatite density in mandibular teeth in newborn strepsirrhines. As in earlier plates, blue coding reveals the 25<sup>th</sup>, 50<sup>th</sup>, 75<sup>th</sup>, and 85<sup>th</sup> percentiles of MHD (light blue = 25<sup>th</sup>; darkest blue = 85<sup>th</sup>).

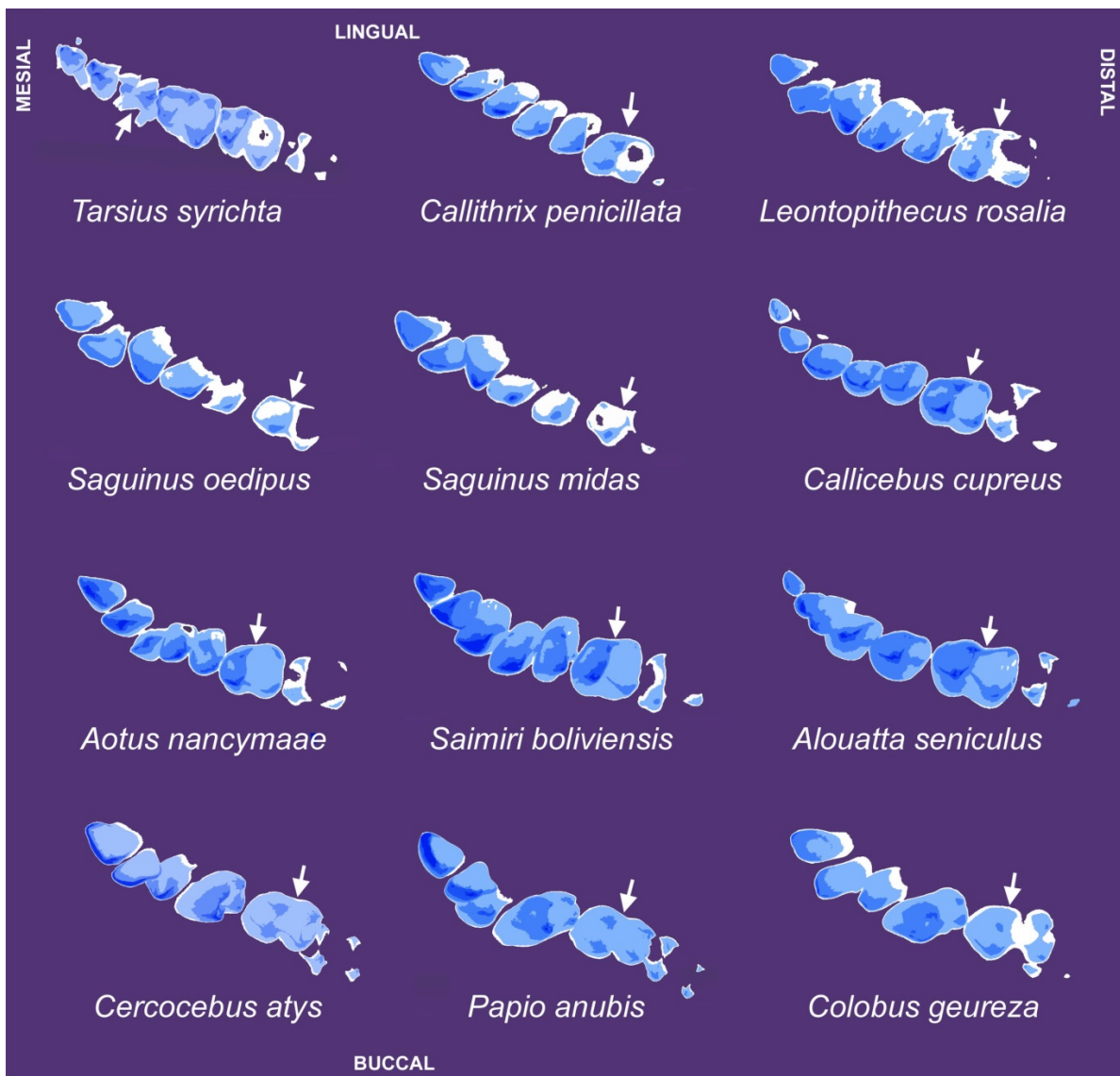


Figure 20: Survey of MHD profiles of mandibular teeth in newborn haplorhines. As in earlier plates, blue coding reveals the 25<sup>th</sup>, 50<sup>th</sup>, 75<sup>th</sup>, and 85<sup>th</sup> percentiles of MHD (light blue = 25<sup>th</sup>; darkest blue = 85<sup>th</sup>).

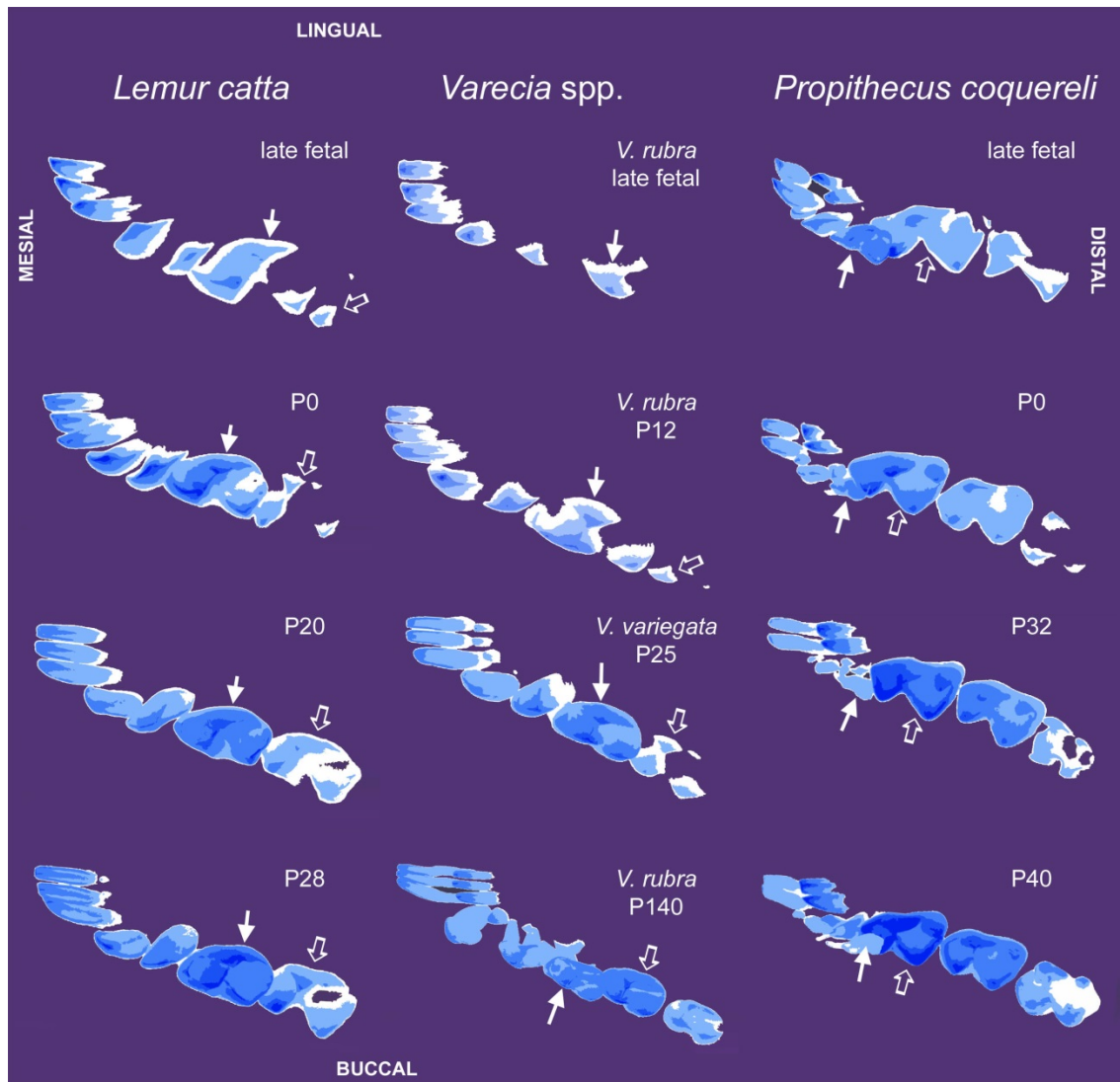


Figure 21: Survey of cusp mineralization patterns in strepsirrhines at late fetal to subadult ages. As in earlier plates, blue coding reveals the 25<sup>th</sup>, 50<sup>th</sup>, 75<sup>th</sup>, and 85<sup>th</sup> percentiles of MHD (light blue = 25<sup>th</sup>; darkest blue = 85<sup>th</sup>). Note that hydroxyapatite density is initially highest anteriorly, and at older ages postcanine teeth contain the peaks in hydroxyapatite density.

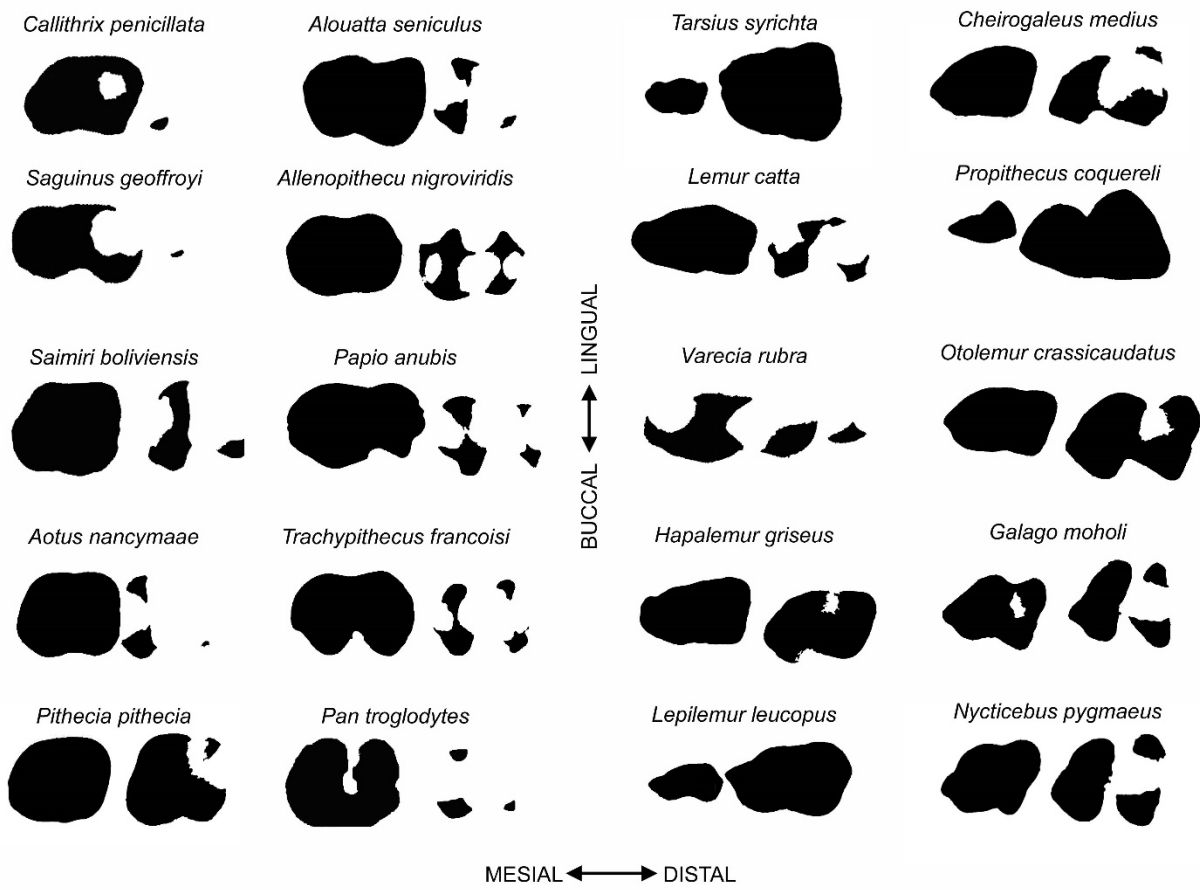


Figure 22: Occlusal view showing extent of mineralization of mandibular dp<sub>4</sub> and M<sub>1</sub> in newborn primates.

## MANDIBULAR TEETH IN NEWBORN LEMURS AND LORISES

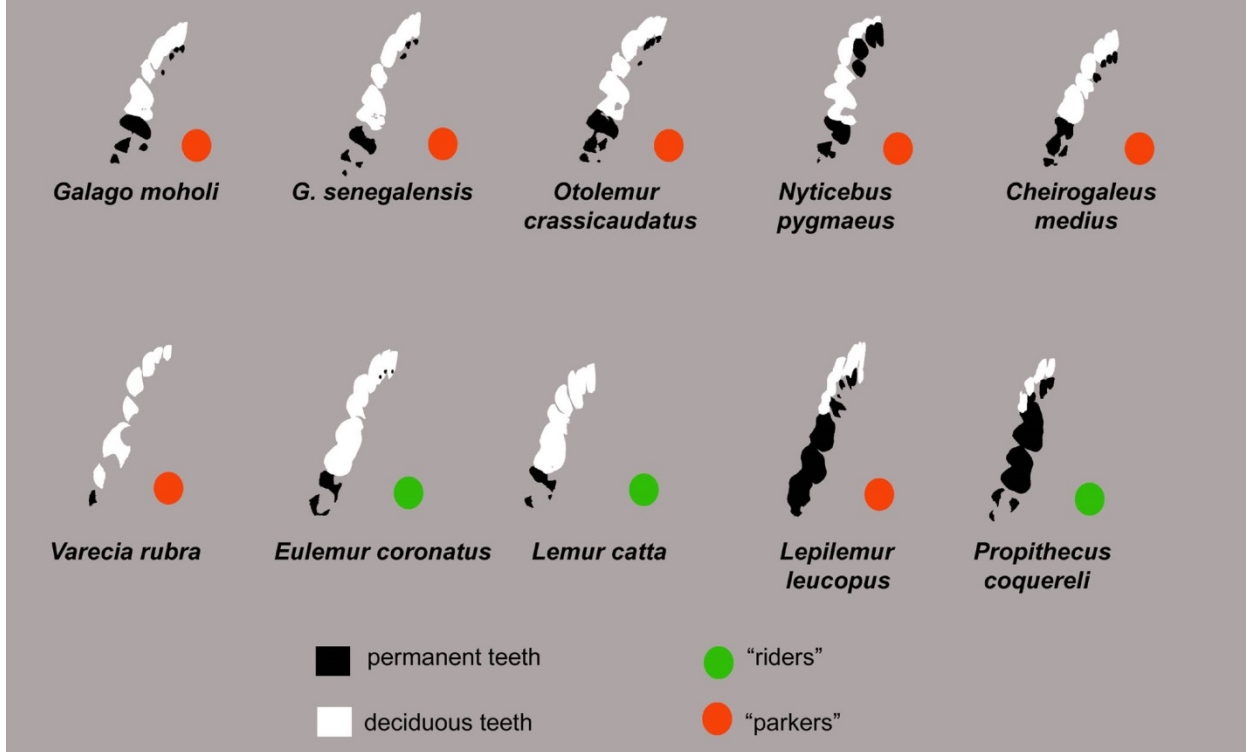


Figure 23: Mineralized portions of deciduous (white) and replacement (black) tooth crowns at birth in newborn strepsirrhines with different parenting strategies.